TECHNICAL REPORT STANDARD TITLE PAGE

1. Report No.	2. Government Accession No.	3. Recipient's Catalog No.
FHWA/TX-85/ +326-2F		

4. Title and Subtitle	5. Report Date
The Behavior of Reinforced Concrete Box Culverts Under Symmetrical and Unsymmetrical Live Loads	January 1986
	6. Performing Organization Code
7. Author(s)	8. Performing Organization Report No
Mark P. Gardner, Jey K. Jeyapalan and Ray W. James	Research Report 326-2F
9. Performing Organization Name and Address Texas Transportation Institute The Texas A&M University System College Station, TX 77843	10. Work Unit No.
	11. Contract or Grant No. Study 2-5-82-326
	13. Type of Report and Period Covered Final - September 1981 January 1986
12. Sponsoring Agency Name and Address Texas State Department of Highways and Public Transportation: Transportation Planning Division P.O. Box 5051 Austin, Texas 78763	14. Sponsoring Agency Code

15. Supplementary Notes
Research performed in cooperation with DOT, FHWA.
Research Study Title: Behavior of Reinforced Concrete Box Culverts Under Backfill and Traffic Loads.

16. Abstract

The design criteria for reinforced box culverts currently used are primarily empirical in nature, and do not allow for the effects of soil-structure interaction. These effects have been shown to make a considerable difference in certain situations. In order to have a better understanding of the field behavior of R.C. box culverts, in another research study, the Texas Transportation Institute is studying the behavior of an instrumented 8' x 8' R.C. box culvert. The purpose of the study presented herein is to perform prediction analyses of the behavior of this 8' x 8' box culvert under traffic loads using a finite element method computer program.

In this study, soil properties determined from laboratory tests of soil samples taken at the site were used to determine the stress-strain parameters for use in the computer analyses. The culvert was represented in the analyses by a series of beam elements connected at common nodes. An incremental analysis was used to represent placement of backfill materials.

Predicted earth pressures, stresses and strains at the instrument locations on the test culvert are presented for symmetrical and unsymmetrical live loading conditions at various backfill cover heights. A no-slip soil-culvert interface condition is used throughout the analyses, due to the fact that this more closely represented actual field conditions. Furthermore, predicted bending moment distributions around the culvert are presented for various loading conditions. In addition, the shear force distributions around the culvert are presented in this report. Also, predicted crown deflections are presented for the various loading conditions.

17. Key Words	18. Distribution Statement
Reinforced Concrete Box Culverts, Prediction Analyses of Behavior, Traffic Loads.	No restrictions. This document is available to the public through the National Technical Information Service, 5285 Port Royal Road, Springfield, Virginia 22161

19. Security Classif. (of this report)	20. Security Classif. (of this page)	21. No. of Pages	22. Price
Unclassified	Unclassified	161	

Form DOT F 1700.7 (8-69)

THE BEHAVIOR OF REINFORCED CONCRETE BOX CULVERTS UNDER SYMMETRICAL AND UNSYMMETRICAL LIVE LOADS

by

Mark P. Gardner
Graduate Research Assistant

Jey K. Jeyapalan
Assistant Research Engineer

Ray W. James
Assistant Professor

Research Report Number 326-2F
Research Project 2-5-82-326

Conducted for
The Texas State Department of Highways
and Public Transportation

In cooperation with the
U.S. Department of Transportation
Federal Highway Administration

by the
TEXAS TRANSPORTATION INSTITUTE
The Texas A&M University System
College Station, Texas

January 1986

METRIC CONVERSION FACTORS

Approximate Conversions to Metric Measures

Symbol	When You Know	Multiply by	To Find	Symbol
		LENGTH		
in	inches	*2.5	centimeters	cm
ft	feet	30	centimeters	cm
yd	yards	0.9	meters	m
mi	miles	1.6	kilometers	km
		AREA		
in^2	square inches	6.5	square centimeters	cm^2
ft^2	square feet	0.09	square meters	m^2
yd^2	square yards	0.8	square meters	m^2
mi^2	square miles	2.6	square kilometers	km^2
	acres	0.4	hectares	ha
		MASS (weight)		
oz	ounces	28	grams	g
lb	pounds	0.45	kilograms	kg
	short tons (2000 lb)	0.9	tonnes	t
		VOLUME		
tsp	teaspoons	5	milliliters	ml
Tbsp	tablespoons	15	milliliters	ml
fl oz	fluid ounces	30	milliliters	ml
c	cups	0.24	liters	l
pt	pints	0.47	liters	l
qt	quarts	0.95	liters	l
gal	gallons	3.8	liters	l
ft^3	cubic feet	0.03	cubic meters	m^3
yd^3	cubic yards	0.76	cubic meters	m^3
		TEMPERATURE (exact)		
°F	Fahrenheit temperature	5/9 (after subtracting 32)	Celsius temperature	°C

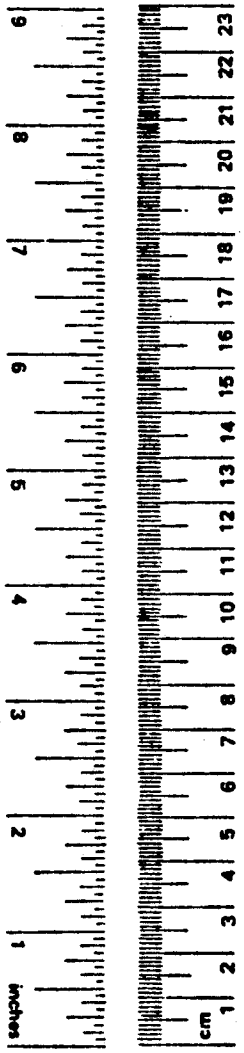

Approximate Conversions from Metric Measures

Symbol	When You Know	Multiply by	To Find	Symbol
		LENGTH		
mm	millimeters	0.04	inches	in
cm	centimeters	0.4	inches	in
m	meters	3.3	feet	ft
m	meters	1.1	yards	yd
km	kilometers	0.6	miles	mi
		AREA		
cm^2	square centimeters	0.16	square inches	in^2
m^2	square meters	1.2	square yards	yd^2
km^2	square kilometers	0.4	square miles	mi^2
ha	hectares (10,000 m^2)	2.5	acres	
		MASS (weight)		
g	grams	0.035	ounces	oz
kg	kilograms	2.2	pounds	lb
t	tonnes (1000 kg)	1.1	short tons	
		VOLUME		
ml	milliliters	0.03	fluid ounces	fl oz
l	liters	2.1	pints	pt
l	liters	1.06	quarts	qt
l	liters	0.26	gallons	gal
m^3	cubic meters	35	cubic feet	ft^3
m^3	cubic meters	1.3	cubic yards	yd^3
		TEMPERATURE (exact)		
°C	Celsius temperature	9/5 (then add 32)	Fahrenheit temperature	°F

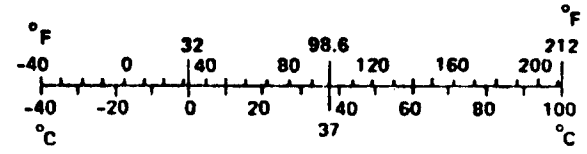

*1 in = 2.54 (exactly). For other exact conversions and more detailed tables, see NBS Misc. Publ. 286, Units of Weights and Measures, Price $2.25, SD Catalog No. C13.10:286.

ABSTRACT

The design criteria for reinforced box culverts currently used are primarily empirical in nature, and do not allow for the effects of soil-structure interaction. These effects have been shown to make a considerable difference in certain situations. In order to have a better understanding of the field behavior of R.C. box culverts, in another research study, the Texas Transportation Institute is studying the behavior of an instrumented 8' x 8' R.C. box culvert. The purpose of the study presented herein is to perform prediction analyses of the behavior of this 8' x 8' box culvert under traffic loads using a finite element method computer program.

In this study, soil properties determined from laboratory tests of soil samples taken at the site were used to determine the stress-strain parameters for use in the computer analyses. The culvert was represented in the analyses by a series of beam elements connected at common nodes. An incremental analysis was used to represent placement of backfill materials.

Predicted earth pressures, stresses and strains at the instrument locations on the test culvert are presented for symmetrical and unsymmetrical live loading conditions at various backfill cover heights. A no-slip soil-culvert interface condition is used throughout the analyses, due to the fact that this more closely

represented actual field conditions. Furthermore, predicted bending moment and shear force distributions around the culvert and crown deflections are presented for various loading conditions.

IMPLEMENTATION STATEMENT

The results of this study show that soil-structure interaction can play a very important role in determining the behavior of certain types of drainage structures under backfill and live loads. This interaction indicates that the design loads specified by present standards may be much simpler than those actually occurring in the field during and after construction of the culvert. By comparing results from finite element method predictions with those from an ongoing study of an instrumented culvert of the same properties and dimensions, good correlation of predicted and measured pressures is found, except for data taken at 2 ft soil cover. While some of the difference may be attributed to measurement errors, it is believed that the finite element model used may in general result in unconservative pressure predictions for concentrated wheel loads and shallow depths of fill. This error is probably due to the increasing importance of the nonlinear soil behavior as soil stresses are increased.

It should be noted that the field data presented herein should not be considered for design purposes without further reference to the final results of the field instrumentation study being conducted by the Texas Transportation Institute, Study Number 2-5-81-294, entitled "Determination of Earth Pressures on Reinforced Concrete Box Culverts". This study is being conducted by Dr. Harry Coyle, Dr. Ray W. James, Richard E. Bartoskewitz, and Dale Brown. Their cooperation and assistance is acknowledged and greatly appreciated.

DISCLAIMER

The contents of this report reflect the views of the authors who are responsible for the facts and the accuracy of the data presented herein. The contents do not necessarily reflect the official views or policies of the Federal Highway Administration. This report does not constitute a standard, specification or regulation.

TABLE OF CONTENTS

LIST OF FIGURES

LIST OF TABLES

CHAPTER 1

INTRODUCTION

Reinforced Concrete Box Culverts are currently being used by state transportation agencies throughout the United States as a means of bridging across canals and streams. The design criteria primarily used for these culverts are presented by the American Association of State Highway and Transportation Officials (AASHTO)(2). Since its' beginning in 1944, the AASHTO specifications have not changed significantly in regard to RC box culvert design specifications. However, great advances in the field of civil engineering have resulted in further insight into the effects of such parameters as geometry and stiffness of the culvert, properties of the surrounding soil medium, and soil-structure interaction phenomenon. Considering these, as well as other secondary parameters affecting culvert behavior, it becomes necessary to reevaluate the current specifications to determine their adequacy. In order to study the behavior of RC box culverts, the Texas Transportation Institute is currently involved with the field instrumentation of an 8'x8' RC box culvert. Earth pressures around the perimeter of the culvert will be measured using pressure cells. In addition, a number of strain gages have been placed on the reinforcing steel at various sections of the culvert to measure strain. Measurements of earth pressure and strain will be taken in order to evaluate the behavior of the culvert under

backfill and traffic loads. These field observations are restricted to one box size and one type of backfill.

In order to derive the maximum benefit from the ongoing field instrumentation study, this research study was initiated so that a series of computer predictions of the behavior of the 8'x8' box culvert can be made.

The purpose of this report is to present the results of the computer predictions for the 8'x8' RC box culvert under traffic loads. The AASHTO (2) standard HS-20 truck was used to determine the live load to be considered, and various backfill cover depths were examined. Soil properties closely resembling those in the field were used to determine the hyperbolic stress dependent stress-strain parameters used in the computer analyses.

The studies undertaken to complete the project objectives are described in subsequent chapters of this report.

Chapter 2 - the results of a literature survey of culvert research are presented. Current design procedures and suggested modifications in light of previous research are also presented in this chapter.

Chapter 3 - presents the material properties used in the computer analyses.

Chapter 4 - includes the computer predictions of the behavior of the 8'x8' RC box culvert under symmetrical and unsymmetrical traffic loads.

Chapter 5 - a comparison of the computer predictions to available field data from the ongoing field instrumentation is

made.

Chapter 6 - contains the conclusions derived from this study and outlines the recommendations for further research.

CHAPTER 2

PREVIOUS RESEARCH

2.1 Introduction

In this chapter the results of previous research studies involving the design and analysis of buried conduits are discussed. The research presented is classified under the following categories and reviewed accordingly:

1) Analytical Studies
2) Numerical Studies, and
3) Empirical Studies.

2.2 Analytical Studies

The analytical procedures reviewed may be divided into two groups: those which do not consider the effects of soil-structure interaction on culvert behavior and those in which these effects are considered.

2.2.1 Studies Without Soil-Structure Interaction

Early design methods for culverts were developed under the assumption that the dead weight of the fill is distributed uniformly over the full width of the culvert. The weight of this fill was considered equal to the weight of a prism of soil whose height is equal to the width of the structure, as given in Polack and DeGroot

(18). This procedure is shown in Figure 2.1. The lateral pressure on the sides of the culvert was taken as one-fourth the weight of the fill uniformly distributed on the side from top to bottom. The pressure exerted on the bottom of the culvert was assumed to be the sum of the superimposed loads on the roof, and the dead weight of the roof and sides of the culvert. The pressure was considered uniformly distributed over the base of the culvert. This is the simplest approach, and is used as the basis for most other analytical procedures in culvert design.

Karadi and Krizek (14) have presented a method of design of rigid culverts used in the Soviet Union. Here, culverts are designed for bending moment by the formula

$$M = \nu r^2 (p+q) [1 - \tan^2 (45 - \phi/2)] \quad (2.1)$$

where

p = vertical pressure due to dead loads

q = vertical pressure due to live loads

ν = coefficient determined by type of foundation

The values of p and q are given by

$$p = C \gamma H \quad (2.2)$$

and

$$q = \frac{19}{H+3} \quad (H > 1 \text{ meter}) \quad (2.3)$$

where in Equation 2.3, H is expressed in meters and q in metric tons per square meter. In Equation 2.2,

$$C = 1 + A \tan \phi \tan^2 (45 - \phi/2) \quad (2.4)$$

and

$$A = m h H^{-3} (2H^2 - m Bh) \quad (2.5)$$

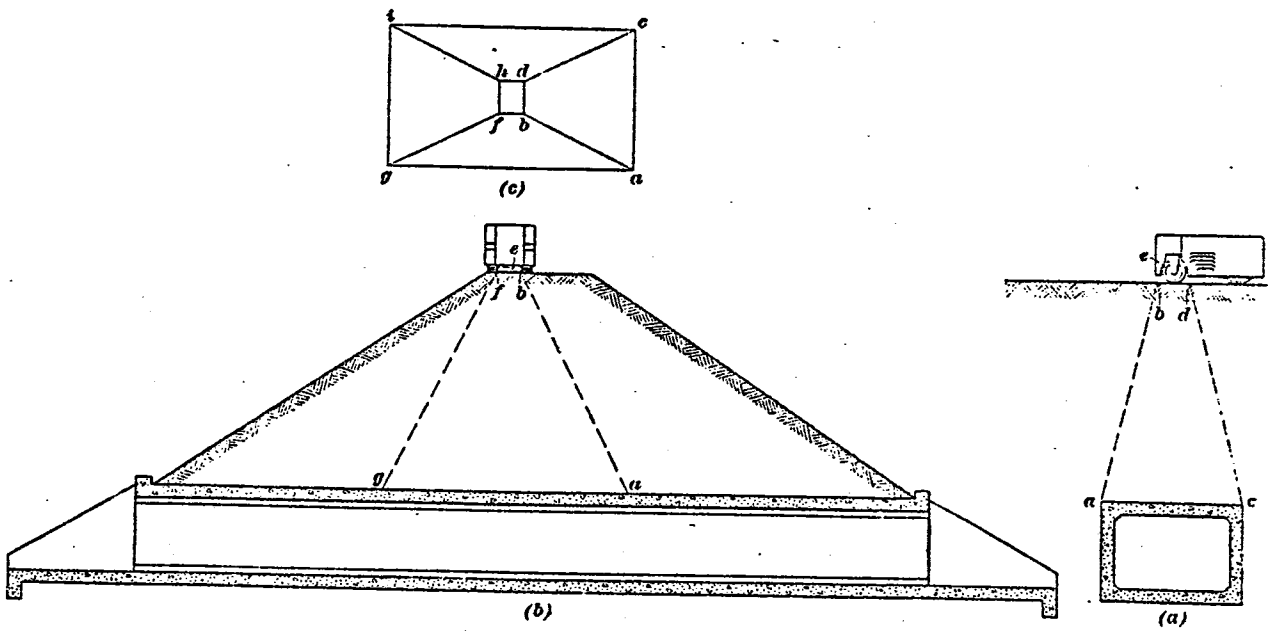

VERTICAL PRESSURE DISTRIBUTION
ON BURIED CONCRETE CULVERTS

FIGURE 2.1

Here, H is the height of the embankment above the crown of the culvert, h is the distance between the plane of the foundation and the crown of the culvert, B is the external span of the culvert, m is a coefficient determined by soil characteristics and and are the angle of internal friction and the density of the soil, respectively.

2.2.2 Studies With Soil-Structure Interaction Effects

If the loading on a buried conduit is determined from classical earth pressure theory, large variations can be expected between the actual and theoretical loads. These variations can result from the buried structure deflecting more than the adjacent soil and thereby causing a reduction in the pressure transmitted to the structure with a corresponding increase in the pressure carried by the adjacent medium. Conversely, under load, the structure may not deform as much as the adjacent soil, and the resulting redistribution can produce an increase in load on the structure and a decrease in the pressure carried by the adjacent medium. The difference in the conditions is determined by the direction of soil stress produced by the soil movement along some slippage plane. Marston (15) recognized this interaction between the structure and the surrounding soil medium while conducting research on earth pressures on buried conduits. Although his original conclusions were limited, they were instrumental in the advancement of knowledge in this field.

Spangler extended Marstons' work on rigid conduits to include flexible conduits as well. In doing this, Spangler introduced the first well defined soil-structure interaction concept. This concept

recognized that a passive type of soil pressure is developed by the horizontal expansion of the conduit which allowed it to carry more load with less deflection than in the unrestrained condition. Also, this deflection might be used as a basis for determining the magnitude of the horizontal pressure developed on the sides of the pipe.

Combining the achievements of both Marston and Spangler to produce a more general theory to predict soil pressures on underground conduits provides a basic concept which encompasses both rigid and flexible conduits.

The Marston-Spangler theory considers four basic classes of conduit installations as shown in Figure 2.2. For each class of installation, the prism of fill over the conduit is assumed to be supported by the conduit and by friction between the adjacent soil prisms on either side of the conduit. Equations of equilibrium are established for an element of backfill such as the ones shown in Figure 2.3. Solution of the equations result in formulae which can be used to compute the total vertical load on the conduit. The formulae are of the form:

$$W_c = C_n \gamma B^2 \tag{2.6}$$

where

W_c = vertical load on top of conduit, plf

γ = unit weight of fill, pcf

B = width of trench or conduit, ft, depending upon class of installation

C_n = load coefficient.

The load coefficient, C_n, may be graphically determined from

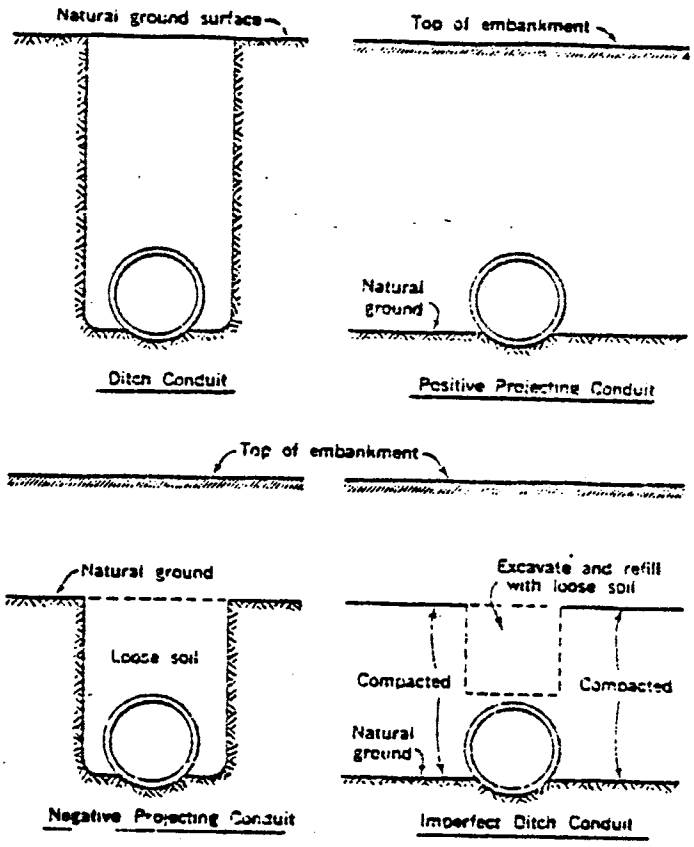

CLASSES OF CONDUIT INSTALLATION CONSIDERED BY MARSTON-SPANGLER THEORY

FIGURE 2.2

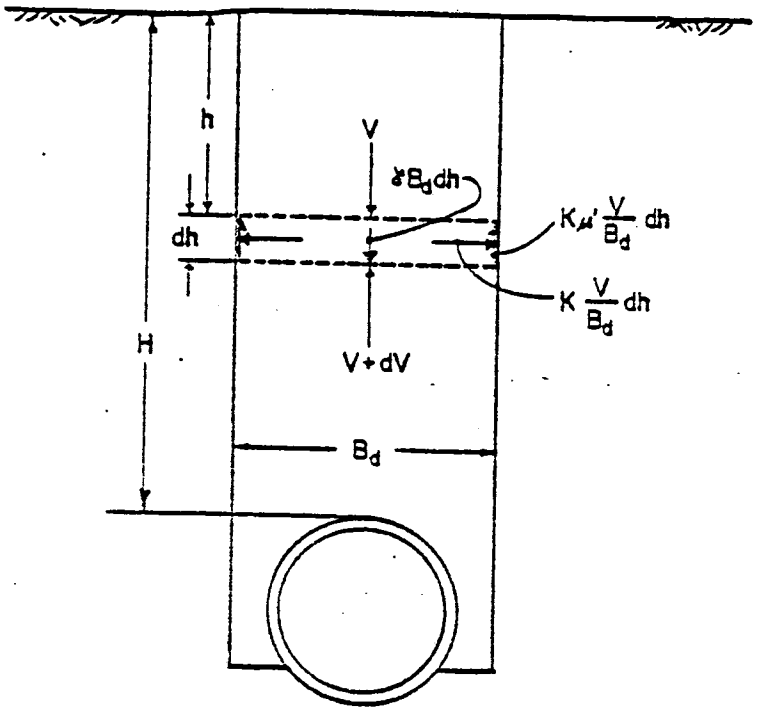

γ = unit weight of fill material, pcf

V = vertical pressure on any horizontal plane, plf

B_d = width of ditch at top of conduit, ft

H = height of fill above top of conduit, ft

h = distance from natural ground surface to horizontal plane, ft

μ' = tan $\emptyset'$ = coefficient of friction between fill material and sides of ditch

K = ratio of active lateral pressure to vertical pressure

FREE-BODY DIAGRAM ASSUMED IN MARSTON-SPANGLER THEORY

FIGURE 2.3

charts such as those shown in Figures 2.4 and 2.5. This coefficient is dependent on such factors as the projection ratio, p, and the settlement ratio, r_{sd}. The projection ratio, p, may have any value, depending on the depth of the trench. Formally, p is the ratio of the trench depth to conduit width. Values of the projection ratio are usually taken as 0.5 or 1.0.

The settlement ratio, r_{sd}, depends on the settlement of the conduit into the foundation, deflection of the conduit, compression of the earth fill and compression of the loose fill material. Values are normally taken from 0 to -1.0, with -0.5 being considered a reasonable design value for most conditions. A representation of the settlement and projection ratios is given in Figure 2.6.

In an attempt to further clarify the interaction of the soil characteristics and the deflection of the structure, Nielson (16) presented a theory for determining loads on buried conduits by an arching analysis. Nielson's theory used an adaptation of the Marston-Spangler theory in order to explain the pressure redistribution across the top of a surface. A representation of the assumed interaction conditions of this theory is given in Figure 2.7.

The term "arching" is used extensively in current analyses of loads on underground structures. In an attempt to clarify this concept, Selig (22) presented the definition of arching as the transfer of load to or away from buried structures as a result of the difference in stiffness properties of the structure with its adjacent encompassing material and the surrounding soil mass. The stress distribution around the structure is different from what would exist

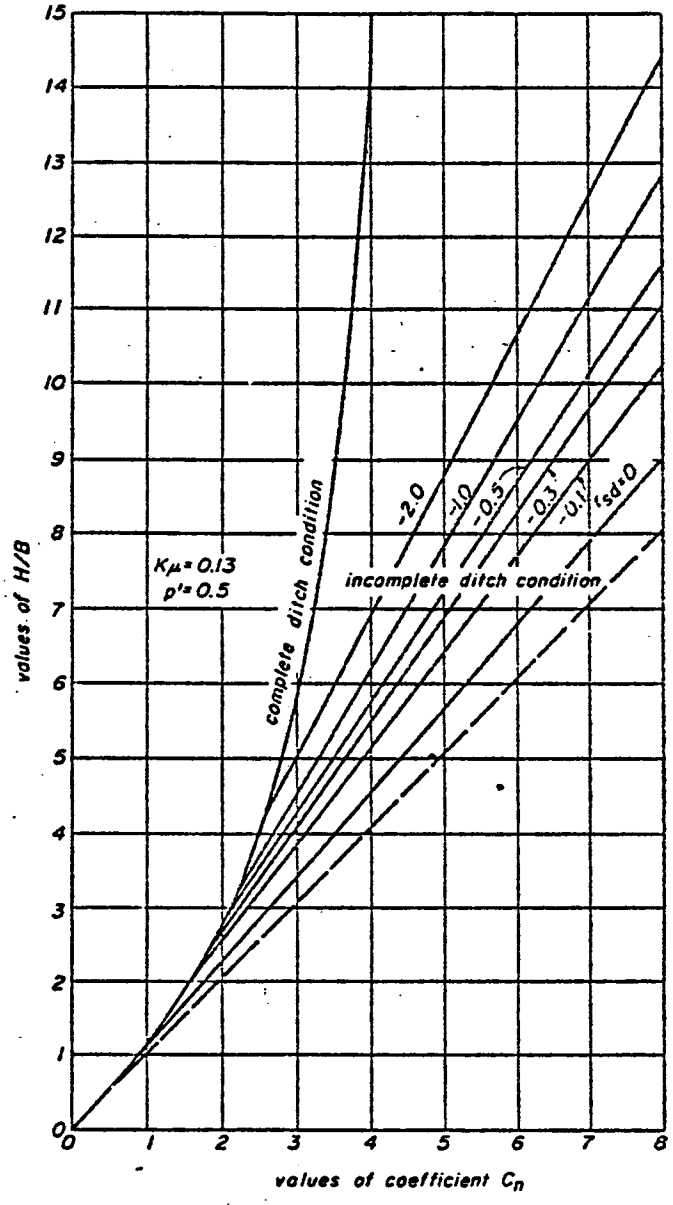

LOAD COEFFICIENT, C_n, FOR IMPERFECT-TRENCH CONDUITS, PROJECTION RATIO p' = 0.5.

FIGURE 2.4

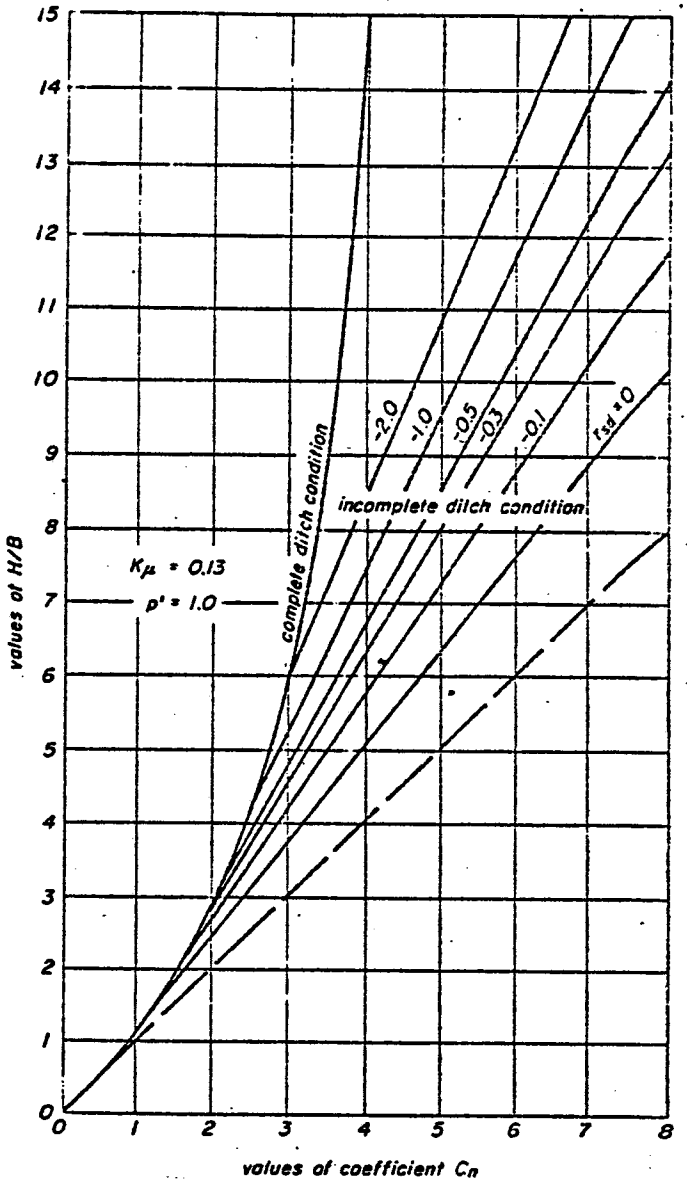

LOAD COEFFICIENT, C_n, FOR IMPERFECT-TRENCH CONDUITS, PROJECTION RATIO p' = 1.0.

FIGURE 2.5

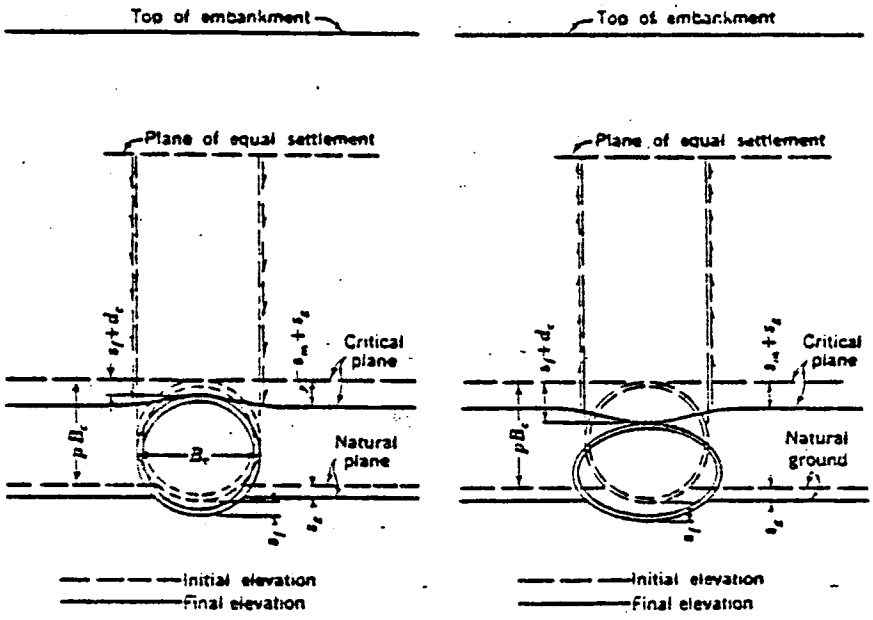

POSITIVE SETTLEMENT RATIO

NEGATIVE SETTLEMENT RATIO

$$\text{SETTLEMENT RATIO, } r_{sd} = \frac{(S_m + S_g) - (S_f + d_c)}{S_m}$$

where, S_m = compression strain of side columns of soil of height pB_c

S_g = settlement of natural ground surface adjacent to conduit

S_f = settlement of conduit into its foundation

d_c = shortening of vertical height of conduit

B_c = outside diameter or width of conduit, ft

p = projection ratio

SETTLEMENT & PROJECTION RATIOS
ACCORDING TO MARSTON-SPANGLER THEORY

FIGURE 2.6

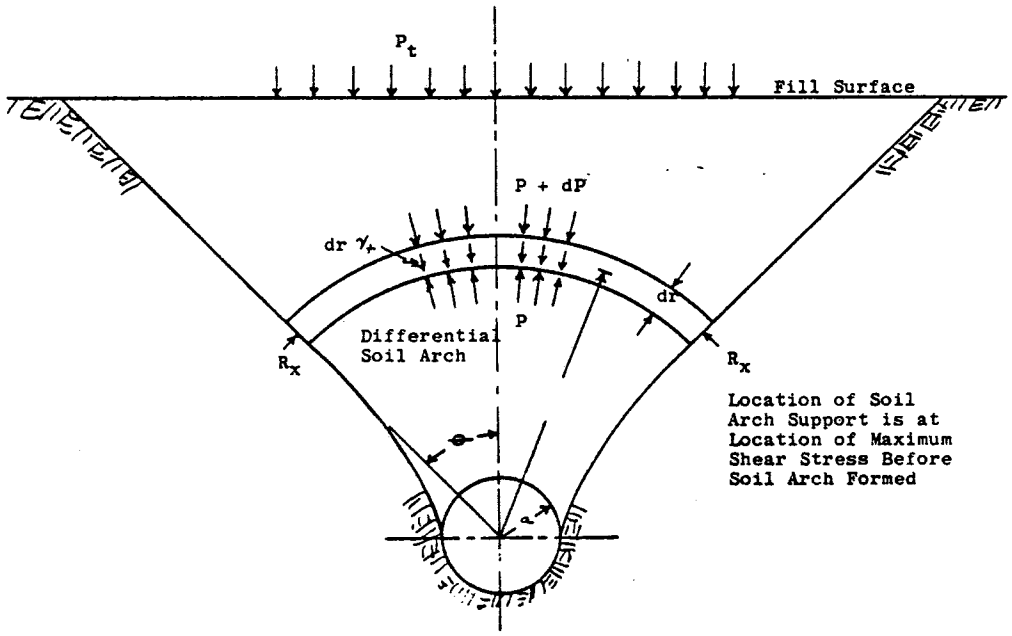

FREE-BODY DIAGRAM FOR DETERMINING LOADS ON
BURIED CONDUITS BY AN ARCHING ANALYSIS

FIGURE 2.7

in the same region of soil, if the structure was not present. By this analysis, if the structure is not as stiff as the soil it replaces, the arching is positive. Conversely, if the structure is stiffer than the soil, then the arching produces a negative effect. Also, if the structure is surrounded by a zone of material that differs from the free field soil, the same concept applies as long as the structural unit is taken to be the structure together with the zone of material. For example, a rigid concrete culvert encompassed in a layer of polyurethane foam or loose soil may have positive arching rather than negative because the composite system is not as stiff as the free field soil. Much consideration has been given to this type of construction installation, termed imperfect-trench installation. The imperfect-trench condition is shown in Figure 2.8.

In an attempt to verify the arching analysis, Watkins (23) conducted a study in which he placed lead shot in a grid pattern in the soil mass around the conduit and measured movement of the lead particles by taking a series of x-ray pictures during the loading sequence. By finding the displacements of the shot without pipe influence (free field condition) and subtracting these from the displacements obtained with the pipe in place, the particle movement due to the conduit influence is obtained. This is shown in Figure 2.9. The arrows indicate the direction of the major principal stresses in the soil mass.

In order to determine the effect of the cell walls on the displacement results, Watkins (23) applied the theory of elasticity, using an infinite elastic plate with a stiffening ring as a model.

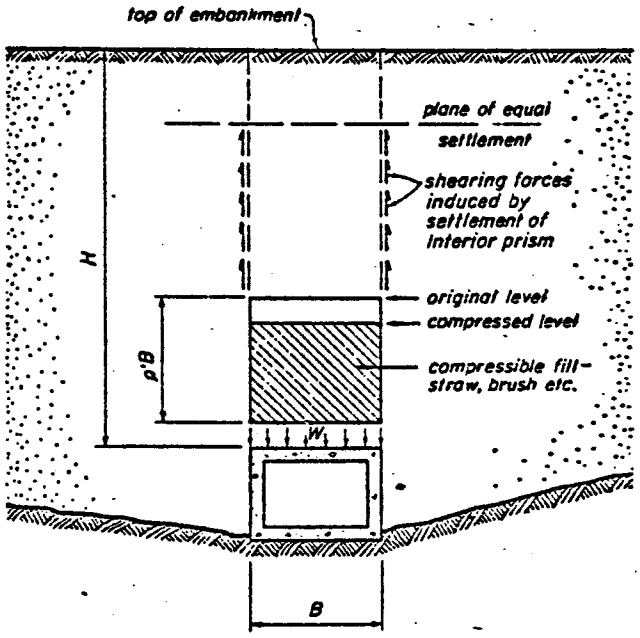

IMPERFECT TRENCH INSTALLATION

FIGURE 2.8

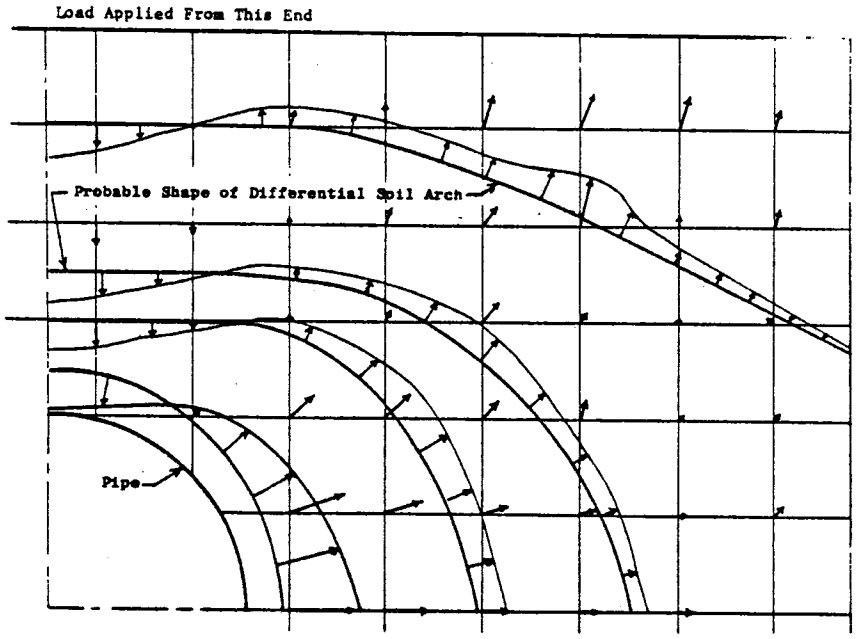

MOVEMENT OF LEAD SHOT DUE ONLY TO INFLUENCE
OF PIPE AS DETERMINED FROM X-RAY STUDY

FIGURE 2.9

Once again, the displacements were determined with and without the ring in order to determine the effect of the ring alone. The results of the theory of elasticity corresponded closely with those obtained using the x-ray analysis, with slight differences occurring directly above the conduit. As a result, Watkins felt justified in assuming the differential arch in the soil mass as a circle, without adding appreciable error to the solution.

The results of another study by Watkins and Nielson (24) are shown in Figure 2.10. This shows only the difference in vertical displacement between the soil mass with the pipe in place and the same soil mass under the same loading conditions without the model pipe or hole. There is one major difference between this study and the x-ray study in that, the pipe in this study was bored into place. The soil was compacted without the pipe, then a hole was bored slightly larger than the diameter of the pipe, and the pipe was inserted into the hole. As the pipe was loaded it could exert only limited, if any, horizontal pressure because the hole was larger than the pipe. Therefore, the horizontal component of the pressure exerted by the pipe on the soil mass was missing.

Heger (11) presents a method which incorporates a soil-structure interaction factor, F. These analyses were performed on rigid concrete pipes, with the objective of improving the correlation between predicted and actual test strengths of these structures.

By this analysis, the total vertical earth load is given by

$$We = F_e \, w \, B_c \, H \tag{2.8}$$

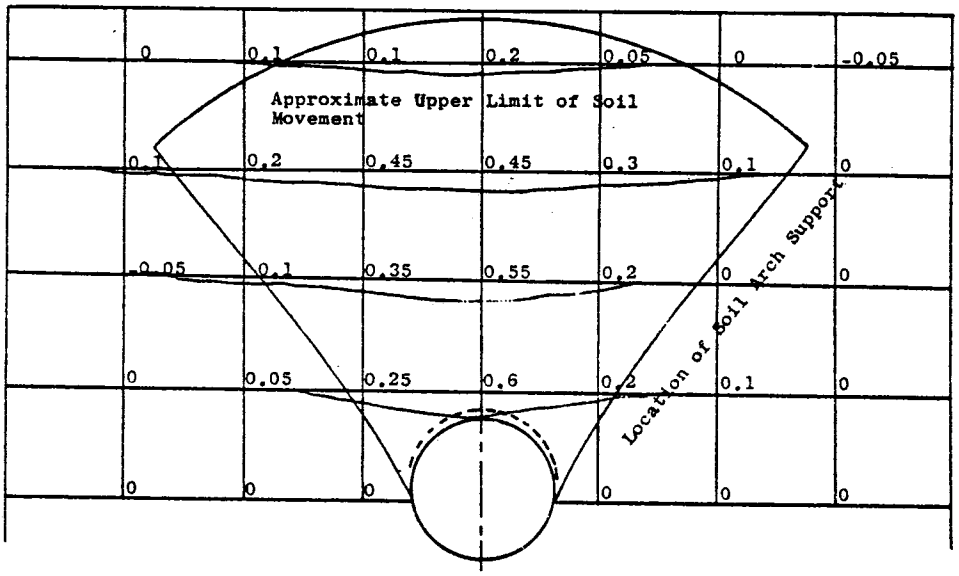

VERTICAL SOIL DEFORMATION AT VARIOUS ELEVATIONS ABOVE A MODEL CONDUIT

FIGURE 2.10

where

B_c = the outside horizontal projection of the pipe,

H = height of cover over the crown of the pipe, and

F_e = soil-structure interaction factor.

For the determination of F_e, Heger presents the equation

$$F_e = [1 + 0.2\ H/B_c] \tag{2.9}$$

The maximum specified value of F_e is taken as 1.5 for uncompacted fills and 1.2 for compacted fills.

In addition to the earth load, a buried pipe is subject to its own weight, W_p. Also, live loads applied on the surface may increase the earth pressure on the pipe. These effects may be approximately taken into account by distributing the live load through the earth cover over the pipe. In this approach, the equivalent surface live load at the crown of the pipe per foot of pipe length, W_L, is treated as additional total earth load to obtain a total equivalent external pressure load, W_T, for use in designing the pipe:

$$W_T = W_e + W_L \tag{2.10}$$

Heger presents assumptions for earth pressure distribution in Figures 2.11 and 2.12. The assumed distribution for the traditionally defined Class C bedding is shown in Figure 2.11. Two possible assumptions are presented. Earth pressure distribution as given by Olander (17) is shown in Figure 2.11a, while uniformly distributed pressures are shown in Figure 2.11b. Earth pressure assumptions for Class B bedding are shown in Figure 2.12.

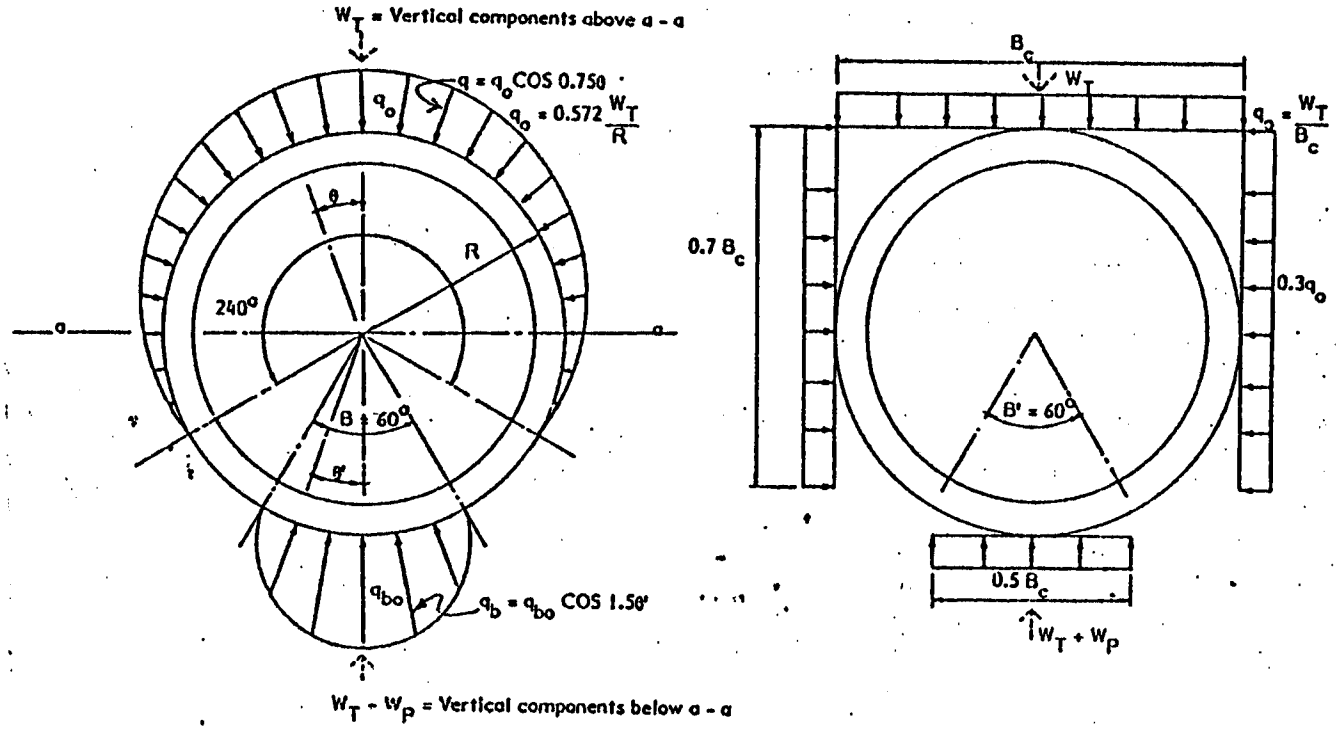

EARTH PRESSURE ASSUMPTIONS FOR EMBANKMENT CLASS C BEDDING

FIGURE 2.11

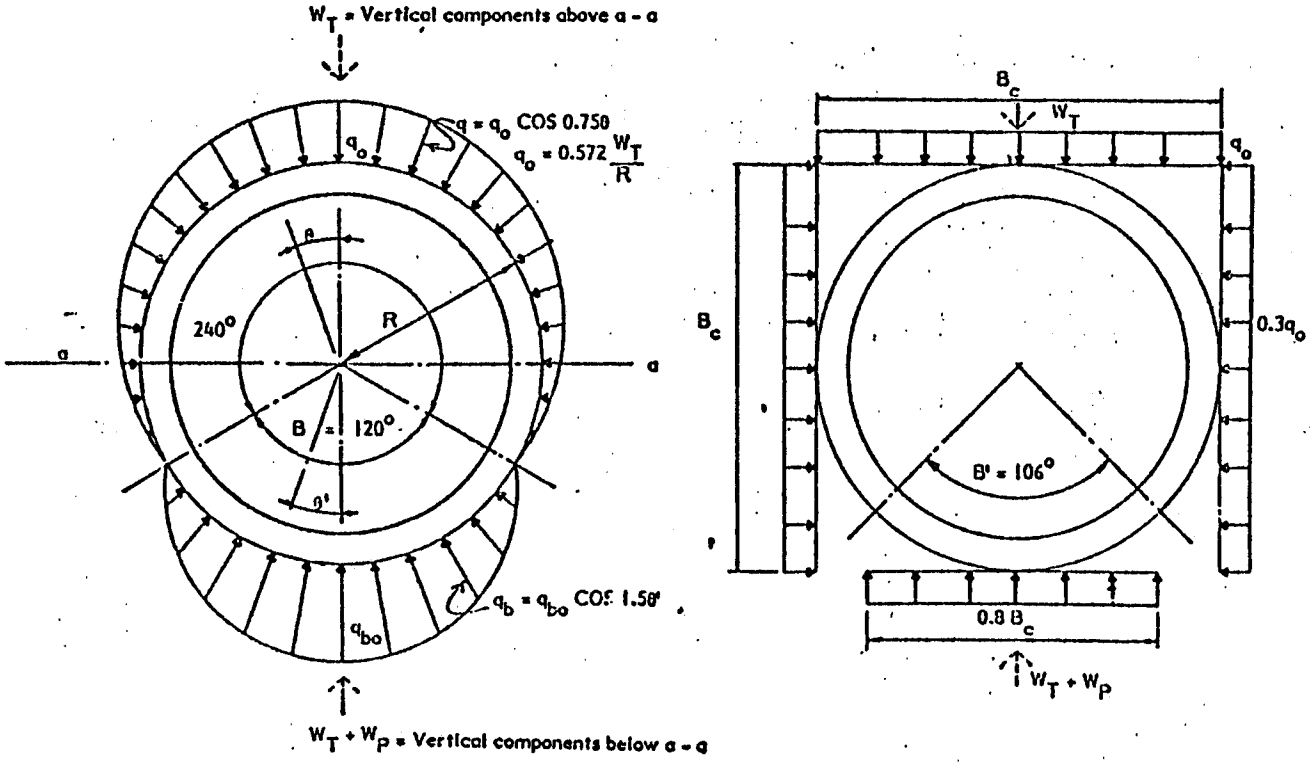

EARTH PRESSURE ASSUMPTIONS FOR EMBANKMENT CLASS B BEDDING

FIGURE 2.12

2.3 Numerical Studies

Numerical studies of the influence of soil-structure interaction on earth pressure distribution on buried structures have been the result of the availability of high-powered modern computers. A number of computer programs have evolved for this type of study, primarily involving the finite element method.

2.3.1 Culvert Analysis and Design Program (CANDE)

One of the most popular programs available is CANDE, developed by Katona (13). CANDE is a plane strain finite element program used for the analysis of buried structures. Katona first used out-of-ground box tests to verify the CANDE model, then used CANDE to evaluate current standards on box culvert design. The out-of-ground box test set-up is shown in Figure 2.13. Katona used four-edge bearing on standard box sections, loaded to the point where 0.01 inch cracking occurs, as well as to ultimate shear or flexural failure.

The CANDE model of the box culvert in four-edge bearing is shown in Figure 2.14. The correlation between the predicted loads and the actual test loads for 0.01 inch cracking to occur is shown in Figure 2.15. Three standard box sizes were analyzed. Although there is some scatter in the data the correlation is good. A comparison of the predicted and actual ultimate loads for shear and flexural failure is shown in Figure 2.16. The correlation of these results is very close for the three box sections tested.

Katona also compared data from previously conducted in-ground box culvert tests with his computer predictions. The culvert-soil system

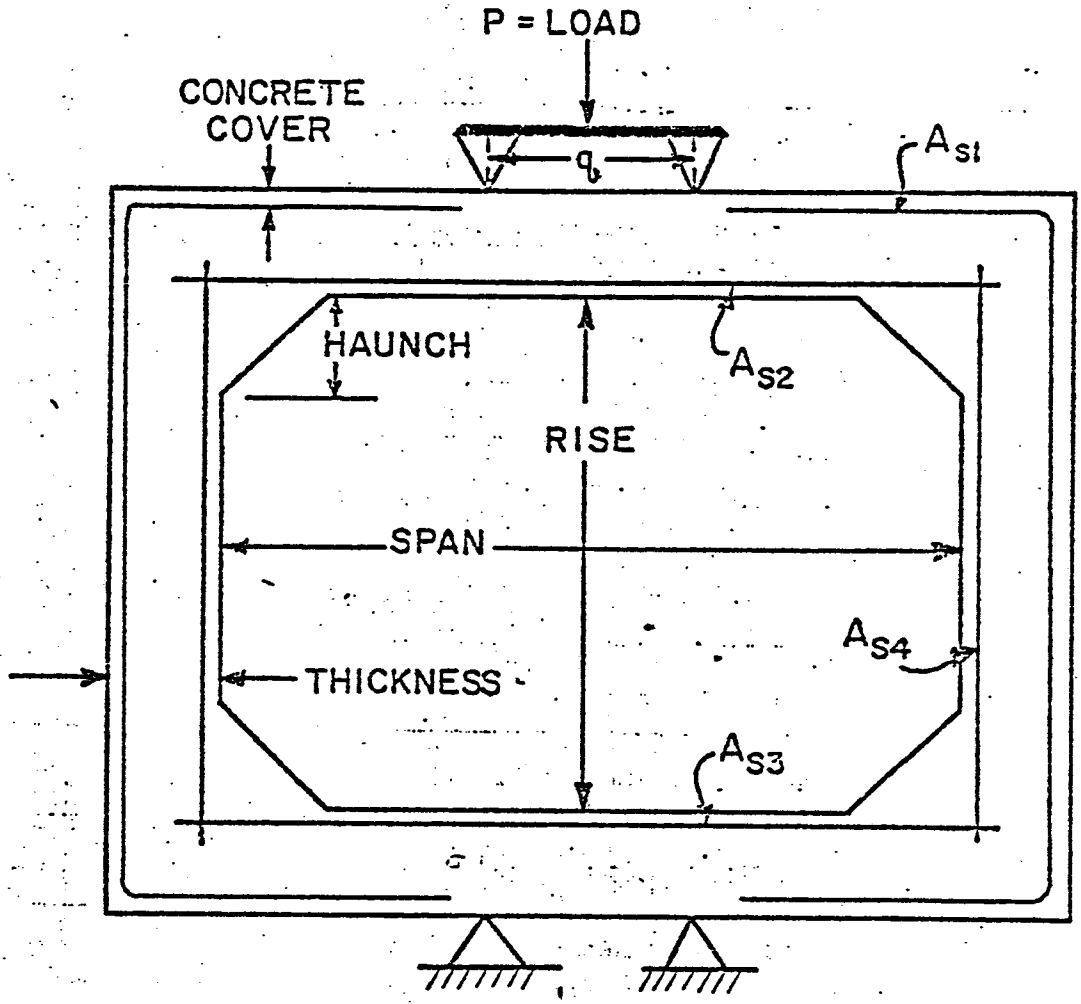

BOX CULVERT IN FOUR-EDGE BEARING

FIGURE 2.13

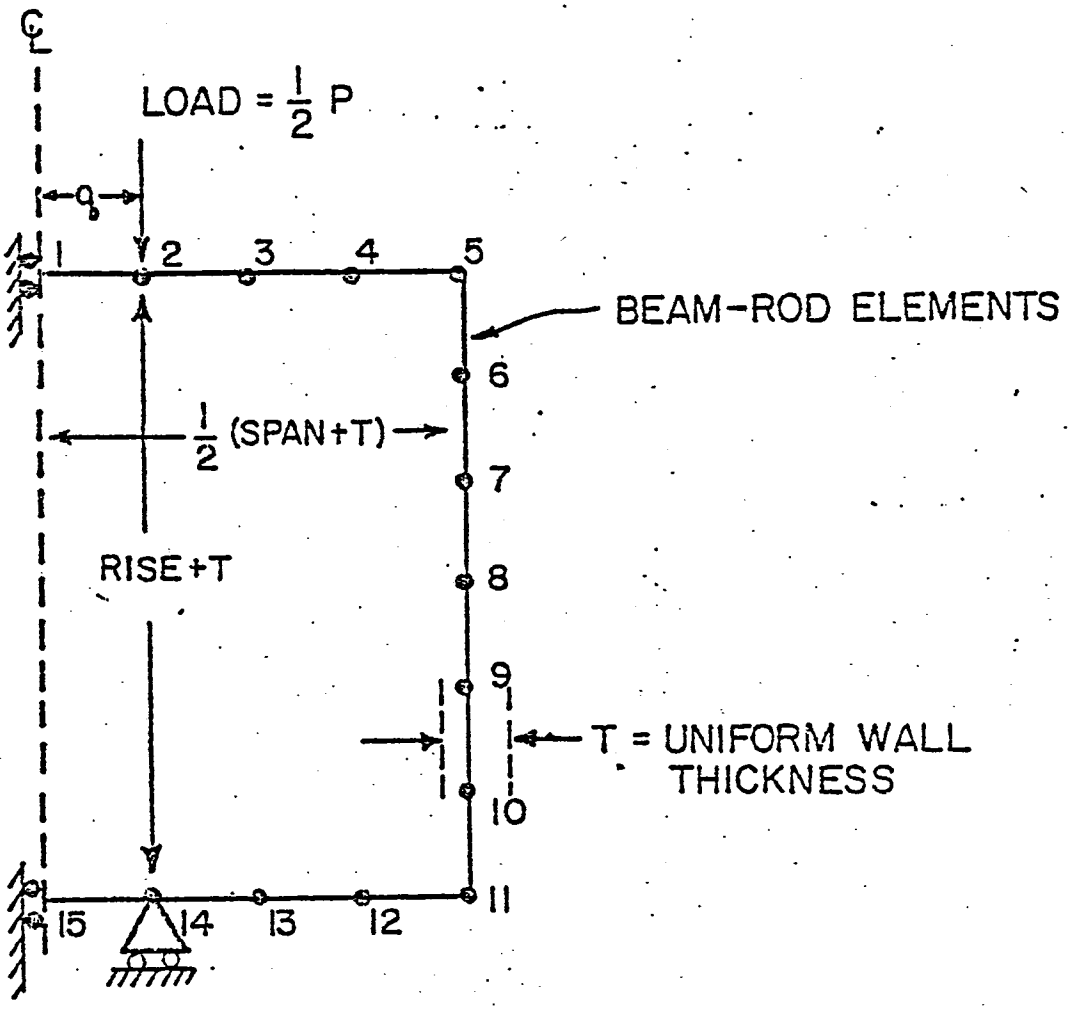

CANDE MODEL OF BOX CULVERT
IN FOUR-EDGE BEARING.

FIGURE 2.14

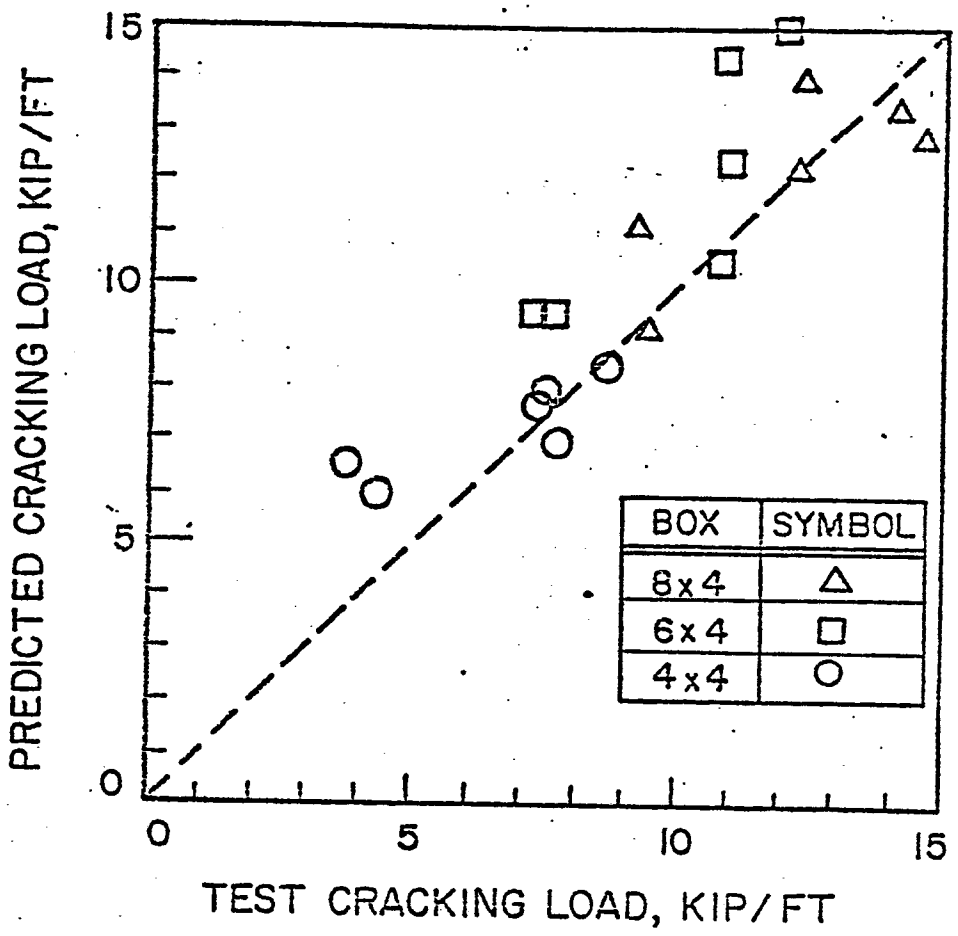

PREDICTION vs. TEST FOR LOAD AT 0.01 INCH CRACKING

FIGURE 2.15

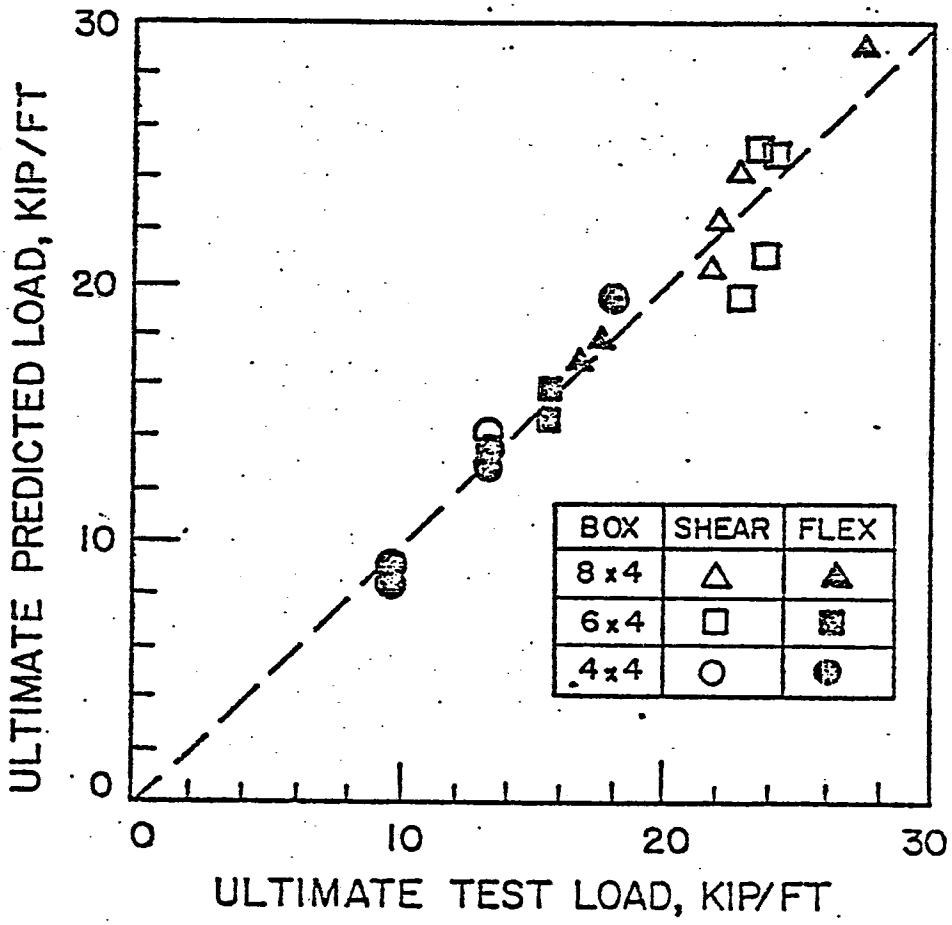

PREDICTIONS vs. TESTS FOR ULTIMATE LOAD

FIGURE 2.16

used for this analysis is shown in Figure 2.17. CANDE was used to predict the earth pressures shown by the eight pressure gages located around the perimeter of the culvert. A summary of his test results is shown in Figure 2.18. The pressures predicted by CANDE and measured by the pressure gages along the top and bottom slabs are not uniformly distributed and this is contrary to what is assumed by most procedures. Also, the correlation of data along the right wall is much closer than the correlation along the left wall of the culvert.

Huang, Gill, and Gnaedinger (12) also used the CANDE program for their analyses. They modeled various combinations of properties in order to evaluate the predicted deflections and earth pressures. The soil-structure system used for this analysis is shown in Figure 2.19. The primary objective of this study was to determine the effects of different soil and structural properties on predicted earth pressures. Using these results a set of earth pressure charts were established to aid in the design of box culverts.

The deflections, as predicted by CANDE for 22 feet of soil cover are shown in Figure 2.20. The inward deflections of both the top and bottom slabs induce an outward deflection of the sides of the culvert. For the same loading conditions, the calculated earth pressures are shown in Figure 2.21. The pressures increase from the center of the culvert to the outside on the top and bottom slabs. The lateral earth pressure increases with depth, although not linearly as expected.

Furthermore, various foundation and backfill soil properties were used to evaluate their effects on calculated earth pressures. Five different variations of bedding and foundation soil properties were

REINFORCEMENT AND CONCRETE PROPERTIES	f_c' psi	fy ksi	STEEL AREAS IN^2/IN A_{s1}	A_{s2}	A_{s3}	A_{s4}
	4500	60	0.037	0.050	0.050	0.017

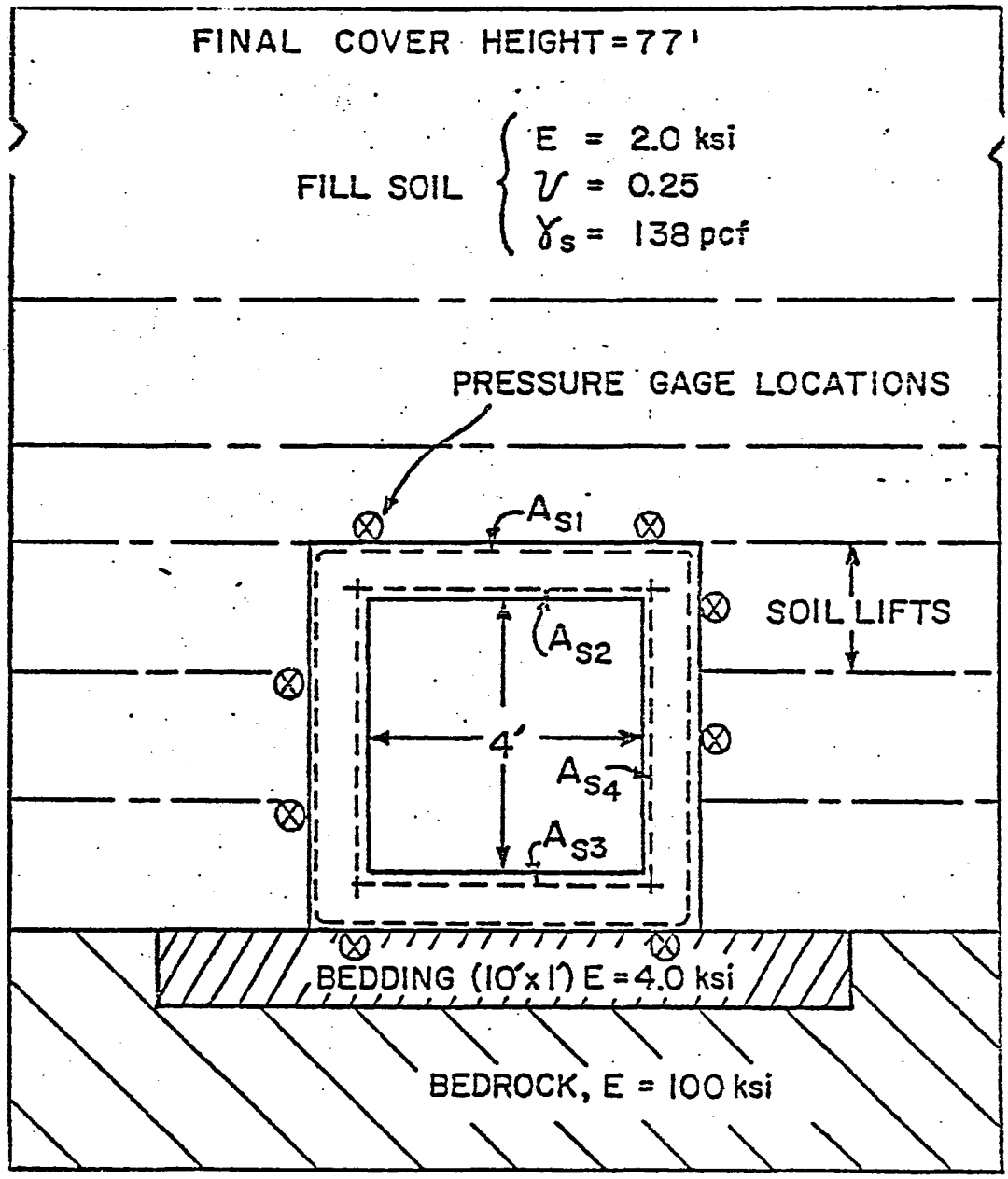

SCHEMATIC VIEW OF BOX-SOIL SYSTEM

FIGURE 2.17

FILL HEIGHT (FT)	LEGEND	
	CANDE	TESTS
21.6	------	o
77.0	———	●

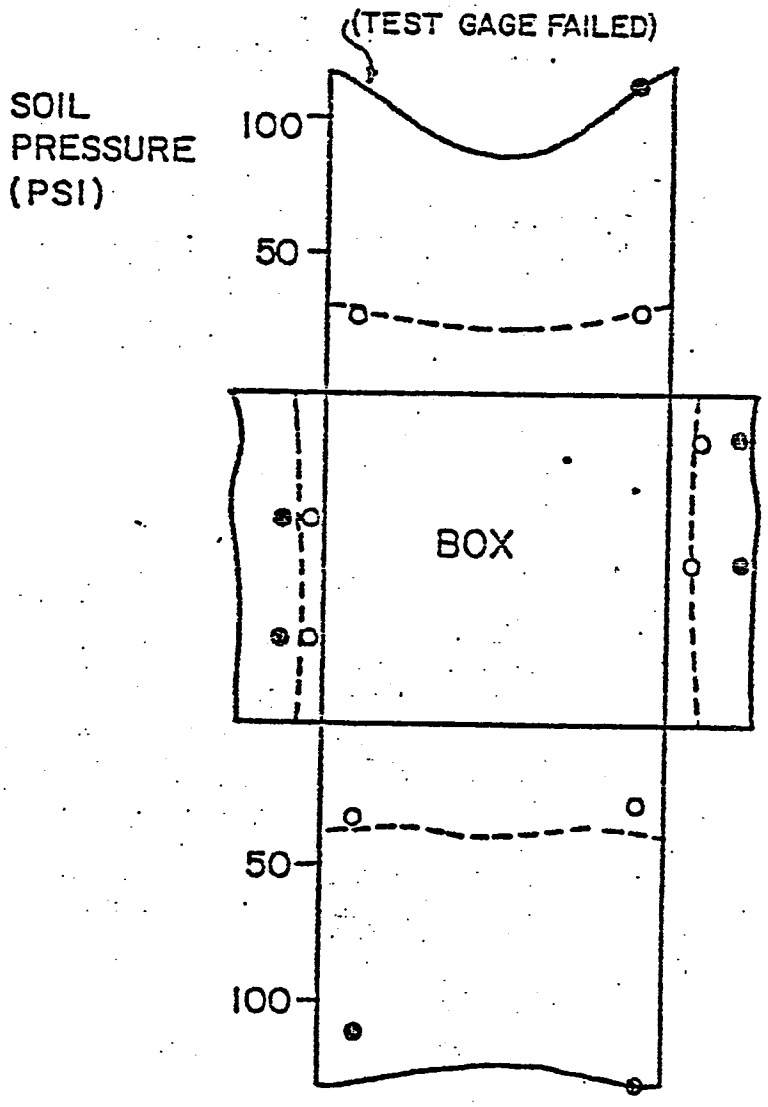

PREDICTION vs. TEST DATA FOR
SOIL PRESSURE AROUND BOX CULVERT.

FIGURE 2.18

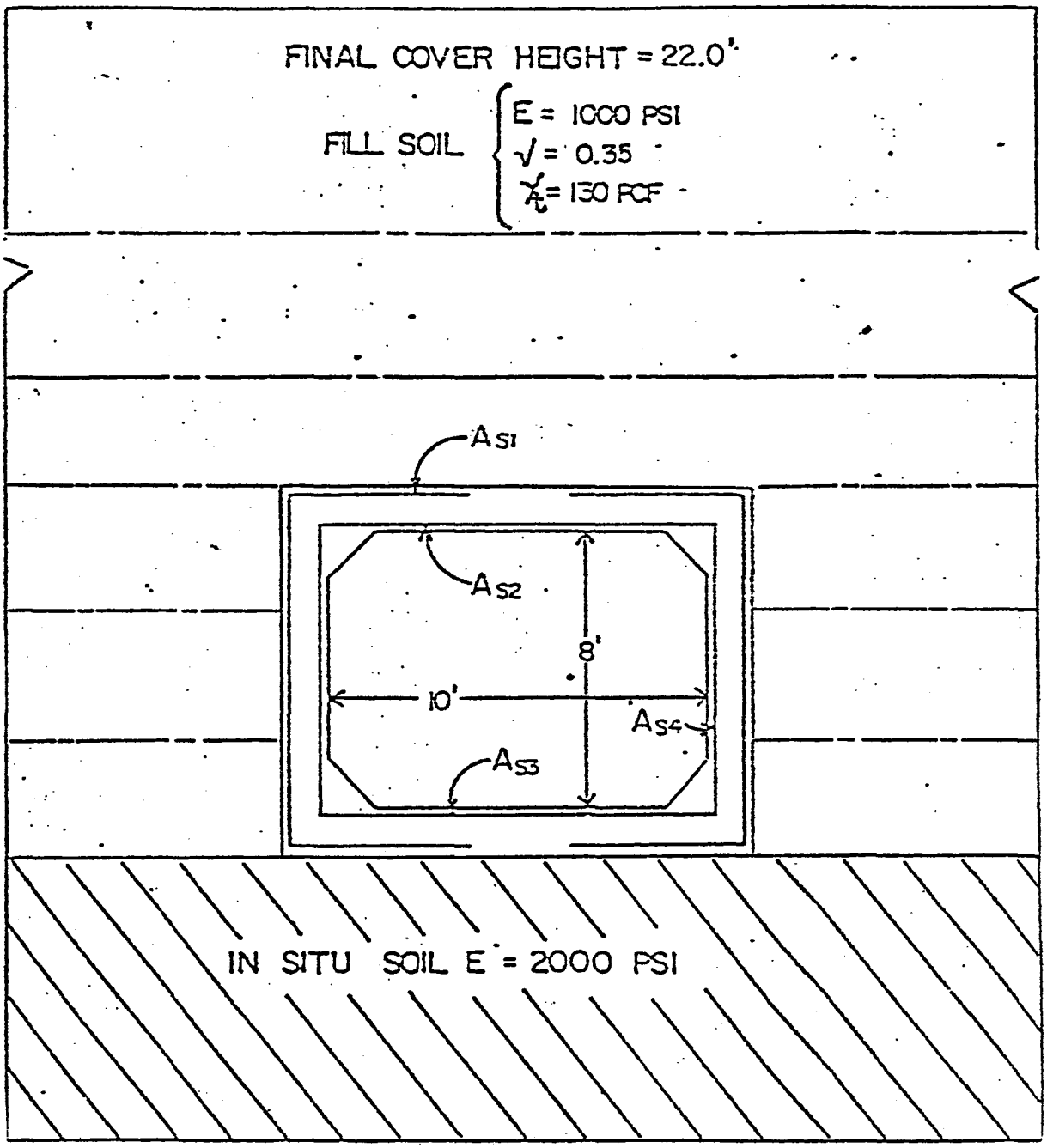

SCHEMATIC VIEW OF SOIL-CULVERT SYSTEM

FIGURE 2.19

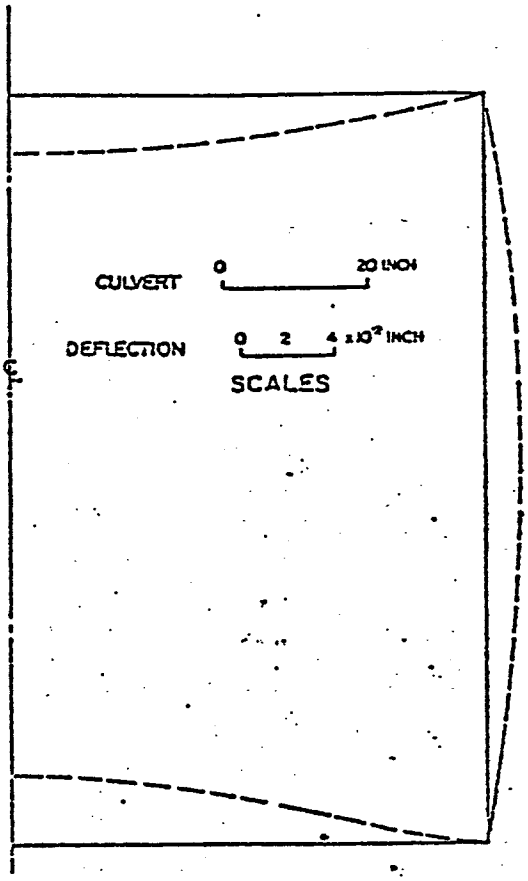

SCHEMATIC VIEW OF CULVERT RELATIVE DEFLECTIONS
UNDER 22 FT OF SOIL COVER

FIGURE 2.20

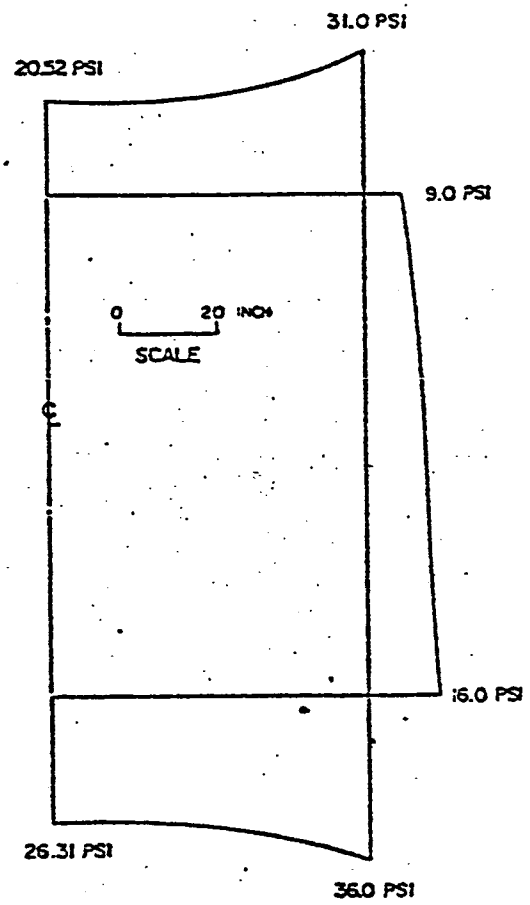

CALCULATED EARTH PRESSURES
ON 8x10-13 BOX CULVERT

FIGURE 2.21

analyzed. The results are shown in Figure 2.22. The earth pressures on the top and the side of the culvert seem to be independent of foundation soil properties. However, the calculated pressures on the bottom slab vary greatly with different foundation soil properties.

Three different variations of backfill soil were analyzed. The calculated earth pressures are shown in Figure 2.23. The results of all three were very similar, with the sides of the culvert showing the greatest difference in fill pressure.

Huang, Gill, and Gnaedinger (12) also studied the effects of culvert geometry on calculated earth pressures. The CANDE input for this analysis is shown in Figure 2.24. A total of six box culvert sizes were used, with the properties of the foundation and fill soils held constant. The calculated vertical earth pressures were converted to dimensionless ratios and plotted against depth-span ratios and culvert height-span ratios. This conversion was accomplished by

$$\frac{W}{W_s} = \frac{\text{Calculated Total Earth Load}}{\text{Weight of Soil above the Culvert}} \tag{2.11}$$

and

$$\frac{P}{\sigma_s} = \frac{\text{Calculated Vertical Earth Pressure}}{\text{Overburden Earth Pressure}} \tag{2.12}$$

The variation of earth load ratio (Equation 2.11) with depth-span ratio is given in Figure 2.25. The culvert height-span ratio (H/S) greatly influences the results shown. An increase in the H/S ratio increases the corresponding earth load ratio. The variation of earth pressure ratio (Equation 2.12) with depth-span ratio is shown in Figure 2.26. The earth pressure ratio also increases with increasing H/S ratio. A comparison of the variation of the earth load ratio and

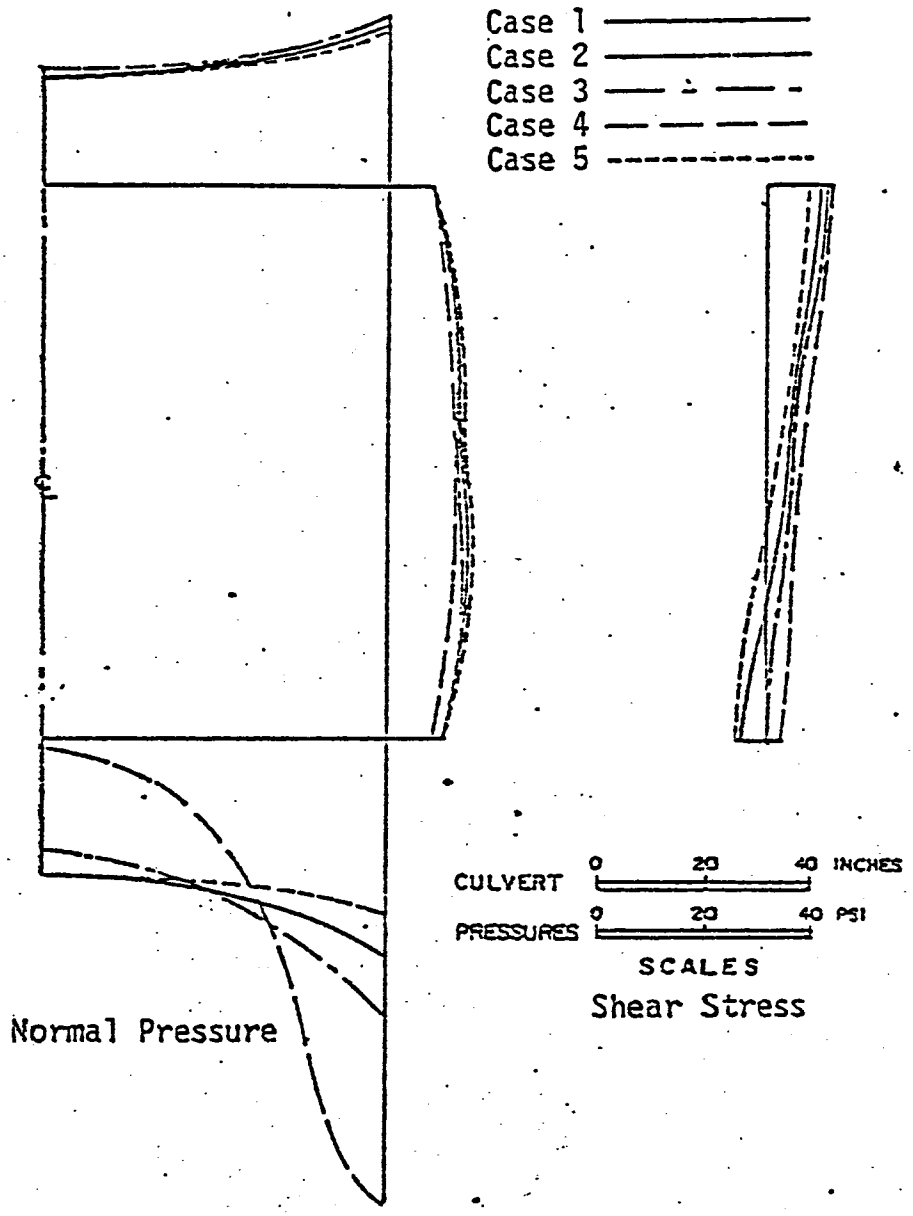

CALCULATED EARTH PRESSURE FOR DIFFERENT BEDDING AND FOUNDATION SOIL PROPERTIES.

FIGURE 2.22

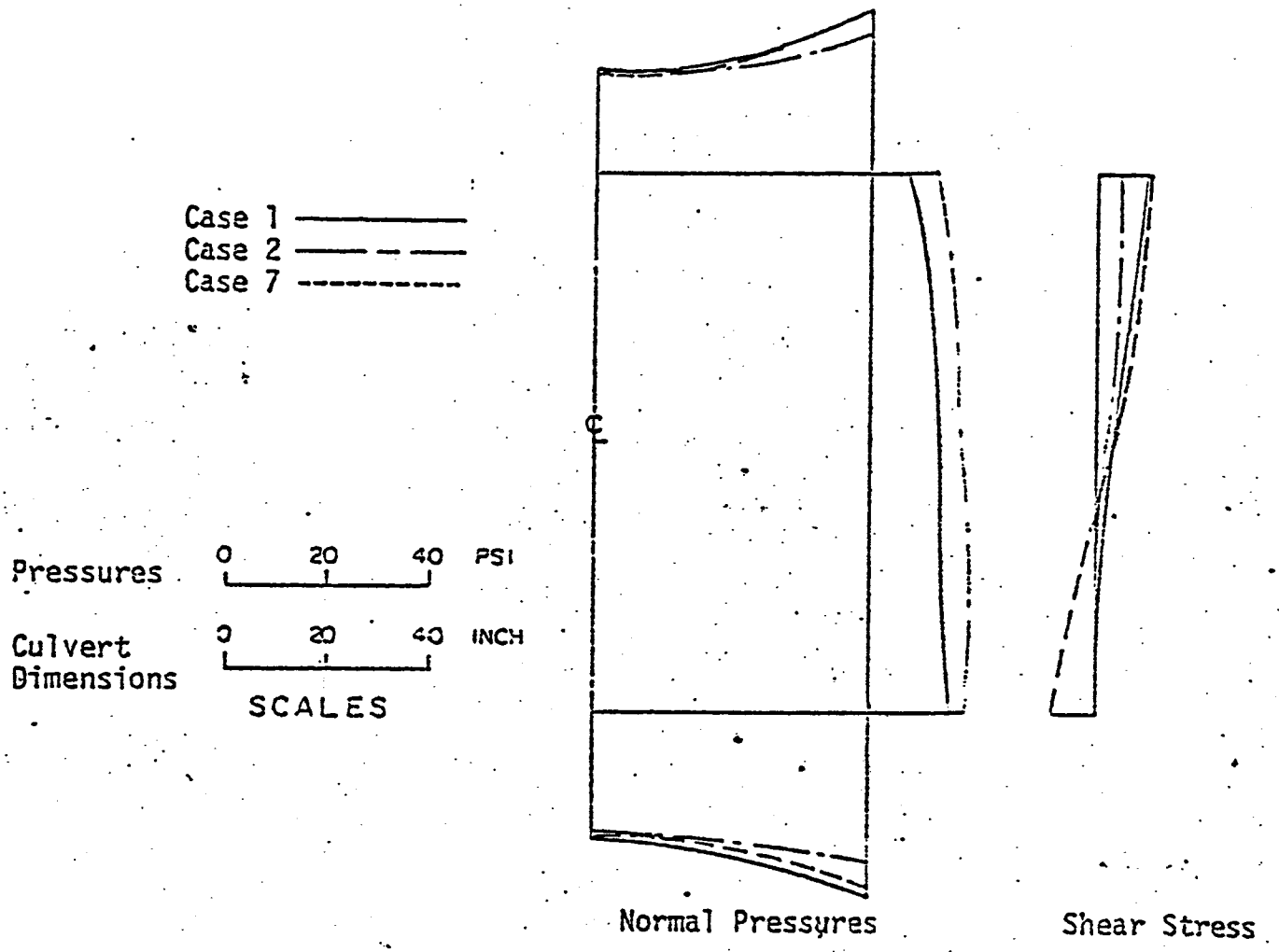

CALCULATED EARTH PRESSURES FOR DIFFERENT SOIL PROPERTIES

FIGURE 2.23

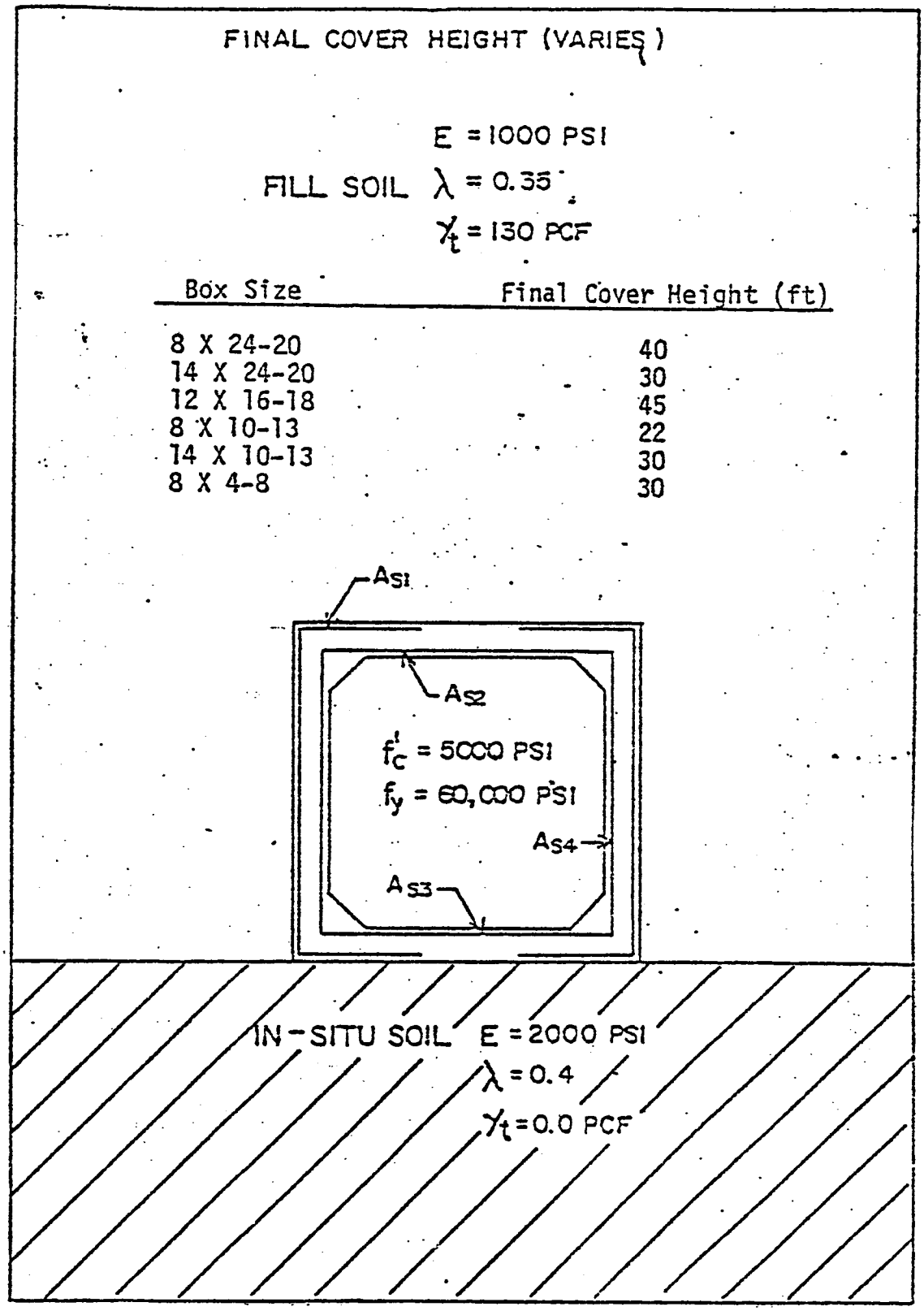

CANDE INPUT DATA FOR DIFFERENT
BOX SIZES AND SOIL COVER

FIGURE 2.24

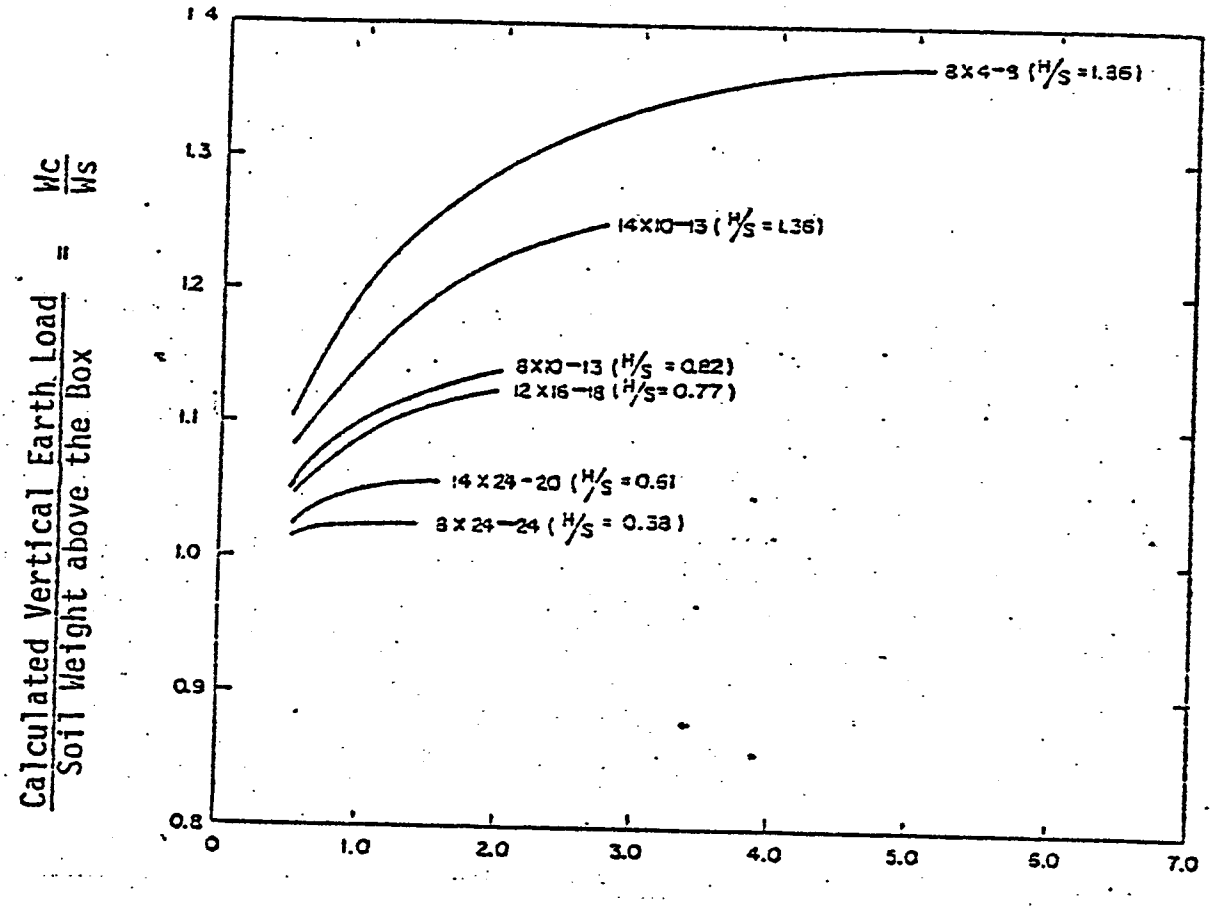

CALCULATED EARTH LOAD RATIO
VS.
SOIL COVER OVER SPAN RATIOS

FIGURE 2.25

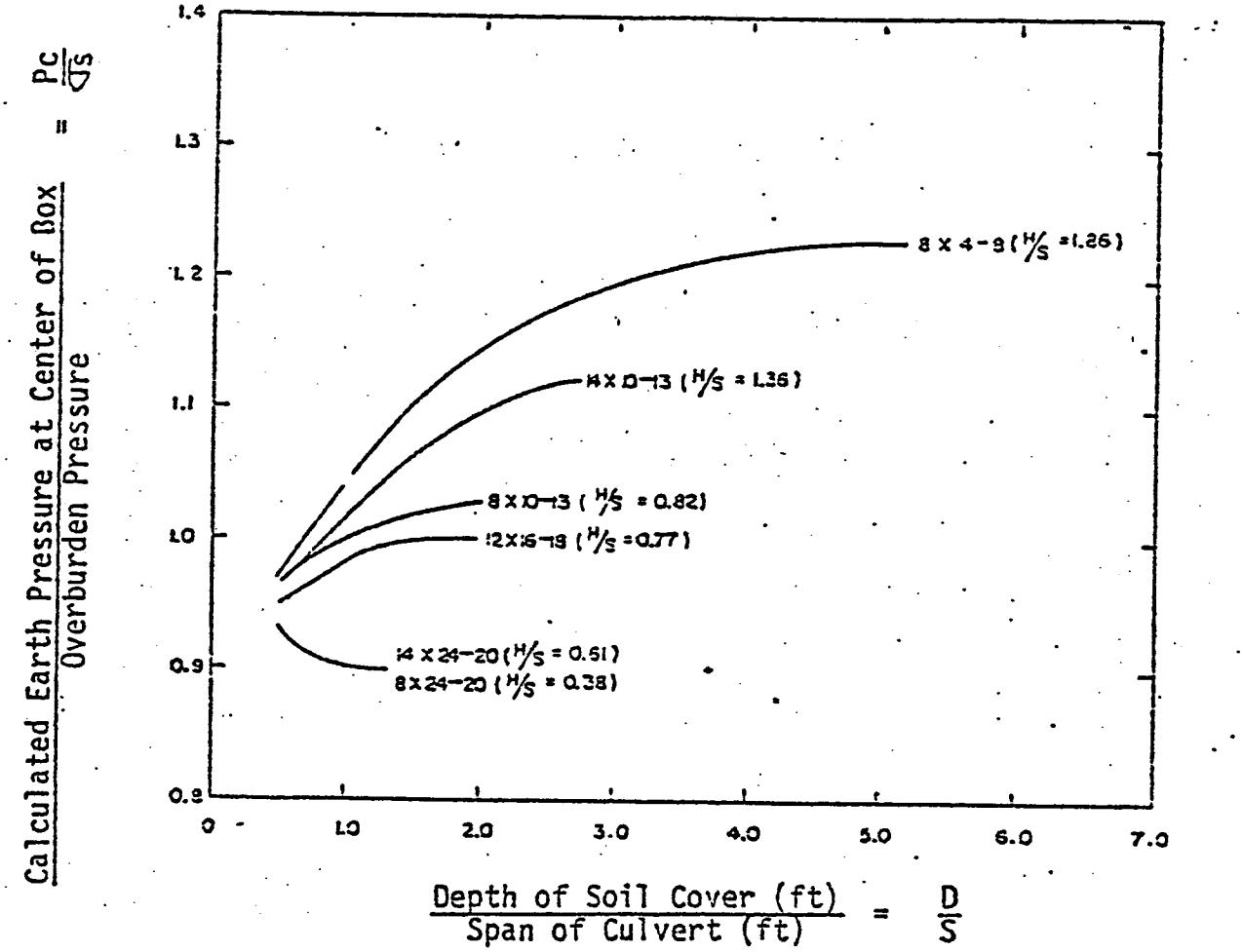

CALCULATED EARTH PRESSURE RATIO
VS.
SOIL COVER OVER SPAN RATIO

FIGURE 2.26

earth pressure ratio with H/S ratio is given in Figure 2.27. The curves are almost identical in shape, with values of the earth load ratio being greater than those for the earth pressure ratio.

Through their analysis, Huang, Gill and Gnaedinger derived a set of design charts for box culverts of various sizes and depths of fill. The earth load ratio may be determined using Figure 2.28, while the earth pressure ratio may be determined using Figure 2.29. To use these charts, the culvert height, span, and depth of fill must be known.

Finally, for the lateral earth pressures, an earth pressure coefficient, K_a, was derived, which may be calculated by

$$K_a = \frac{\text{Integral of Calculated K Along Wall}}{\text{Culvert height, H}} \qquad (2.13)$$

A design chart is given in Figure 2.30 for the determination of K_a. By knowing the culvert span and the depth of fill-height ratio, the lateral earth pressure coefficient can be easily found. Although Huang et.al. presented extensive results on the behavior of box culverts, in their analyses the nonlinear stress dependent stress-strain behavior of the soil was not modeled. Furthermore, the soil-structure interface was assumed to be fully bonded.

2.3.2 Soil-Structure Interaction Program (SSTIPN)

Another widely used finite element program for the study of buried structures is SSTIPN, developed at the University of California at Berkeley. Studies using SSTIPN to analyze soil- structure interaction effects include the analysis of the Tice Valley

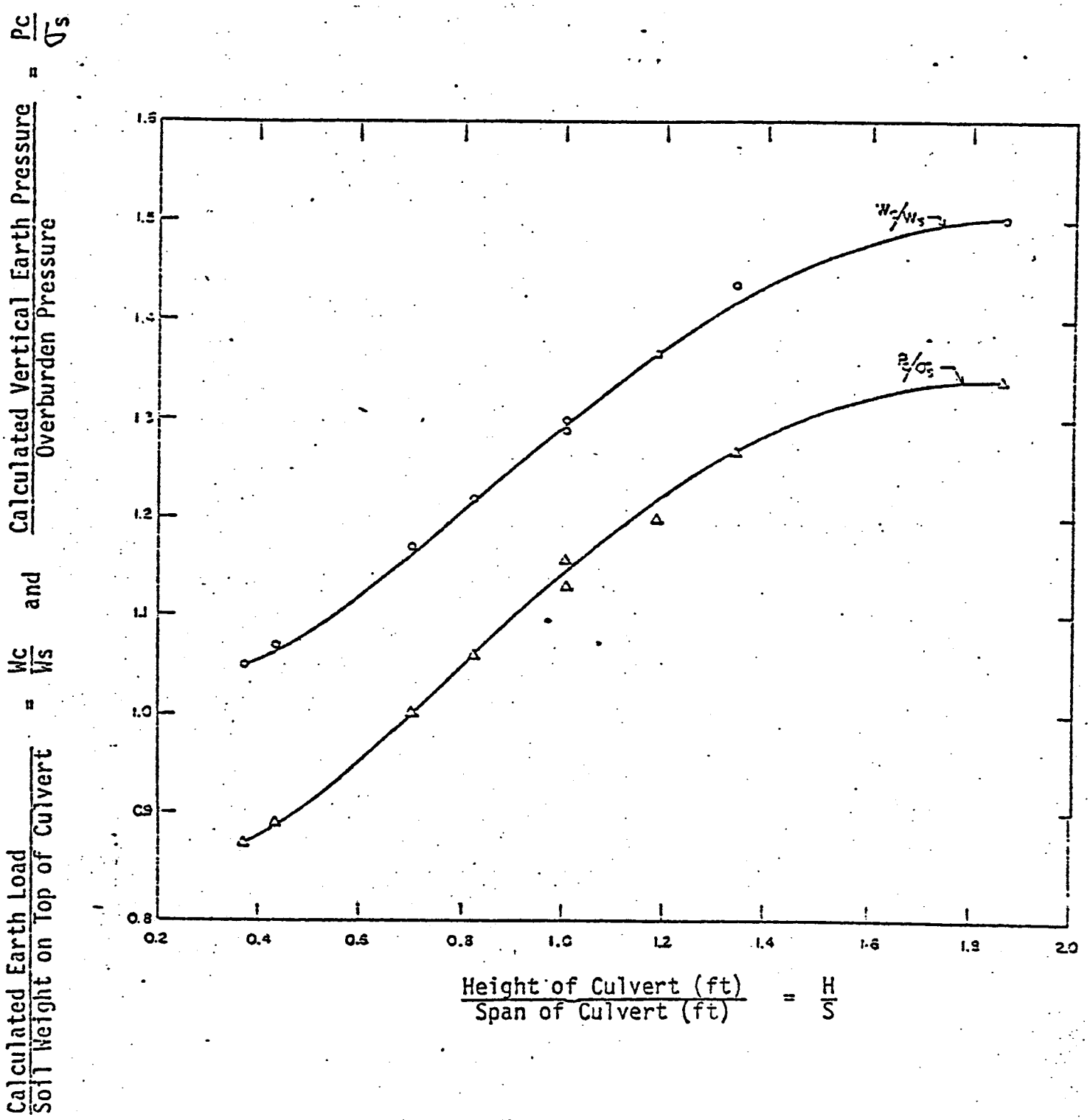

CALCULATED EARTH LOAD AND EARTH PRESSURE RATIOS
VS.

HEIGHT OF CULVERT OVER SPAN RATIO

FIGURE 2.27

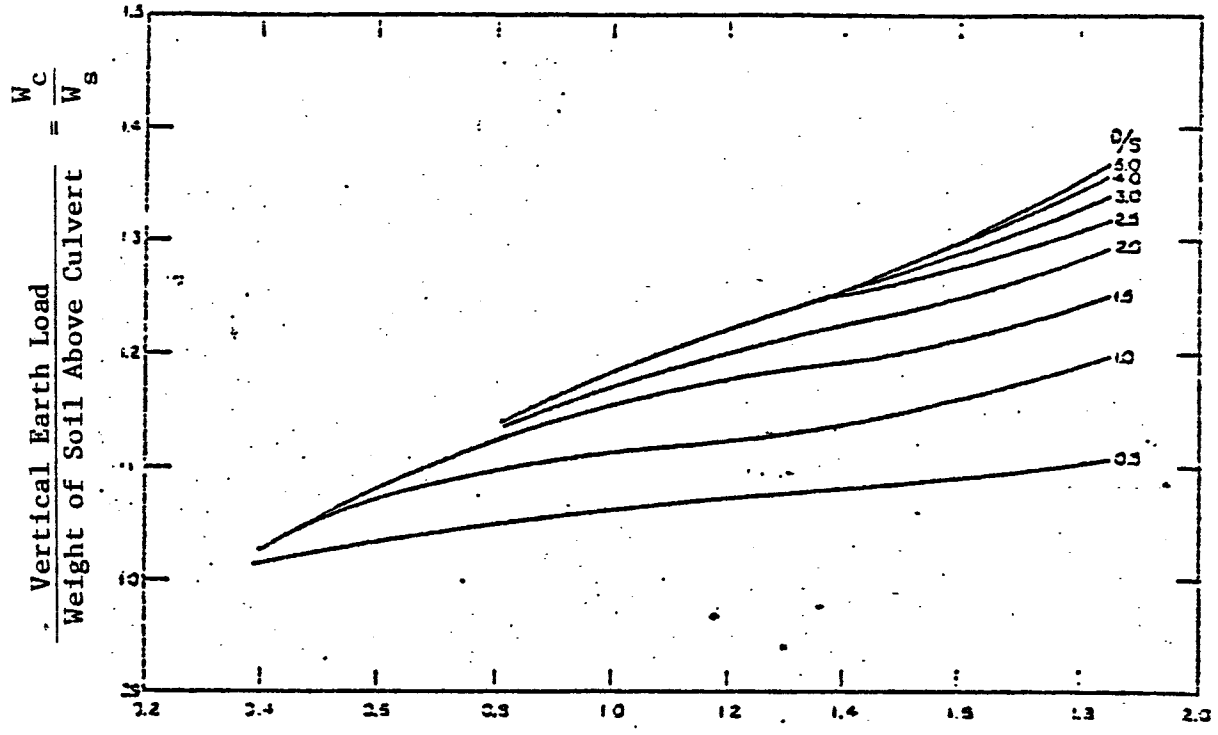

$$\frac{\text{Height of Culvert}}{\text{Span of Culvert}} = \frac{H}{S}$$

VERTICAL EARTH LOAD VS. H/S RATIO

FIGURE 2.28

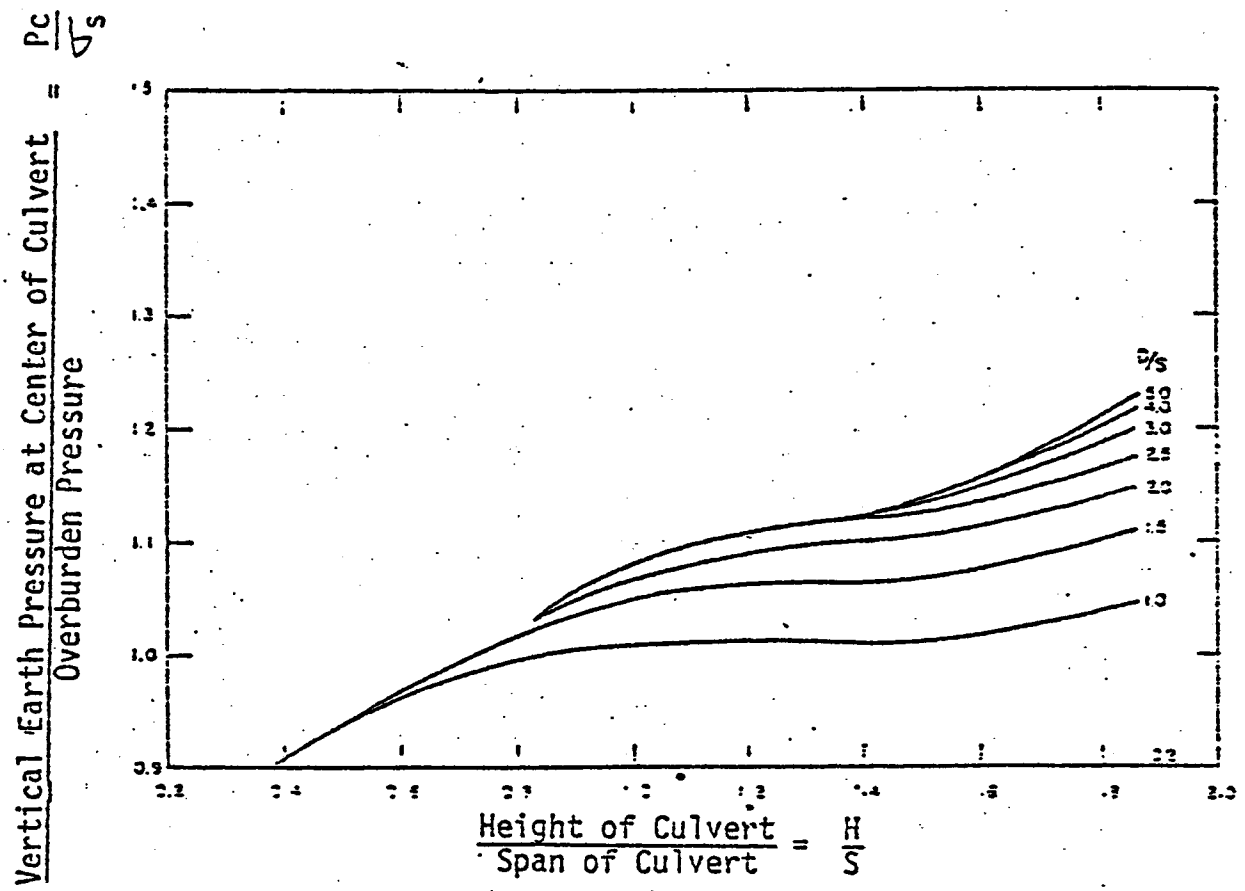

VERTICAL EARTH PRESSURE AT BOX CENTER VS. $^{H}/_{S}$ RATIO

FIGURE 2.29

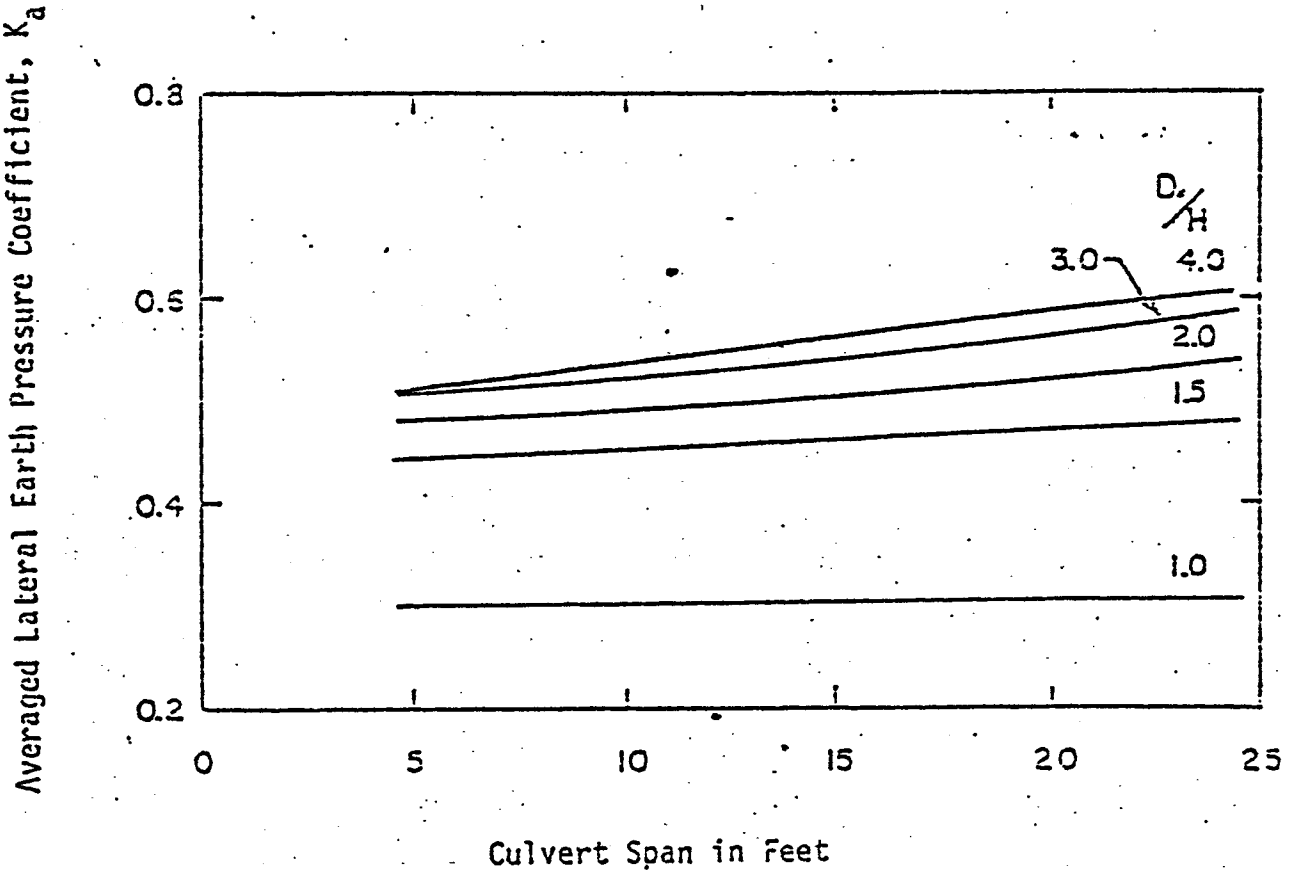

AVERAGE LATERAL EARTH PRESSURE COEFFICIENT,
K_a VS. CULVERT SPAN

FIGURE 2.30

culvert structure in Walnut Creek, California by Duncan and Jeyapalan (10). In this study, deflection gages were mounted around the perimeter of the culvert, and measurements were plotted with respect to the level of fill. Deflection measurements were taken both before and after compaction as shown in Figures 2.31 and 2.32.

The measured variation in span with respect to fill height is shown in Figure 2.31. These measurements were taken at two cross-sections, A and B. The span decreases slightly during back-filling, and then a much greater decrease in span is seen during compaction.

The measured crown deflections are shown in Figure 2.32. Here, deflections are greatly affected by the compaction effort applied.

The measured and calculated haunch movements are shown in Figure 2.33. It may be seen that the calculated values agree quite well with those measured up to H = -2.0 ft. Subsequently, the calculations indicate a considerable increase in span (about 2.0 inches) whereas very little occurred in the field. This lack of agreement indicates that the soil alongside the structure was probably considerably more stiff on reloading than was assumed in the analyses. It may be seen that the difference between the measured and calculated changes in span is as great for conditions before compaction as for conditions after, indicating that the calculated deflections due to compaction are approximately equal to those measured.

The measured and calculated crown movements are shown in Figure 2.34. It may be seen that they are in good agreement up to the stage when the crown begins to move down. Subsequently, the calculated

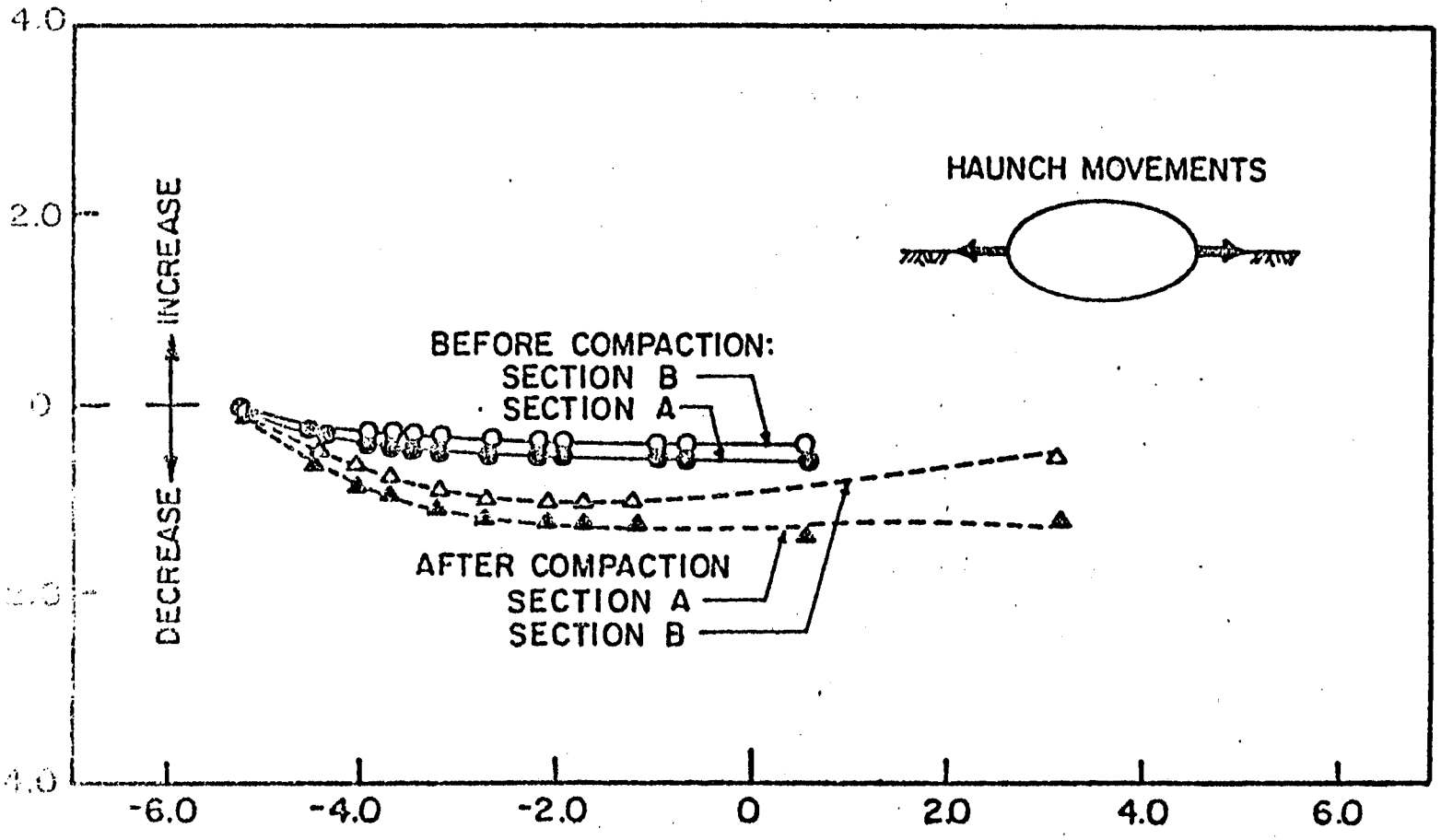

FIGURE 2.31

VARIATION IN SPAN WITH FILL HEIGHT

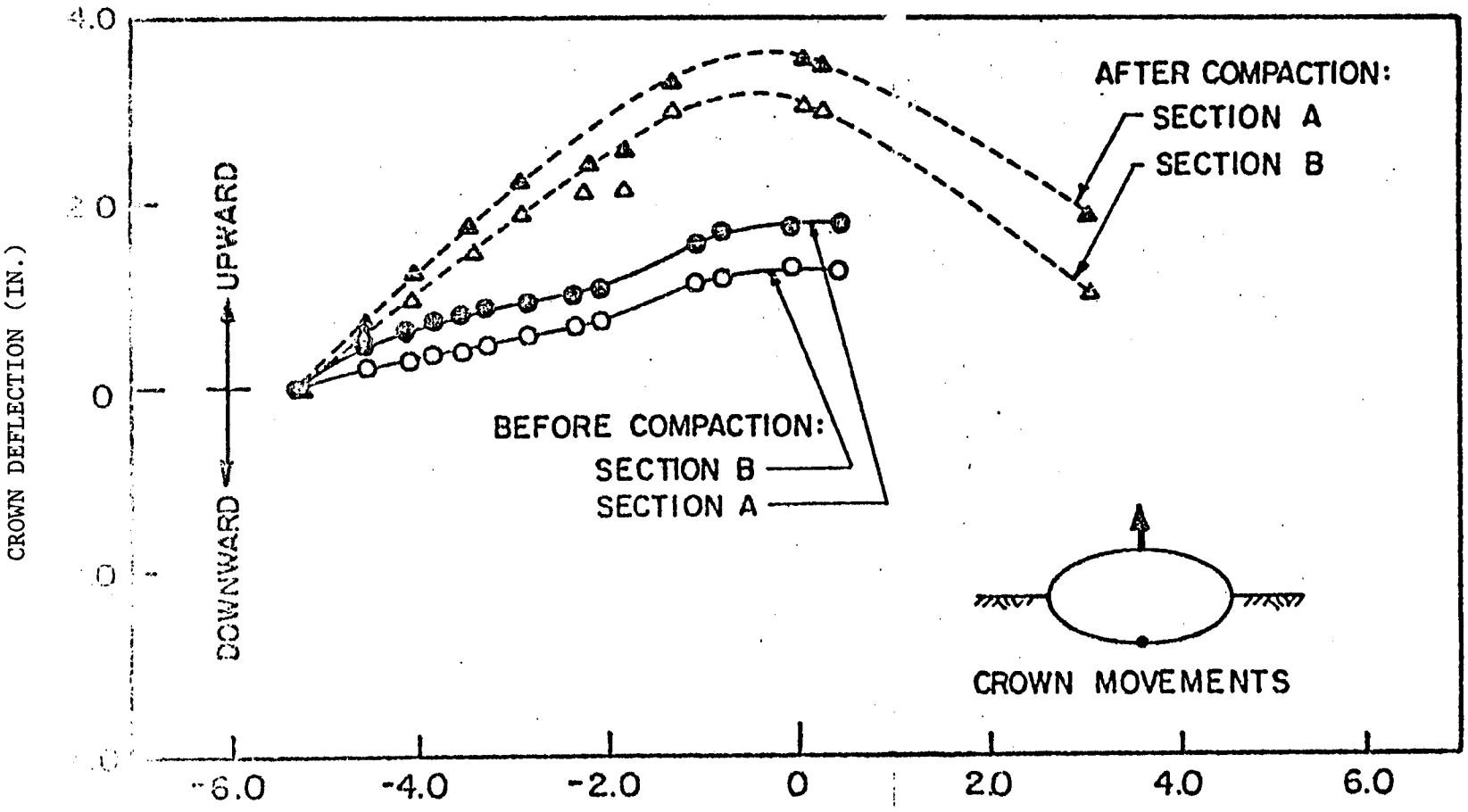

FIGURE 2.32

VARIATION IN CROWN DEFLECTION WITH FILL HEIGHT

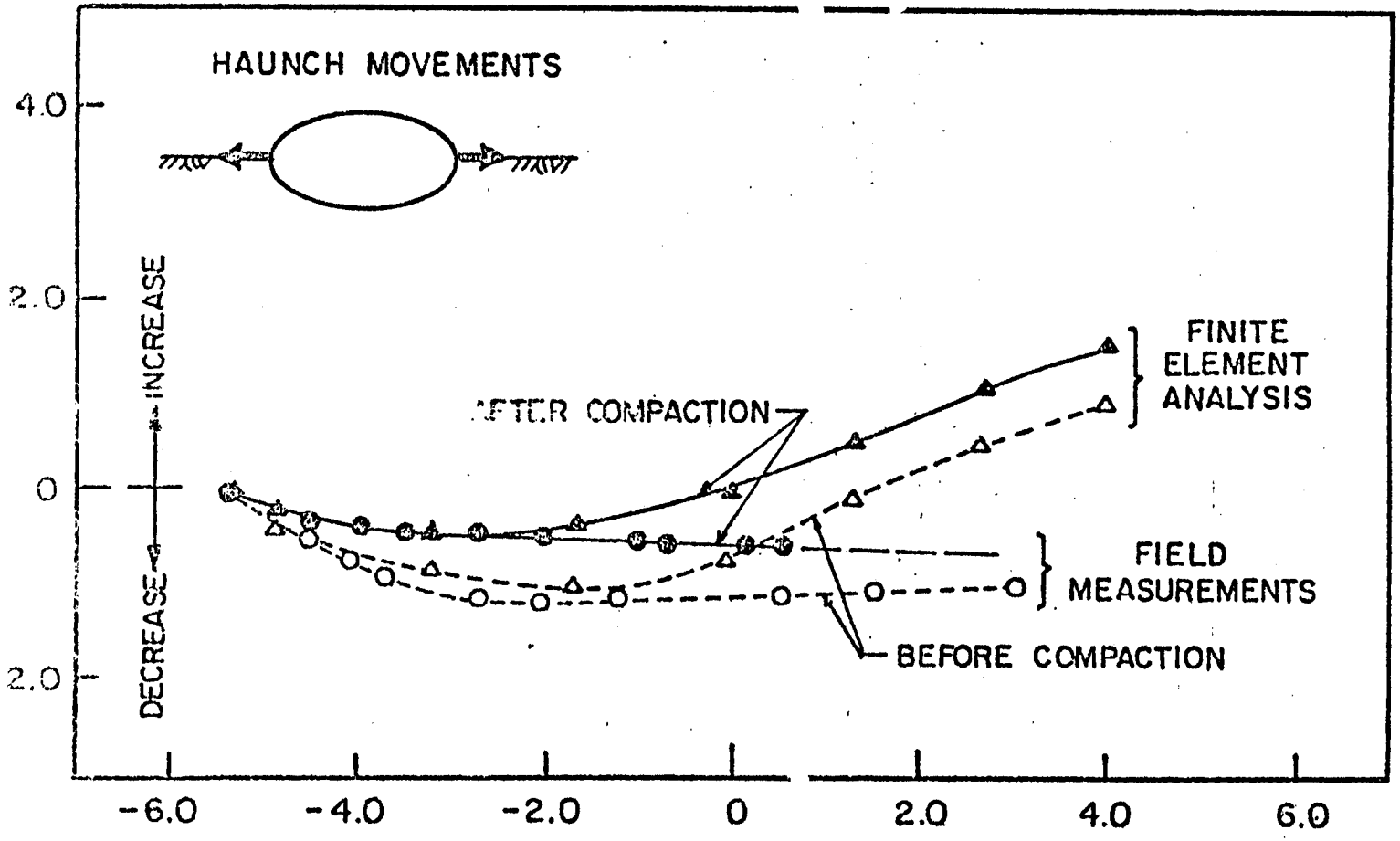

FIGURE 2.33

VARIATION IN SPAN WITH FILL HEIGHT

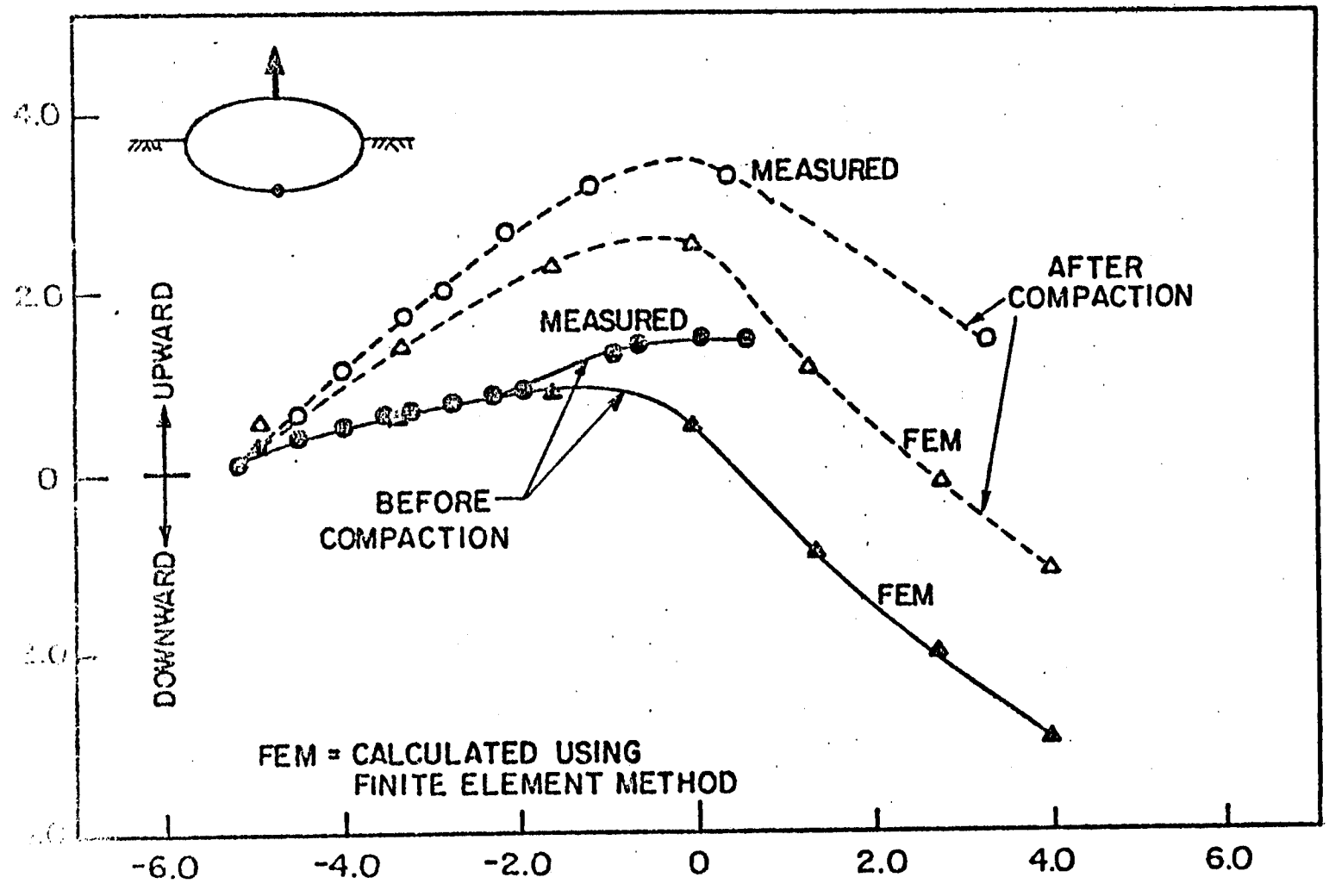

FIGURE 2.34

VARIATION IN CROWN DEFLECTION WITH FILL HEIGHT

downward movements are larger than those measured. It seems likely that the discrepancy is due to the fact that the soil adjacent to the haunches of the structure was actually stiffer than assumed for the analyses, as mentioned previously, restricting outward movement of the haunches, and the soil in this zone also inhibits downward movement of the crown. The magnitude of the differences between the measured and calculated deflections are about equal before and after compaction, indicating that the calculated deflections due to compaction are reasonably accurate.

Another study conducted by Duncan and Jeyapalan (9), involves the analysis of an underground oil pipeline under granular backfill and heavy live loads. The objective was to determine the stresses induced in the steel pipe by the loads from the heavy vehicles, and those due to the earth pressures from the backfill around and over the pipe.

A cross-section through the fill showing the location of the pipeline is given in Figure 2.35. The steel pipe and the outer ethylene jacket were modeled by beam elements. The gravel backfill, the urethane foam insulation around the pipe, and the styrofoam insulation beneath the pipe were modeled by two-dimensional elements.

In some of the analyses interface elements were used to allow free slip between the ethylene jacket and the backfill. In others, these interface elements were not included, thus simulating a no-slip condition at the interface between the ethylene jacket and the gravel.

The analyses were performed in increments, simulating first the placement of backfill around the pipe and subsequently the application of live loads to the surface of the fill. The non-linear stress-

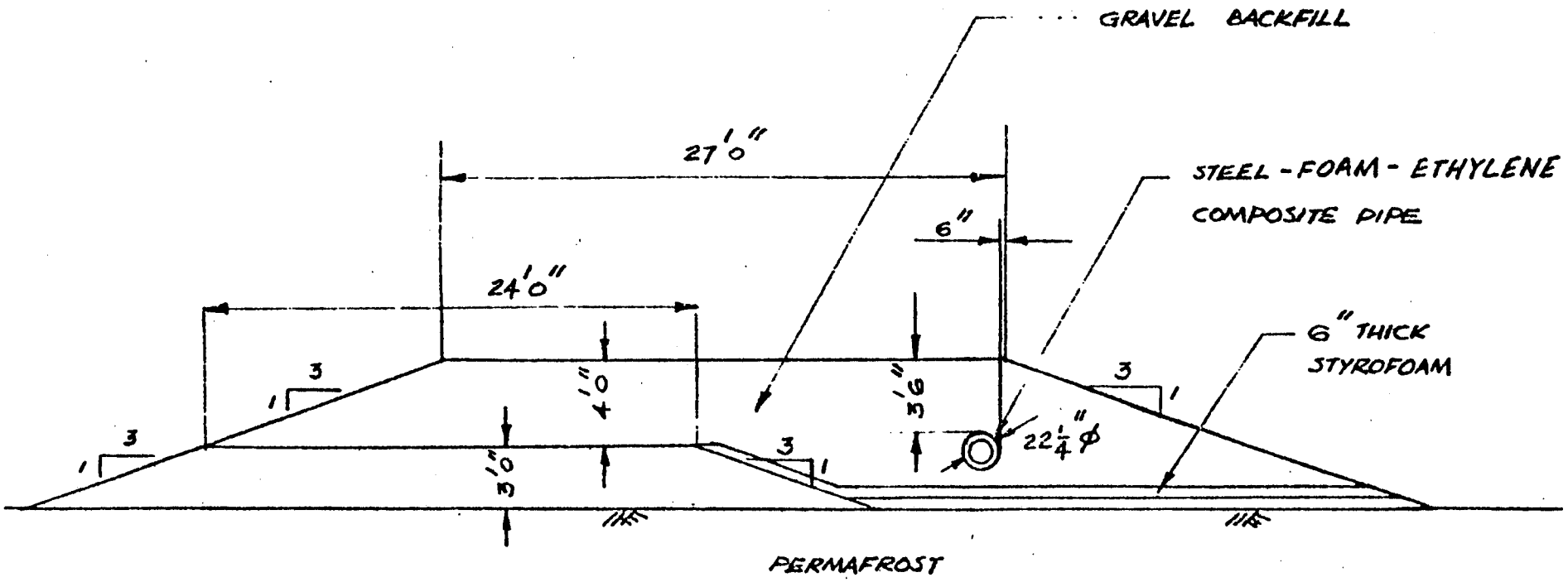

CROSS SECTION OF PIPE STUDY

FIGURE 2.35

strain behavior of the gravel backfill, the urethane foam surrounding the pipe and the styrofoam insulation, was simulated in the analyses by varying the values of modulus in each element of the materials at each step of the analysis, in accordance with the calculated values of stress in each element.

The live load model used in this study is shown in Figure 2.36. The position of the load was varied in the analyses to find the location which produced the greatest stresses in the pipe. During preliminary analyses in which an equivalent live load was used, it was found that an off-center load produced the greatest stress in the steel pipe. However, subsequent analyses showed that this result was influenced by failure of soil elements above and around the pipe, which resulted in unreasonable distribution of the load through the unfailed portions of the fill. When more appropriate strip loading was used it was found that the greatest stress in the steel pipe occurred when the load was centered over the pipe.

Distributions of the stresses in the steel pipe due to backfill and traffic loads are shown in Figures 2.37 and 2.38. Stresses on the inside of the pipe are shown in Figure 2.37, and stresses on the outside of the pipe are shown in Figure 2.38. The largest calculated tensile stress due to backfill and live load is about 13,800 psi, at the top of the pipe on the inside.

Results for both the no-slip case and the free-slip case are shown in Table 2.1. The stresses due to backfilling and internal pressure were analyzed only for the no-slip condition. It was believed that they would be little affected by the condition of the

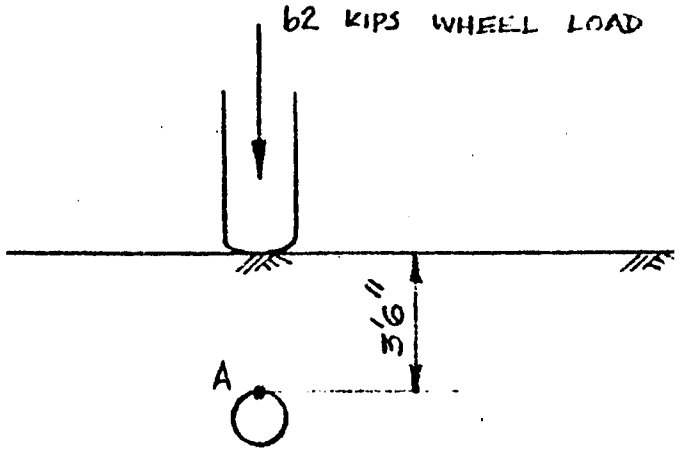

SECTIONAL ELEVATION

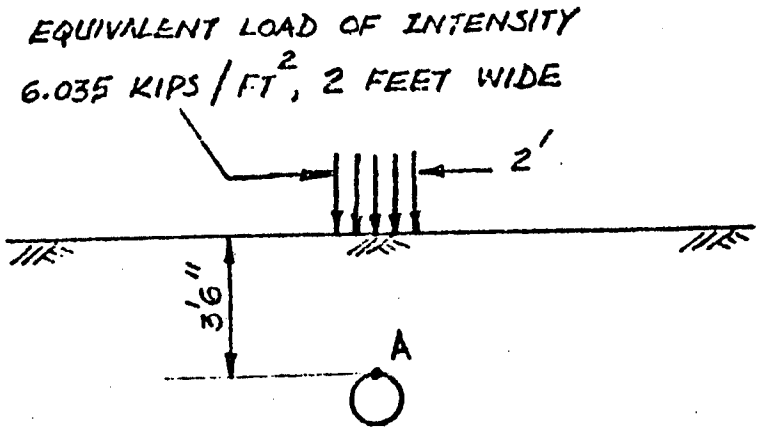

SECTIONAL ELEVATION

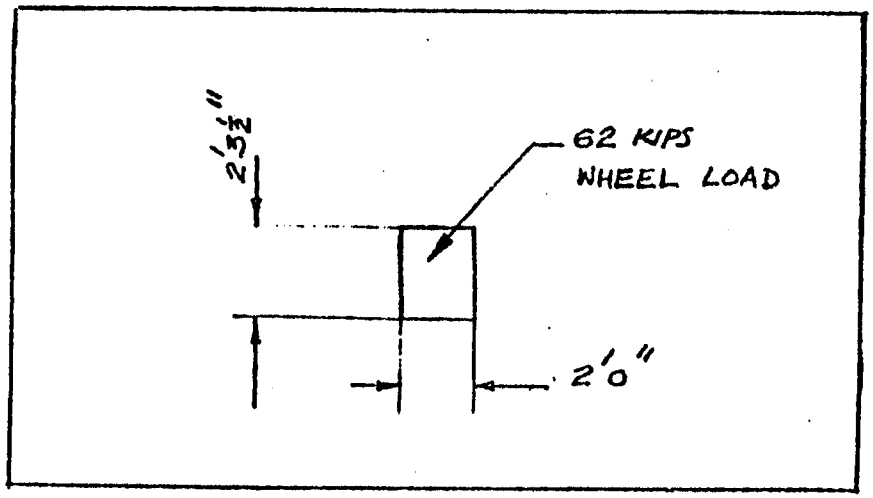

PLAN

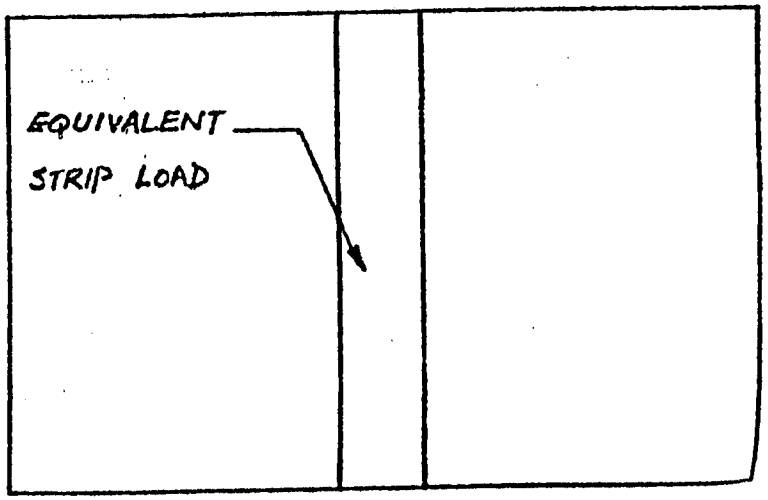

PLAN

EQUIVALENT STRIP LOAD

FIGURE 2.36

SIGN CONVENTION: TENSILE STRESSES ARE POSITIVE

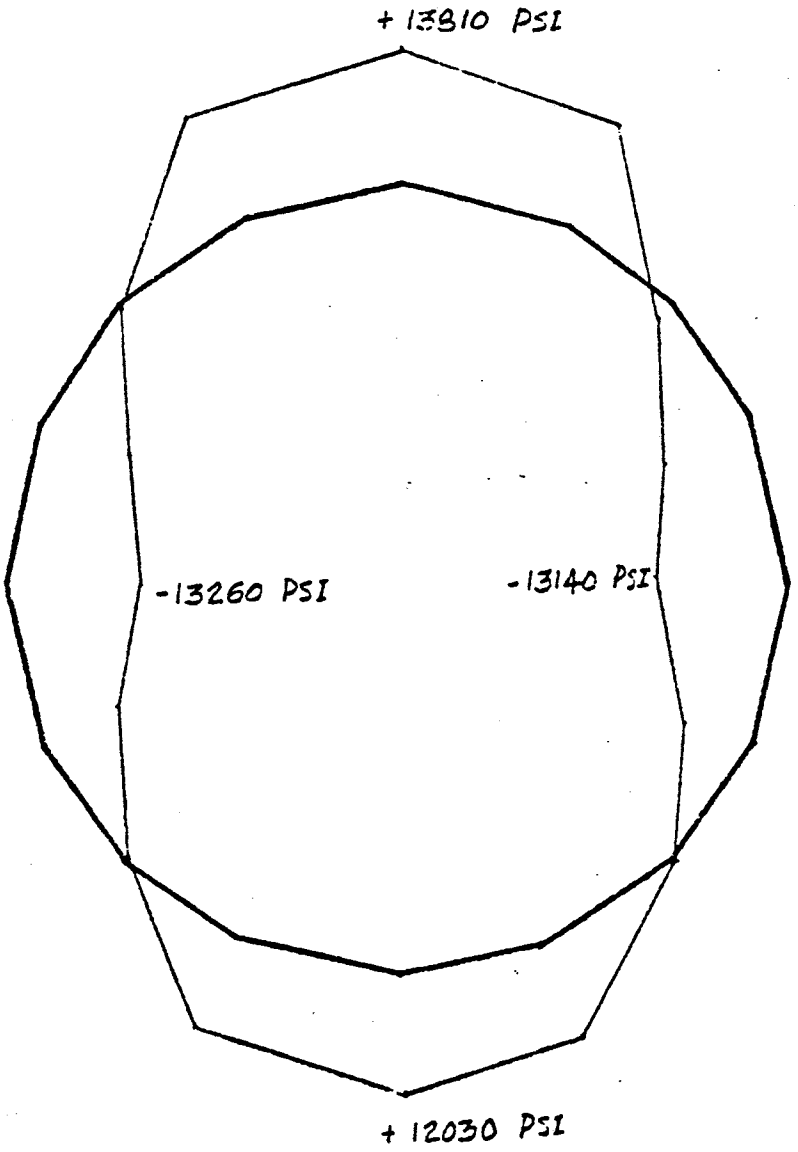

1. THESE STRESSES ARE ON THE INSIDE OF PIPE
2. INTERFACE ELEMENTS ARE USED IN THESE ANALYSES (FREE SLIP)

STRESS DISTRIBUTION IN STEEL PIPE DUE TO BACKFILLING AND LIVE LOAD

FIGURE 2.37

SIGN CONVENTION: TENSILE STRESSES ARE POSITIVE

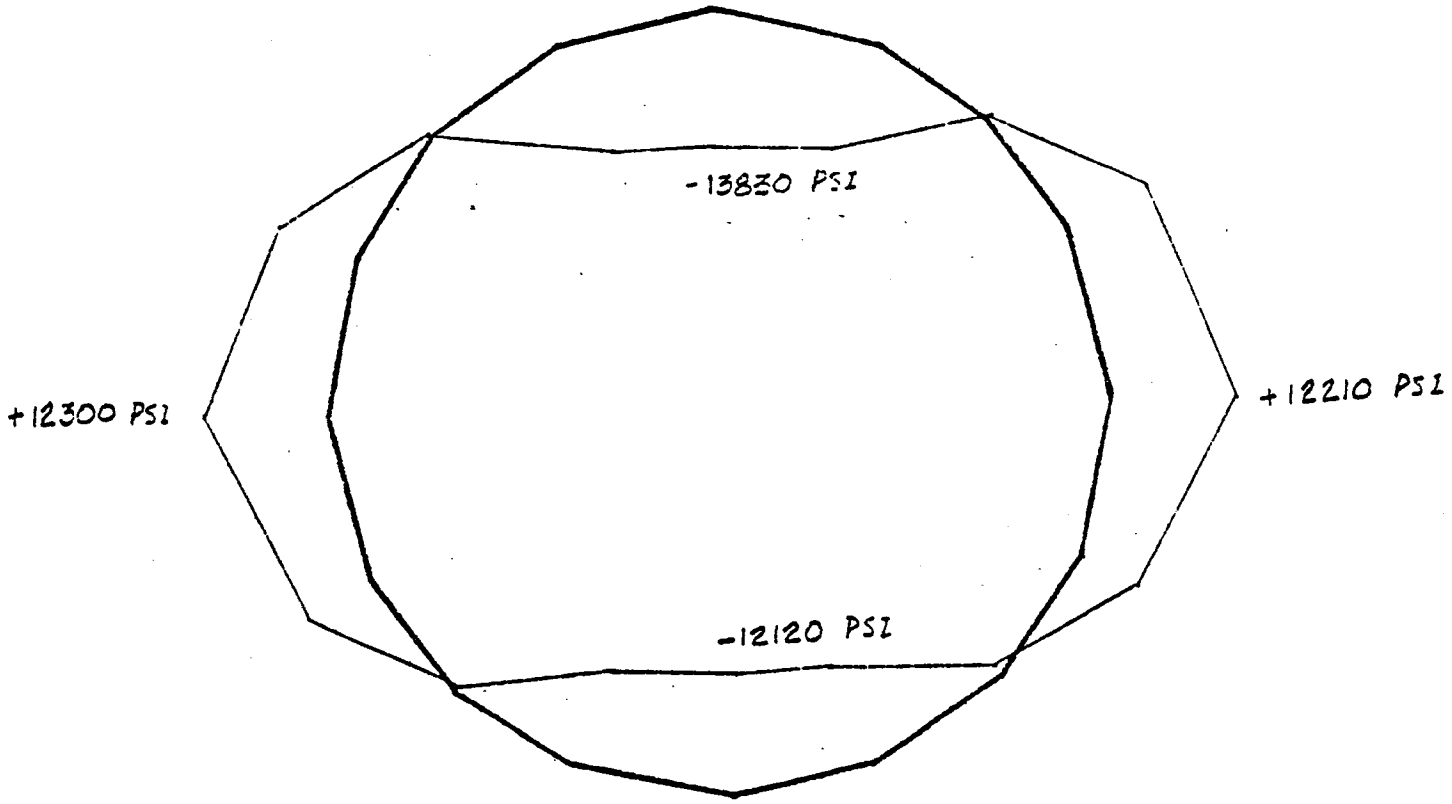

1. THESE STRESSES ARE ON THE OUTSIDE OF PIPE
2. INTERFACE ELEMENTS ARE USED IN THESE ANALYSES (FREE SLIP)

STRESS DISTRIBUTION IN STEEL PIPE DUE TO BACKFILLING AND LIVE LOAD

FIGURE 2.38

TABLE 2.1 Critical Stresses in Steel Pipe from Finite Element Analyses (Duncan and Jeyapalan, 9)

Type of Loading	Stress Without Interface Elements (psi)	Stress With Interface Elements (psi)
Due to backfilling	1568	1568
Due to scraper live load	14248	12236
Due to internal pressure	31480	31480
Total	47296	45284

interface between the gravel and the jacket, and in Table 2.1 the values calculated for the no-slip case are shown also for the case of free-slip. The stress due to traffic loading is about 2000 psi larger in the no-slip case than in the free-slip case.

2.3.3 Finite Element, Isoparametric, Non-Linear, with Interface Interaction and No-Tension Program (FINLIN)

FINLIN is a finite element method computer program developed at Purdue University for soil-structure interaction studies. Like the other programs mentioned, small displacement formulation is adopted, time dependent response is assumed, the soil-conduit interaction is treated as a plane-strain problem, and the incremental construction technique is used.

Two types of soil models are incorporated into the FINLIN code. These are a linear elastic and a nonlinear, incrementally elastic soil model. The nonlinear soil model uses a cubic spline function to represent actual test data. Plane strain soil test results were used directly as input data. The appropriate soil moduli for any soil element are interpolated using cubic spline function in accordance with the existing octahedral normal and shear stress conditions.

The conduit materials are assumed to exhibit linear elastic behavior.

2.3.4 CANDE-SSTIPN Comparison

In order to determine which program would best fit the needs of this analysis, a comparison of the two programs, CANDE and SSTIPN was

conducted. For the comparison, such aspects as the available options, soil and structural models, verification with controlled tests, interpretation of results, and estimated operating expense were considered. The conclusions of this comparison may be stated as follows:

1) Where unsymmetrical loading configurations are to be considered, solution level 3 of the CANDE code must be used. Therefore, it is not possible to take advantage of the automated mesh generation sheme available.
2) Although the CANDE code does include four possible soil models, the Duncan soil model is thought to be the best representation of non-linear soil behavior for routine studies of conduit behavior. This soil model is incorporated into the SSTIPN program.
3) The advanced beam-rod element incorporated in the CANDE program for modeling a reinforced concrete section gives a better indication of the performance of the structural elements. However, in the present analyses, the culvert stresses are much smaller than those required for failure. Therefore the internal structural performance is not of primary importance.
4) Both SSTIPN and CANDE have been verified with actual test results, and have been shown to produce acceptable results for soil-structure interaction analyses.
5) The SSTIPN program is presently compiled and ready for use on the computer facilities available at Texas A&M. Excessive time and expense would be required to prepare the CANDE program for use. Also, estimated operating costs for CANDE on the available

facilities are greater than those for SSTIPN.

Based on these, it was determined that the SSTIPN program would best fit the needs of our analyses. Therefore, this program has been used in producing the results presented herein.

2.4 Empirical Studies

2.4.1 General

Beginning in 1923, the American Railway Engineering Association (AREA) (4) conducted a series of tests at Farina, Illinois to determine culvert loading conditions. Earth pressure cells were placed on culvert sections of varying material types, which were then buried under varying depths of fill. A layout of the test site is given in Figure 2.39(a) and the results of the tests are presented in Figure 2.39(b). For a rigid culvert, the horizontal pressures are approximately 40% of the weight of the overlying soil. However, the vertical pressures are greater than the weight of the soil above the culvert.

Marston (15) also conducted many empirical studies at the Iowa State College on the subject of culvert loading and earth pressures. The earth pressure distribution on a circular pipe under 15 feet of fill, presented by Marston (15), is given in Figure 2.40. Three material types are given in order to evaluate the pressure differences caused by the degree of flexibility of the conduit. The rigid culvert exhibits the greatest pressures on the top and bottom portions of the

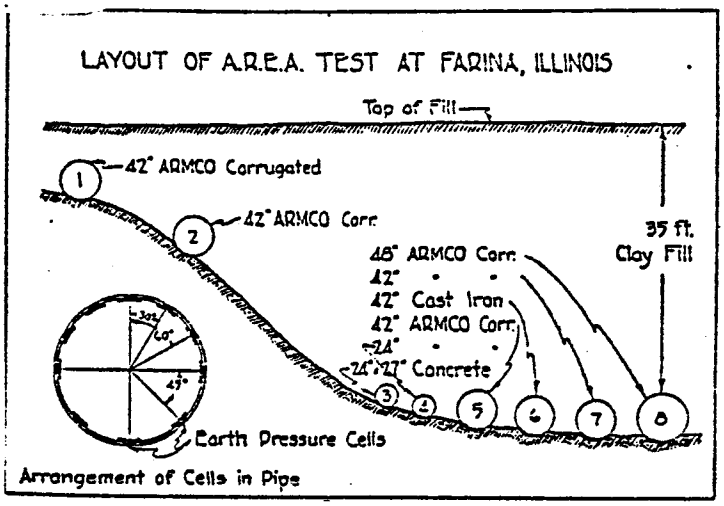

a) Field Conditions of AREA Tests

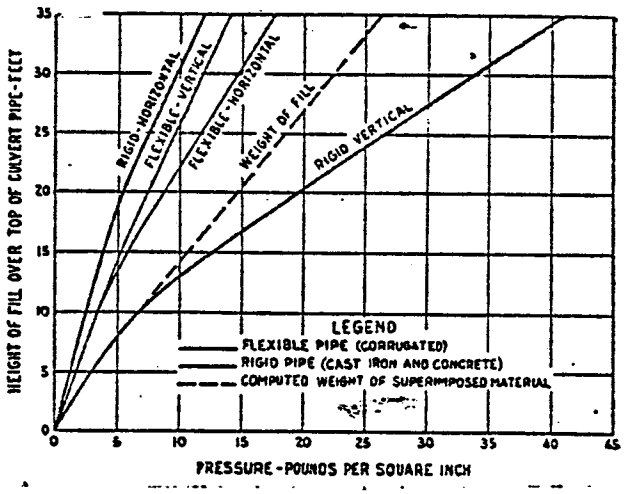

b) AREA Results

AREA TESTS AT FARINA, ILLINOIS
ON CULVERT LOADING

FIGURE 2.39

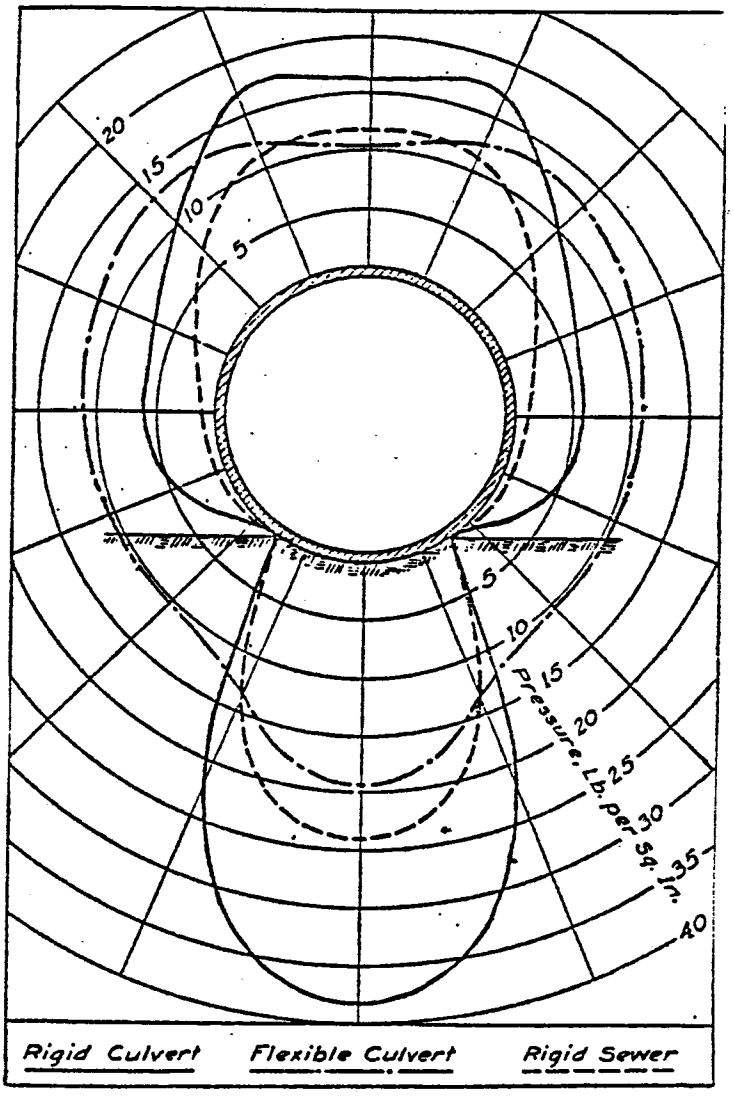

DISTRIBUTION OF RADIAL PRESSURE
ON THREE TYPES OF CONDUITS UNDER A FILL HEIGHT OF 15 FEET

FIGURE 2.40

conduit. However, the pressures exerted on the sides of the flexible culvert are much greater than those on the rigid culvert. This may be explained by the difference in deflection between the rigid and flexible conduit and the associated degree of arching that takes place.

The United States Corps of Engineers (6) use a design method for rigid conduits and culverts which depends on the construction methods used for installation. The Marston-Spangler theory is recommended for determining vertical loads on conduits placed in ditches, i.e. loading Condition I as described in Figure 2.41. The horizontal pressure is assumed to be equal to the Rankine active value. For conduits beneath embankments (Condition III) uniformly distributed vertical and horizontal soil pressures are assumed for design. Two loading cases are considered: Case 1, where the vertical and horizontal pressures of 150 and 50 percent of the overburden soil pressure, respectively; and Case 2, where the vertical and horizontal pressures are assumed to be the same and equal to the overburden pressure.

For the intermediate Condition II, where the conduit is placed in a shallow trench beneath an embankment, the design manual recommends that the soil pressures be determined by interpolation between values calculated by the Conditions I and III. For all conditions, it is recommended that conduits with vertical walls, which are cast directly against rock, should be designed for no lateral soil pressure. For the structural design of circular and oblong conduits, tabulated values of moment, thrust and shear coefficients at various sections of the conduits are given for different loading assumptions. Bedding

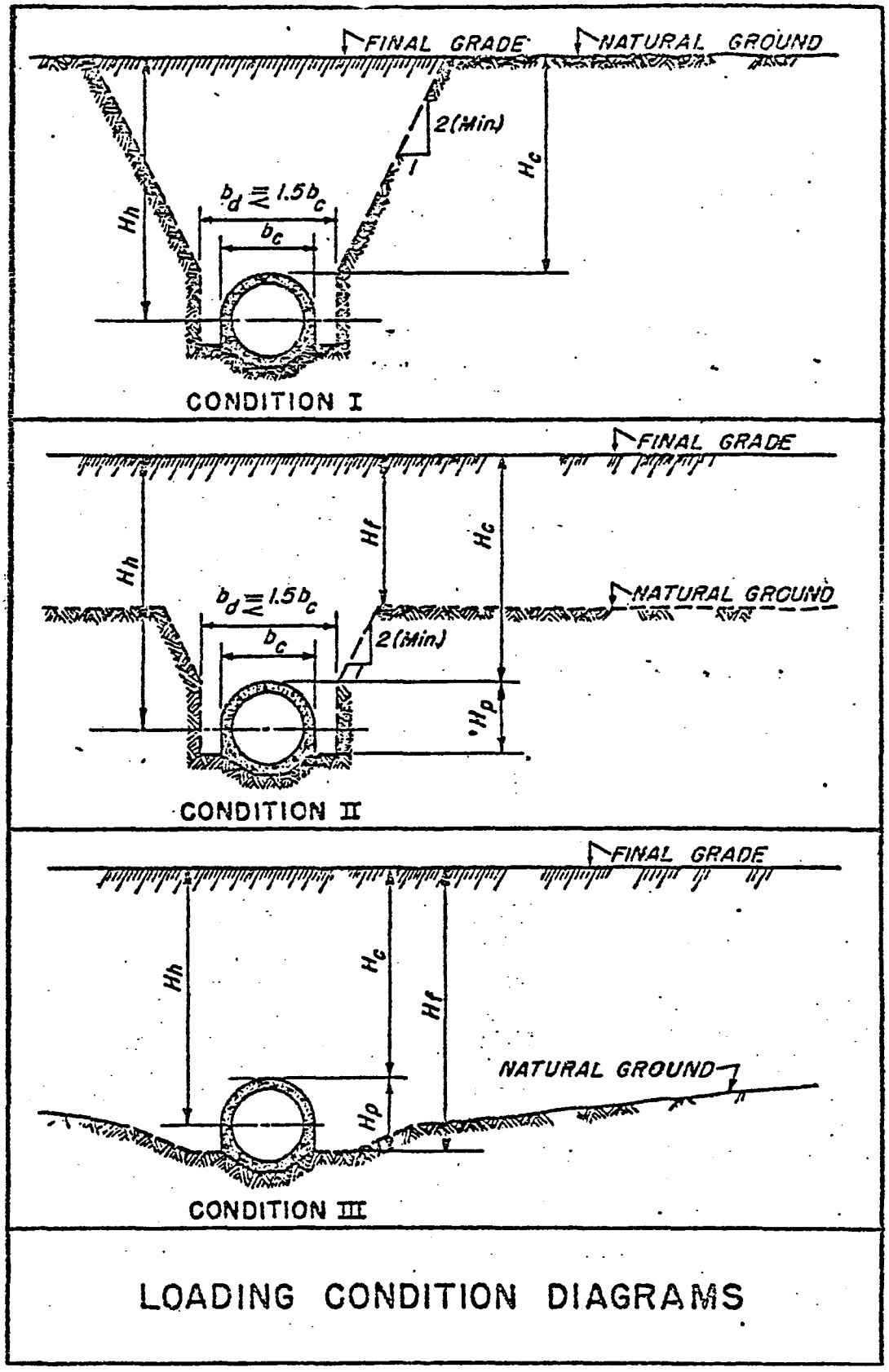

LOADING CONDITION DIAGRAMS

FIGURE 2.41

load factors to be used in the selection of standard, precast concrete pipe are also given.

2.4.2 Specifications

The American Association of State Highway and Transportation Officials (AASHTO) (2) deals with design loadings on box culverts in their bridge specifications. The vertical and horizontal pressures due to soil fill are estimated by using an assumed equivalent fluid weight. These are divided into two cases. The first case involves a culvert in a trench or on a yeilding foundation. Moreover, this is divided into three areas. These deal with rigid culverts except reinforced concrete boxes, reinforced concrete boxes, and flexible culverts. For reinforced concrete boxes, the suggested equivalent weight for vertical pressure is 120 pcf, while for lateral pressure it is 30 pcf.

For the case of a culvert untrenched or on an unyielding foundation, AASHTO specifications require a special analysis.

American Society of Testing and Materials (ASTM) specifications (3) also cover the design loads for box culverts. These are very similar to the AASHTO specifications previously mentioned. For the vertical earth pressure, ASTM recommends that the pressure be taken as the weight of a column of earth of a width equal to the outside width dimension of the box section and a height equal to the depth of cover over the top of the section. Lateral earth pressures are taken as a minimum of 0.25 times vertical pressures. For the soils used in the ASTM design tables, an assumed unit weight of 120 pcf was used, which

is equal to the suggested value of the equivalent unit weight in AASHTO specifications.

2.4.3 California Division of Highway Studies

The California Division of Highways is presently involved in a great deal of research involving the structural behavior of buried conduits. Unfortunately, none of their efforts have been applied to the study of the behavior of reinforced concrete box culverts. For the design of reinforced concrete box culverts, they primarily use the current AASHTO Specifications for Highway Bridges.

The California Division of Highways has, however, conducted extensive research and field investigations using reinforced concrete arches and pipes. Davis and Bacher (5) have presented the current status and observations of some of these studies.

For the San Luis Reservoir arch, where a rigid concrete culvert was buried in a 200-feet deep rock fill, three major findings are presented. First, the pressure-height curves were linear up to the full fill height. Second, the pressure configuration was vastly different from that assumed in initial design. Because the California Division of Highways assumes a linear lateral pressure distribution increase with depth, this indicates that this assumption may not be valid. Finally, the change in the effective density of the backfill material after embankment completion was negligible.

Other studies show similar trends, with slight variations due to the use of straw or some compressible material around the barrel of the arch culvert. Here, the curvilinear stress-strain function of

straw influences the peripheral pressures measured.

2.5 Conclusions

As may be seen, the behavior of a rigid conduit under backfill and traffic loads is much more complex than has been previously assumed. Specifications are primarily empirical in nature, assuming a linear pressure distribution with depth. However, the studies presented have shown that this is not necessarily the case. The stiffness properties of the combined soil-culvert system have been shown to produce a marked influence on the behavior of the culvert.

Most of the contemporary research done in this area has involved some type of finite element study of the problem. These studies have produced a great amount of information concerning the behavior of culverts, although the amount of field information available to verify calculated results is limited.

In order to explain differences between calculated predictions and actual results, an arching effect has been introduced. This effect primarily involves the difference between the stiffness properties of the culvert and those of the surrounding soil mass. This concept partially accounts for the difference in pressure distribution measured around the culvert perimeter.

CHAPTER 3

MATERIAL PROPERTIES FOR THE LIVE LOAD ANALYSES

3.1 Soil Properties

In order to accurately model the soil-culvert system for an analysis of the behavior of a RC box culvert under live loads, the soil properties must be determined. These properties are then used to calculate hyperbolic parameters for use in the finite element method computer program. Representative soil samples were obtained from the culvert backfill materials and standard laboratory procedures were used to determine their properties. Also, field density measurements were made in order to determine the in-situ density of the soil surrounding the culvert after backfill compaction. Three instruments were used to obtain the in-situ density of the backfill around the instrumented box culvert. These are the balloon volumeter, the Texas Highway Department Harris cup, and the nuclear density gage. Twelve points around the construction site were chosen as soil sampling locations. At each of the stations, in-situ measurements of soil density were obtained, and samples were taken for the determination of moisture content in the laboratory.

The results of preliminary measurements showed an average density of 117 pcf, and an average moisture content of approximately 18 percent. These measurements were made after only two feet of backfill soil had been placed with little or no compaction. It was felt that

with time, the density of the soil would increase slightly, while the moisture content would decrease as drainage occurred.

Subsequent measurements of the in-situ density and the moisture content using the nuclear density gage were taken after the level of backfill had exceeded the crown of the culvert. At the time of these measurements, the backfill had been placed and compacted, and sufficient time had elapsed for drainage to occur. The results of these measurements showed an average density of 123 pcf and an average moisture content of 12 percent.

The soil properties used for the live load analyses are shown in Table 3.1. The moist unit weight is 125 pcf at a moisture content of 13 percent. These values were obtained through controlled laboratory tests on samples taken from the site, and correspond to 95 percent compaction on the wet side of the optimum moisture content. The values used to perform the live load analyses are very close to those determined by in-situ measurements at the time of field testing the instrumented culvert. It is felt that these values adequately represent the actual field conditions.

Other properties presented in Table 3.1 are hyperbolic parameters required as input for the soil model used in the finite element method computer program. These values were determined using the results of a number of triaxial tests, as discussed in the preliminary report "Preliminary Analyses of the Behavior of Reinforced Concrete Box Culverts", Research Report 326-1, Study 2-5-82-326, Texas Transportation Institute, Texas A&M University.

TABLE 3.1 Soil Properties Used In the Live Load Analyses

Property	Value
Dry Unit Weight, γ_d [kcf]	0.110
Moisture Content, w [%]	13.0
Moist Unit Weight, γ_m [kcf]	0.125
Degree of Compaction, [% γ_{max}]	95
Modulus Number, K	50
Modulus Exponent, n	0.2
Failure Ratio, R_f	0.6
Bulk Modulus Number, K_b	40
Bulk Modulus Exponent, m	0.2
Angle of Friction, ϕ	34.8
Reduction in Angle of Friction, $\Delta\phi$	5
Cohesion, C	0
Earth Pressure Coefficient, K_o	0.5

3.2 Structural Properties

The RC box culvert was modeled in the finite element analyses as a series of beam elements connected at common nodes. The geometry and the sectional properties of the culvert used in the analyses are discussed in the sections below.

3.2.1 Geometry of the Culvert

The culvert analyzed in this study is an 8 ft. x 8 ft. reinforced concrete box culvert as shown in Figure 3.1. The side walls have a thickness of 8 inches and the top and bottom slabs have a thickness of 7 inches. Longitudinal and transverse reinforcing steel bars are present in the concrete sections.

3.2.2 Sectional Properties

The culvert was represented as a series of beam elements in the analyses. The cross-sectional properties for the plane-strain analyses were calculated by transforming areas of reinforcing steel into equivalent areas of concrete. Due to similarities between the sectional properties of groups of beam elements, the culvert was divided into four material types as shown in Figure 3.1. The sectional properties for each of these materials used in the live load analyses are summarized in Table 3.2.

3.2.3 Interface Conditions

As determined from the analysis of backfill loads, interface conditions seem to exhibit very small effects on the calculated

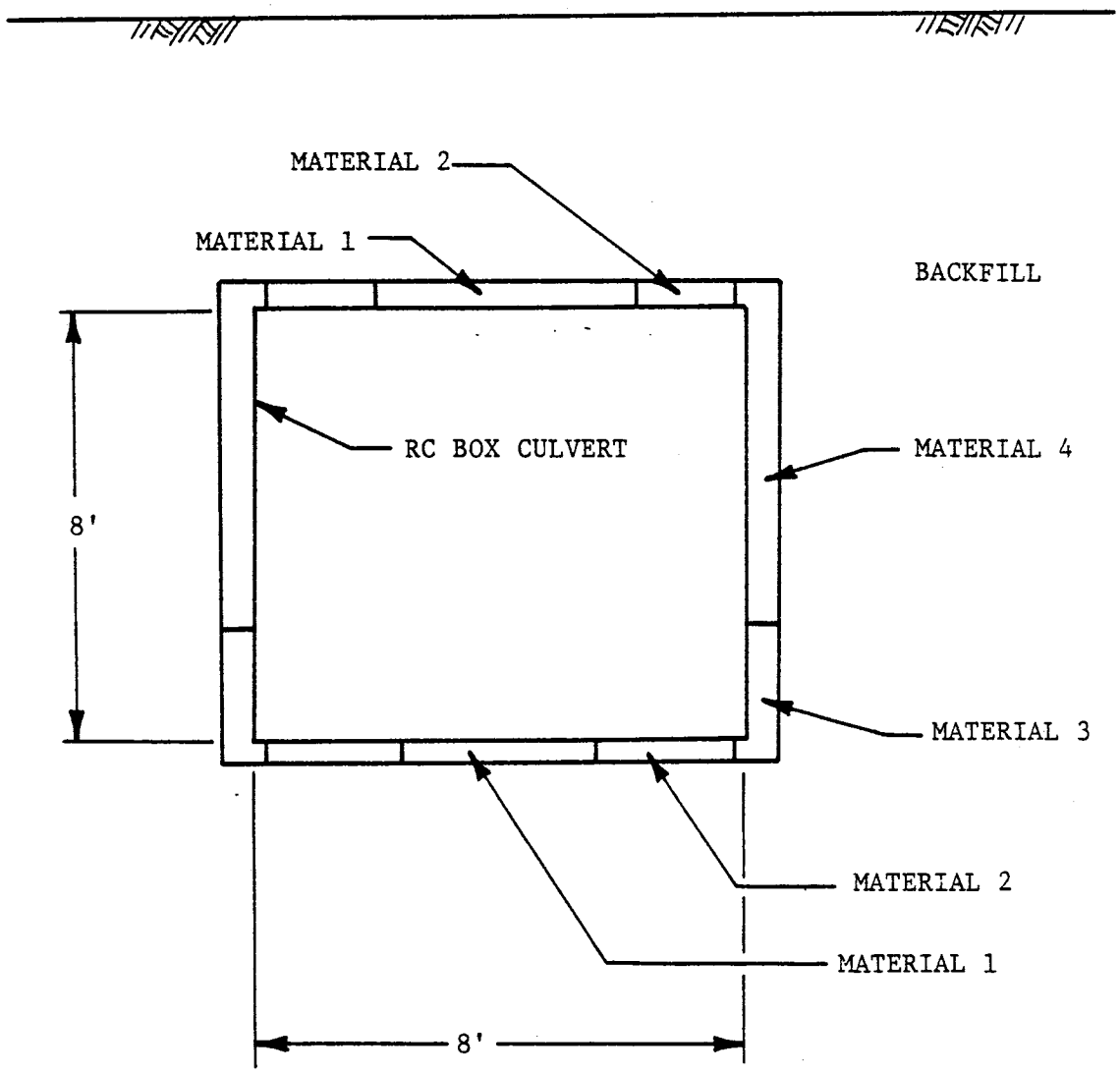

Cross-section of Box Culvert

FIGURE 3.1

TABLE 3.2 Structural Properties Used in the Analyses

Property	Material Type Number			
	1	2	3	4
Young's Modulus, E [ksf]	519119.0	519119.0	519119.0	519119.0
Moment of Inertia, I [ft]	0.0170	0.0172	0.0256	0.0253
Cross Sectional Area, A [ft]	0.601	0.612	0.700	0.689
Shear Area, ASH [ft]	0.601	0.612	0.700	0.689
Weight Per Unit Length, [kips/ft]	0.0875	0.0875	0.100	0.100
CTOP [ft]*	0.287	0.289	0.331	0.333
CBOTTOM [ft]*	0.297	0.294	0.331	0.333

*CTOP - Distance to the top-most fiber from the neutral axis.

CBOTTOM - Distance to the bottom-most fiber from the neutral axis.

results. Also, for an analysis in which no slippage is allowed at the soil-structure interface, the special soil-structure interface element available in SSTIPN can be omitted. This results in an appreciable reduction in computing costs. Therefore, a no-slip soil-structure interface was assumed in the analyses of the culvert under live loads.

CHAPTER 4

BEHAVIOR OF THE STRUCTURE UNDER SYMMETRICAL AND UNSYMMETRICAL LIVE LOADS

4.1 Introduction

This chapter presents the results of a finite element study conducted to analyze the behavior of an 8' x 8' reinforced concrete box culvert when subjected to symmetrical and unsymmetrical live loads. A live load model was derived in order to transform the finite tire load pattern into a semi-infinite strip load applicable to the plane strain finite element study. The results presented include predicted earth pressures, bending moments, shear stresses, stresses at the extreme fibers, strains in the reinforcing steel, and crown deflections. These are compared with results obtained for soil loads only to evaluate the effects of the applied live loads.

4.2 The Live Load Model

In order to model the live load to be used in the finite element analyses, it was necessary to determine an infinite strip load which was equivalent to the live loads actually applied. The live loads to be considered are those produced by a 4 ft tandem axle, such as the alternate interstate loading. These design loads are shown in Figure 4-1. Due to the long span of the trailer in the companion experimental study, and the relatively short width of the reinforced concrete box culvert, it was assumed that the critical live loading condition

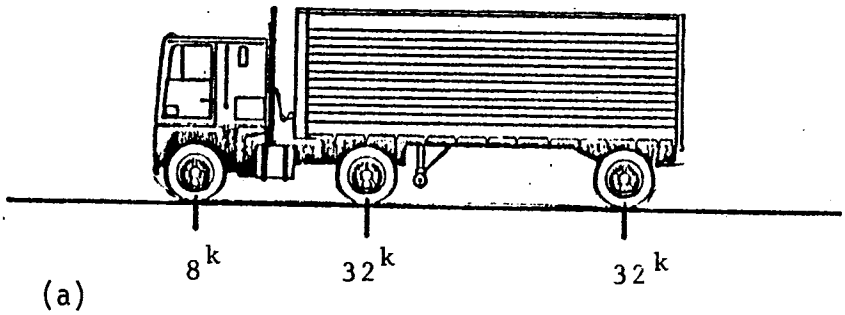

(a)

STANDARD HS-20 TRUCK LOADING

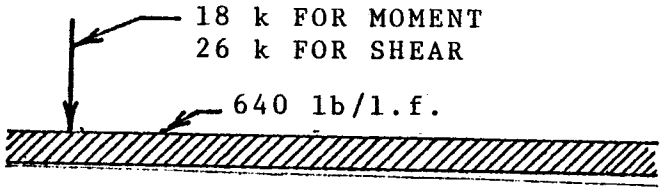

(b)

STANDARD HS-20 LANE LOADING

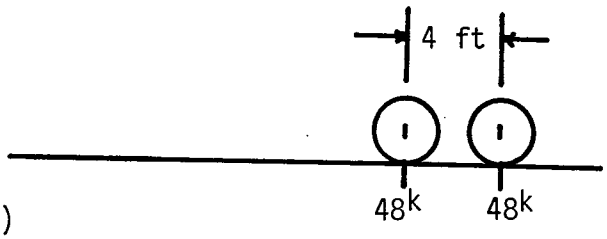

(c)

ALTERNATE INTERSTATE LOADING

Design Wheel Loadings

FIGURE 4-1

would be produced by the rear axle loads alone. In this manner, it is hoped to obtain a close correlation between the actual field results and those results from the finite element analyses.

A diagram of the tire loading pattern produced by the test vehicle tandem axle is given in Figure 4-2. Using the known load on each wheel and the tire pressure of the truck, it is possible to determine the area of contact for each tire. Assuming a square area of contact, and using the known truck dimensions, the loading pattern was developed.

It was then necessary to develop a uniform strip load which would produce an equivalent loading condition. This was accomplished using elastic solutions as presented by Poulos and Davis [20]. Four points of interest were considered and are shown as A, B, C, and D in Figure 2-4. Also, depths of fill of 2, 4, 6, and 8 feet have been considered. In this manner, the most critical loading configuration could be determined for each depth of fill.

In order to determine the magnitude of the equivalent strip load to be used, the stresses induced by the actual loads were calculated at the four points and at the four heights of fill considered. An elastic solution for the sterss beneath the corner of a uniformly loaded rectangular area was used in the calculation and is given as:

$$\sigma_z = \frac{p}{2\pi} \left[\tan^{-1} \frac{lb}{zR_3} + \frac{lbz}{R_3} \left(\frac{1}{R_1^2} + \frac{1}{R_2^2}\right)\right] \qquad (4.1)$$

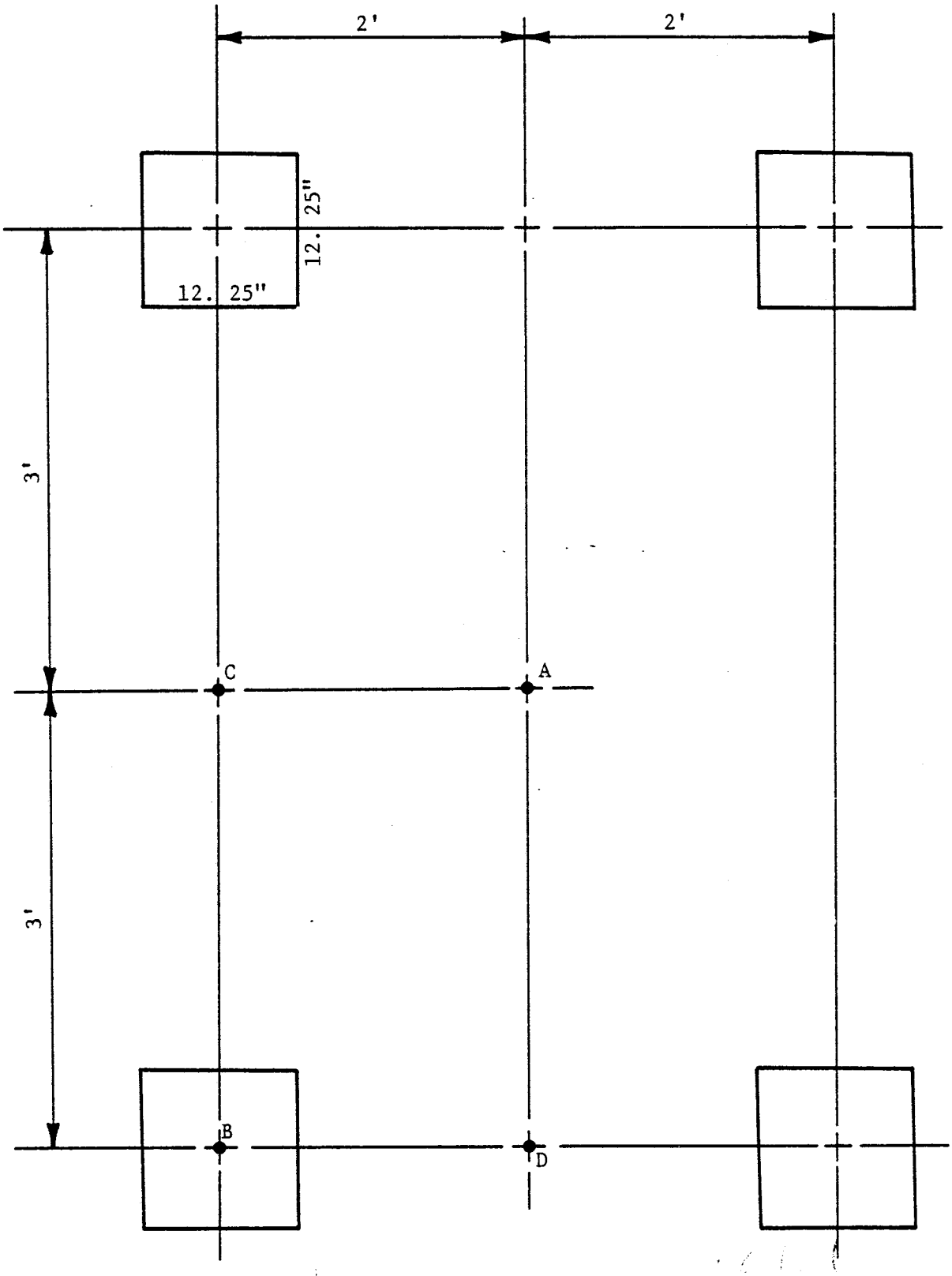

Simplified Representation of Actual Tire
Load Pattern for Test Vehicle (Rear Axles)

FIGURE 4-2

where

$$R_1 = (l^2 + z^2)^{1/2},$$

$$R_2 = (b^2 + z^2)^{1/2}, \text{ and}$$

$$R_3 = (l^2 + b^2 + z^2)^{1/2}.$$

This loading is shown in Figure 4-3. The principle of superposition was employed in order to obtain the total influence of the four loads at each point.

After determining the stresses due to the actual loads, the stresses produced by a uniform strip load were calculated in terms of the unknown uniform pressure, p. The idealized loading configuration for this case is shown in Figure 4-4. The width of the strip load was assumed to be that of the tire print. These stresses were determined by applying the strip load directly above the point, at depths of 2, 4, 6, and 8 feet. From Poulos and Davis [20], the vertical stress at the point in question is given by

$$\sigma_z = \frac{p}{\pi} [\alpha + \sin \alpha \cos (\alpha + 2\delta)] \qquad (4.2)$$

The calculated vertical stress at the crown of the culvert for the actual loads was then equated to the calculated vertical stress at the crown of the culvert for the uniform strip load for each of the heights of fill considered. In this way, the magnitude of the equivalent strip load for each height of fill was determined. By matching the stresses at the crown of the culvert, the best representation of the actual loads on the culvert were determined. The calculated values of the magnitude of the uniform strip load for each of the four points beneath the actual loads and the four heights

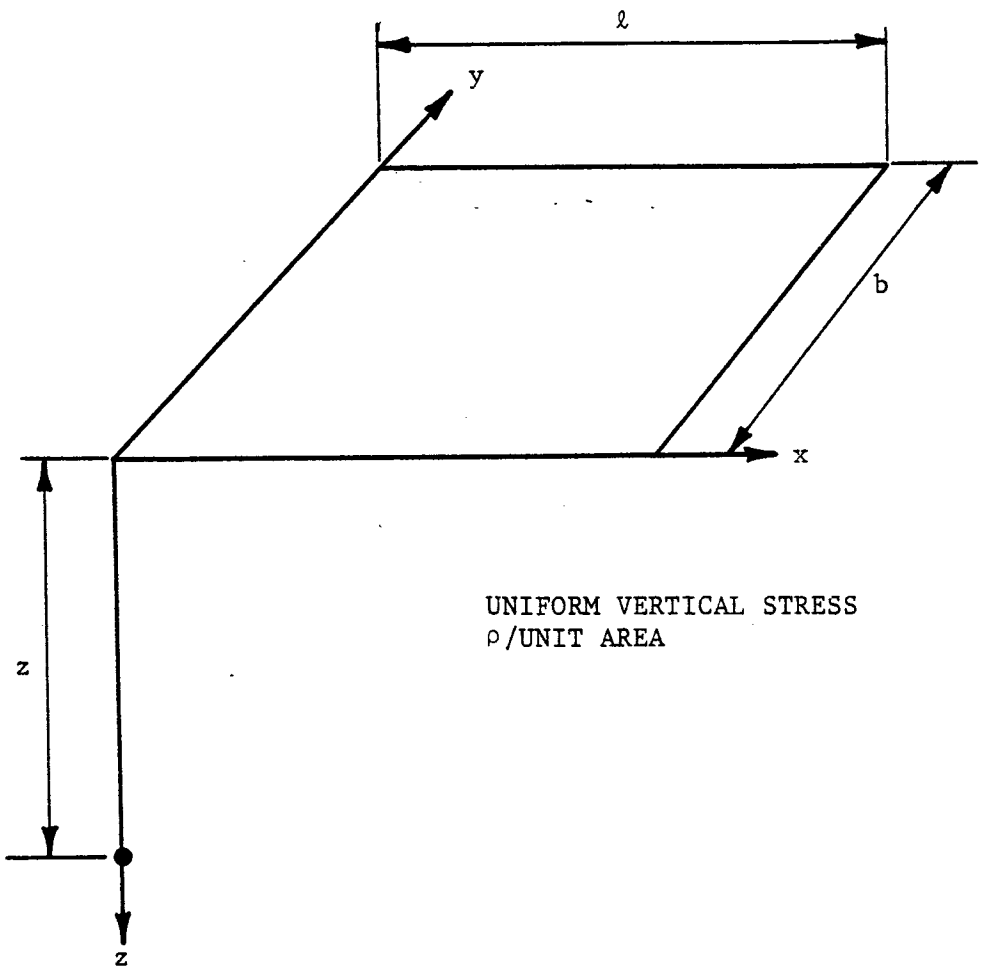

Model Load Configuration for Stress Beneath a Uniformly Loaded Rectangle

FIGURE 4-3

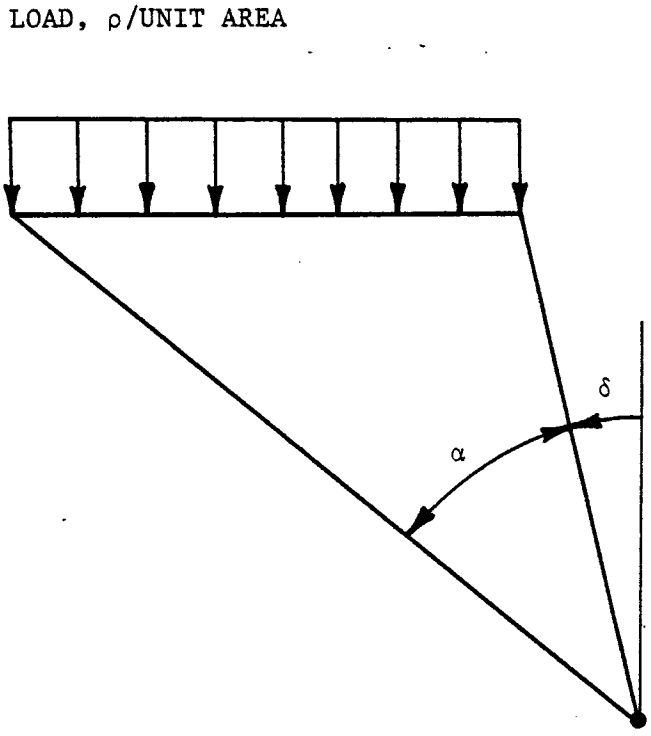

Model Load Configuration for Infinite Strip Load

FIGURE 4-4

of fill considered are given in Table 4-1. The critical loads are underlined, and were used in the analyses of the behavior of the culvert due to traffic loads.

It is interesting to note that beneath tire loading points A and C, the equivalent strip load pressure increases with depth. However, beneath point B, the equivalent strip load pressure decreases with depth. This difference may be attributed to the fact that for points A and C, as the depth of fill becomes greater, more influence from the surrounding loads is being applied. However, for point B directly beneath a tire, as the depth of fill becomes greater, the influence becomes smaller from the other three tires, causing a reduction in the vertical stress at this point. It is assumed that at some depth beneath points A and C the influence from all of the tire loads would begin to decrease. This is shown by looking at the strip load values calculated for point D. These values reach a maximum at approximately 4 feet, and then begin to decline at greater depths.

For the live load analyses conducted, finite element computer runs were made at heights of fill of 2, 4, and 8 feet above the crown of the culvert. Two loading positions were used in the analyses. First, the strip load was applied over the center line of the culvert. In the second loading condition, the strip load was offset approximately 2 feet from the center line. These loadings are shown in Figure 4-5 a and b, respectively.

TABLE 4-1. Equivalent Strip Load Results

Height of fill H, ft.	Calculated Strip Load Values for live loads applied at: PT. A	PT. B	PT. C	PT. D
2	3.64	30.11	4.05	12.11
4	14.39	19.52	13.43	19.35
6	19.34	17.67	17.56	19.23
8	19.81	16.65	18.13	18.11

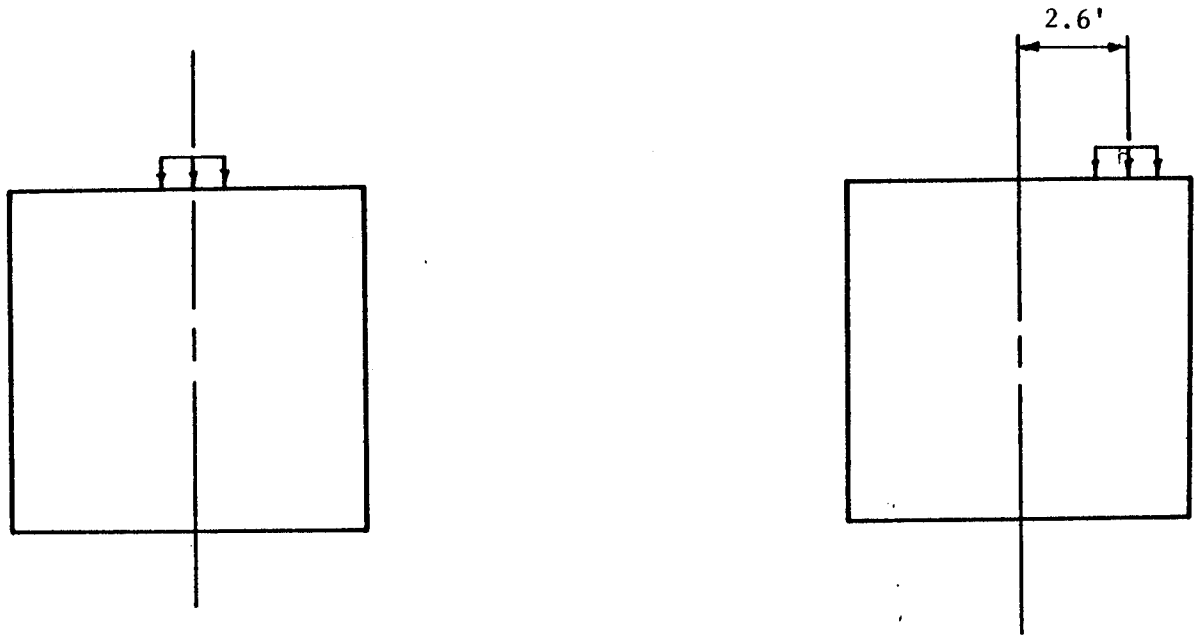

(a) CENTERED LOAD

(b) OFFSET LOAD

Positions of the Applied Live Load

FIGURE 4-5

4.3 Results of the Analyses

4.3.1 Earth Pressures

The variations in earth pressure with depth of fill for pressure cells P-1 through P-7 are given in Figures 4-6 to 4-12. As may be seen in Figures 4-6 to 4-8, the live load effects at these cells is almost negligible. However, as shown in Figure 4-9, there is a significant reduction in the predicted earth pressure for pressure cell P-4 as a result of the live load. Furthermore, the reduction in earth pressure is greater for the offset load. This reduction may be attributed to the arching effect around the culvert, which would cause a relief in pressure at the top corner. Also, the position of the offset load causes a greater influence than does the live load applied at the center of the culvert. As the depth of fill increases beyond about 6 feet, the earth pressures tend to approach the predicted values for the backfill loads only.

The variation in earth pressure with depth of fill along the top of the culvert is shown in Figures 4-10 to 4-12. A large difference in pressures may be seen as a result of the application of the live loads. For pressure cell P-5 in the center of the culvert, the center loading creates the largest pressures as would be expected. These values decrease with depth of fill to a point, and then approach the predicted earth pressures for backfill only. The offset load has a much less noticeable effect, but still influences the earth pressures greatly.

For pressure cell P-6, located almost directly beneath the point

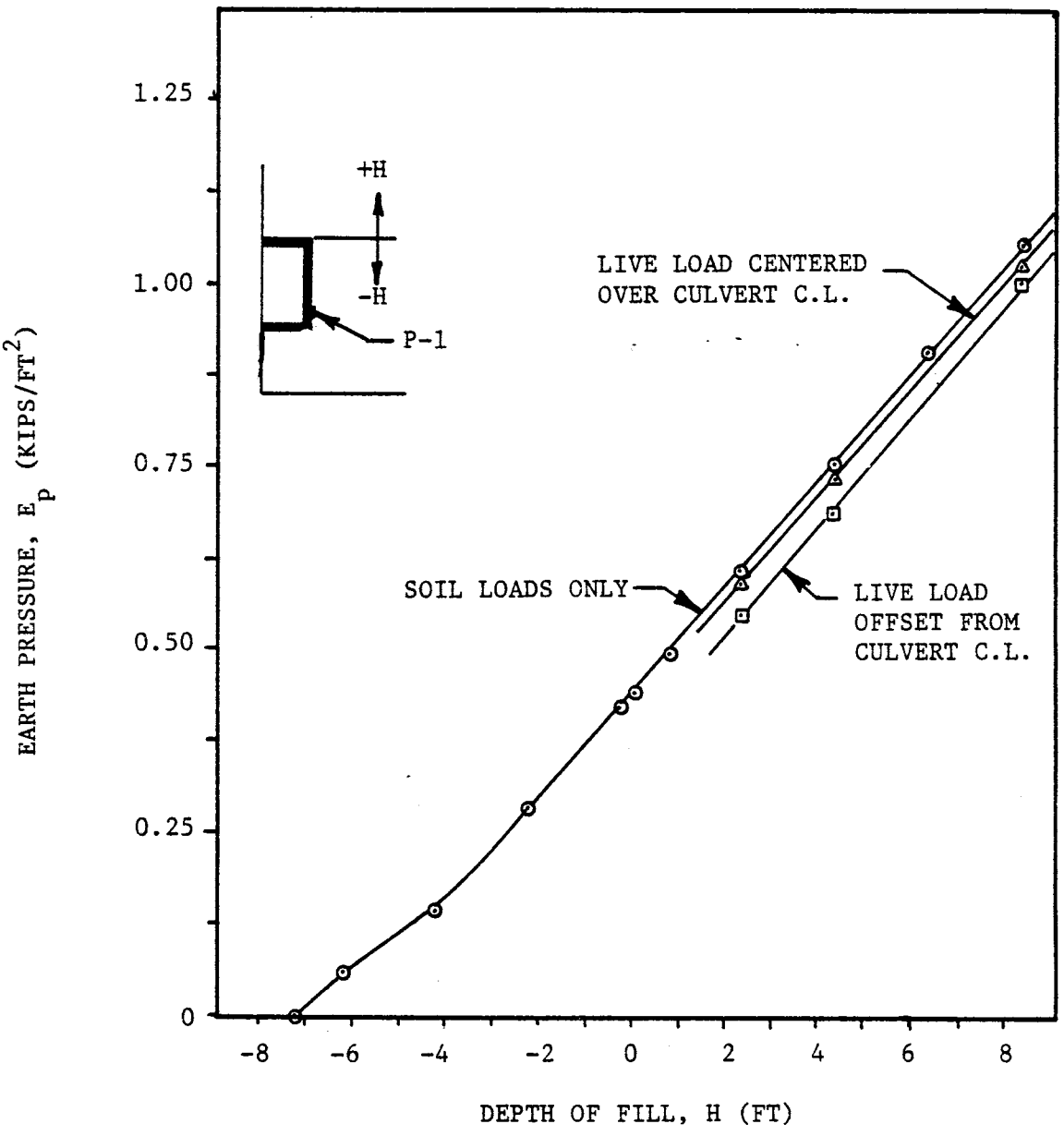

Variation of Earth Pressure with Depth
of Fill for Pressure Cell P-1

FIGURE 4-6

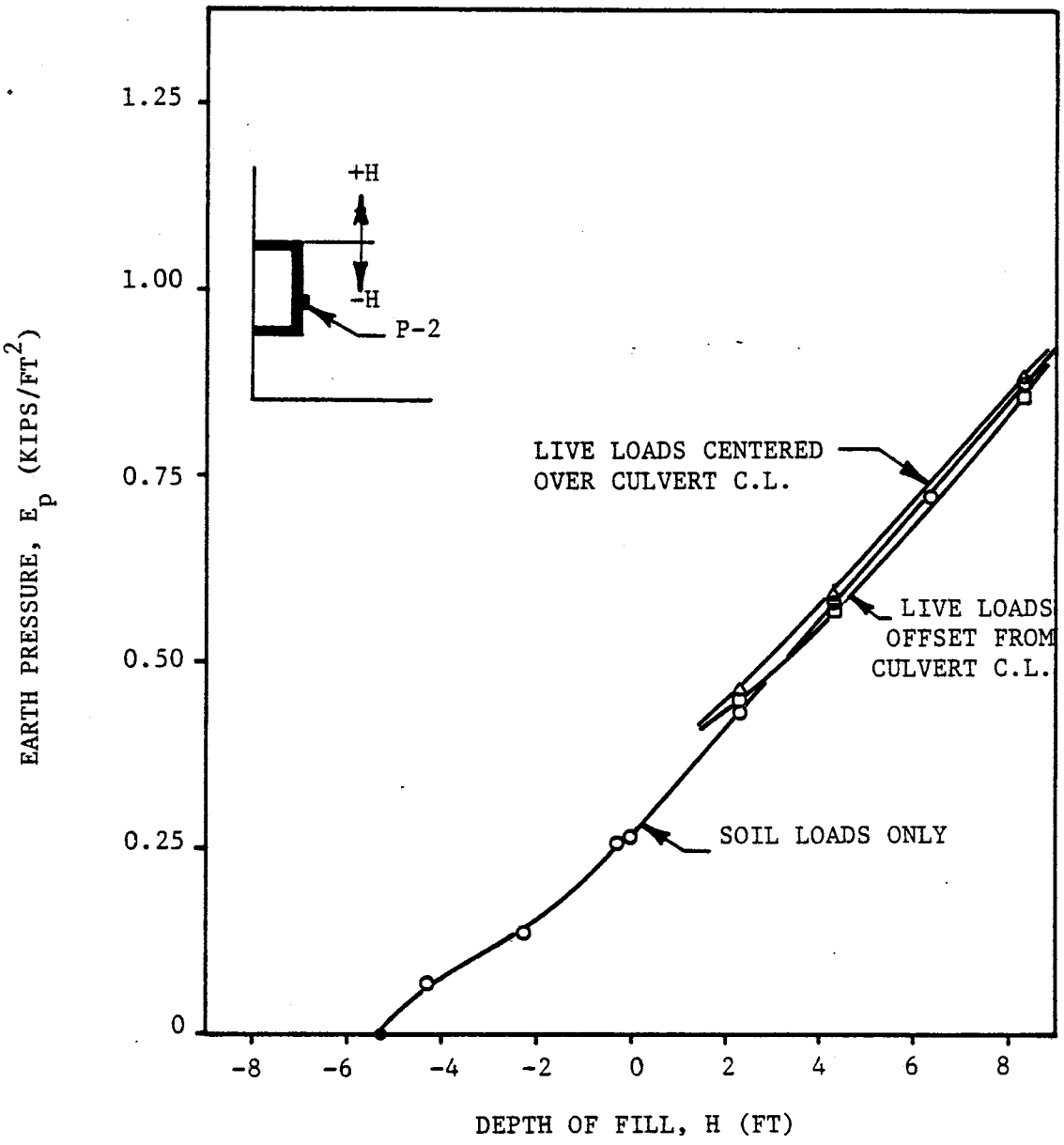

Variation of Earth Pressure with Depth
of Fill for Pressure Cell P-2

FIGURE 4-7

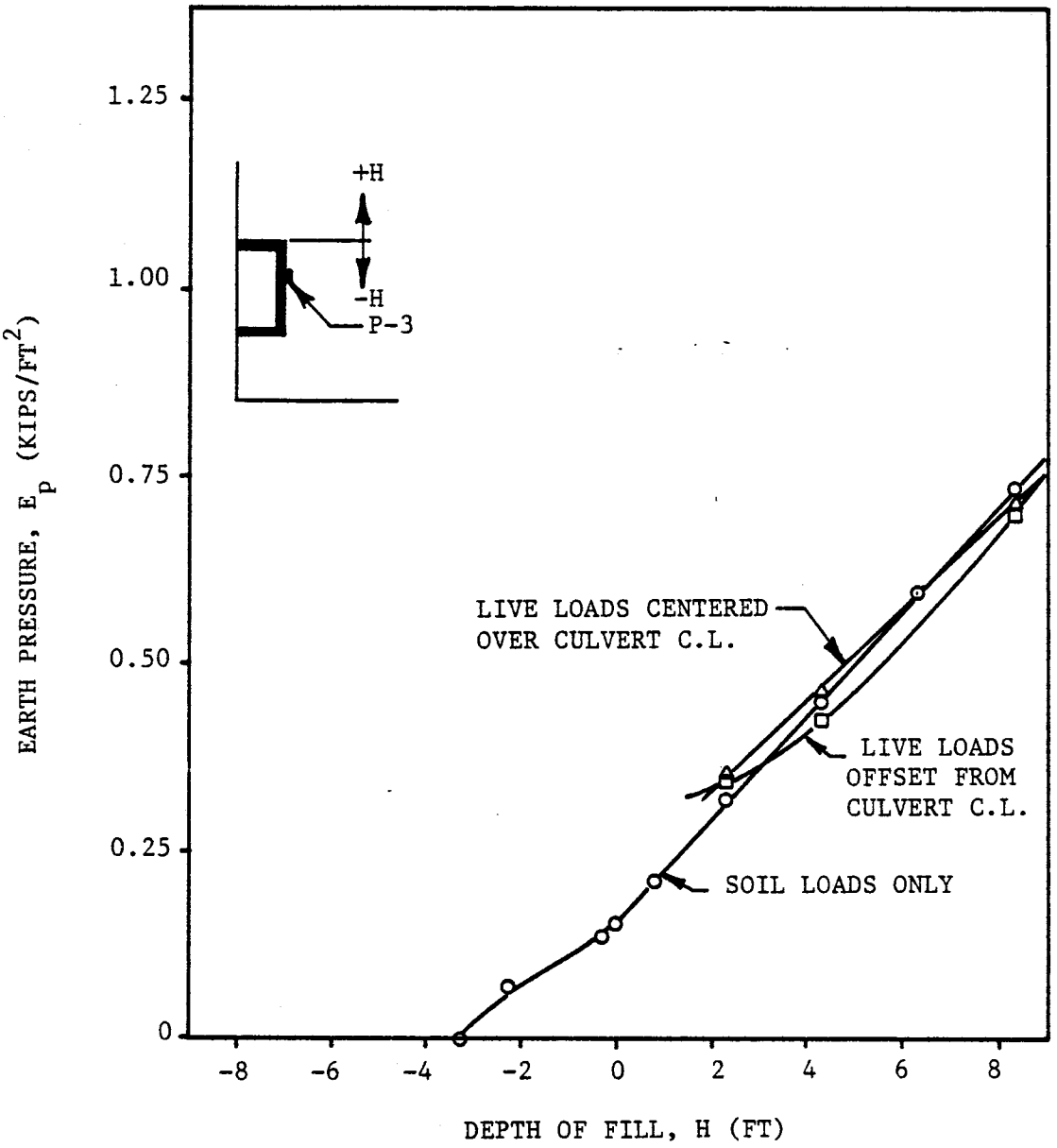

Variation in Earth Pressure with Depth
of Fill for Pressure Cell P-3

FIGURE 4-8

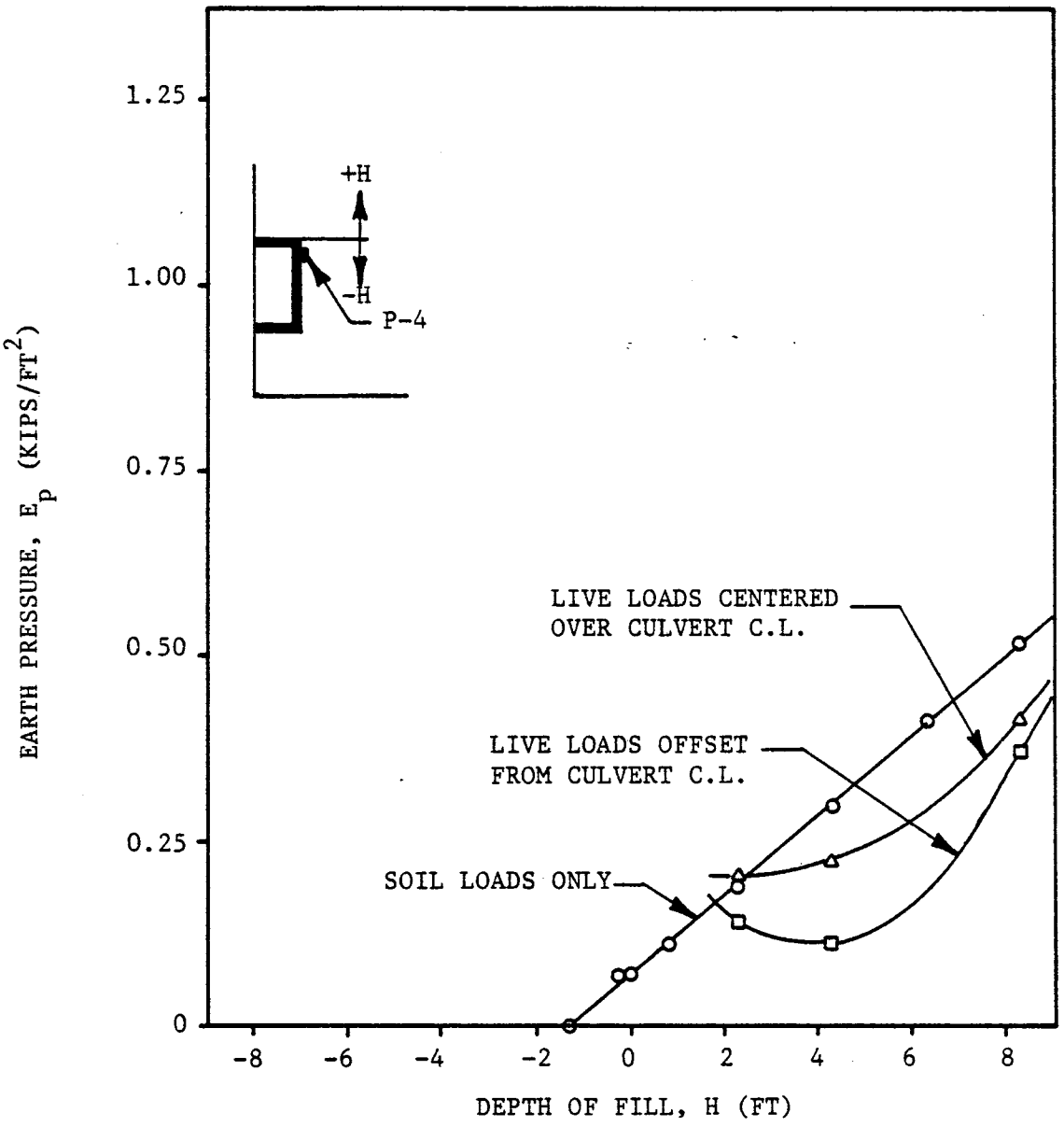

Variation of Earth Pressure with Depth
of Fill for Pressure Cell P-4

FIGURE 4-9

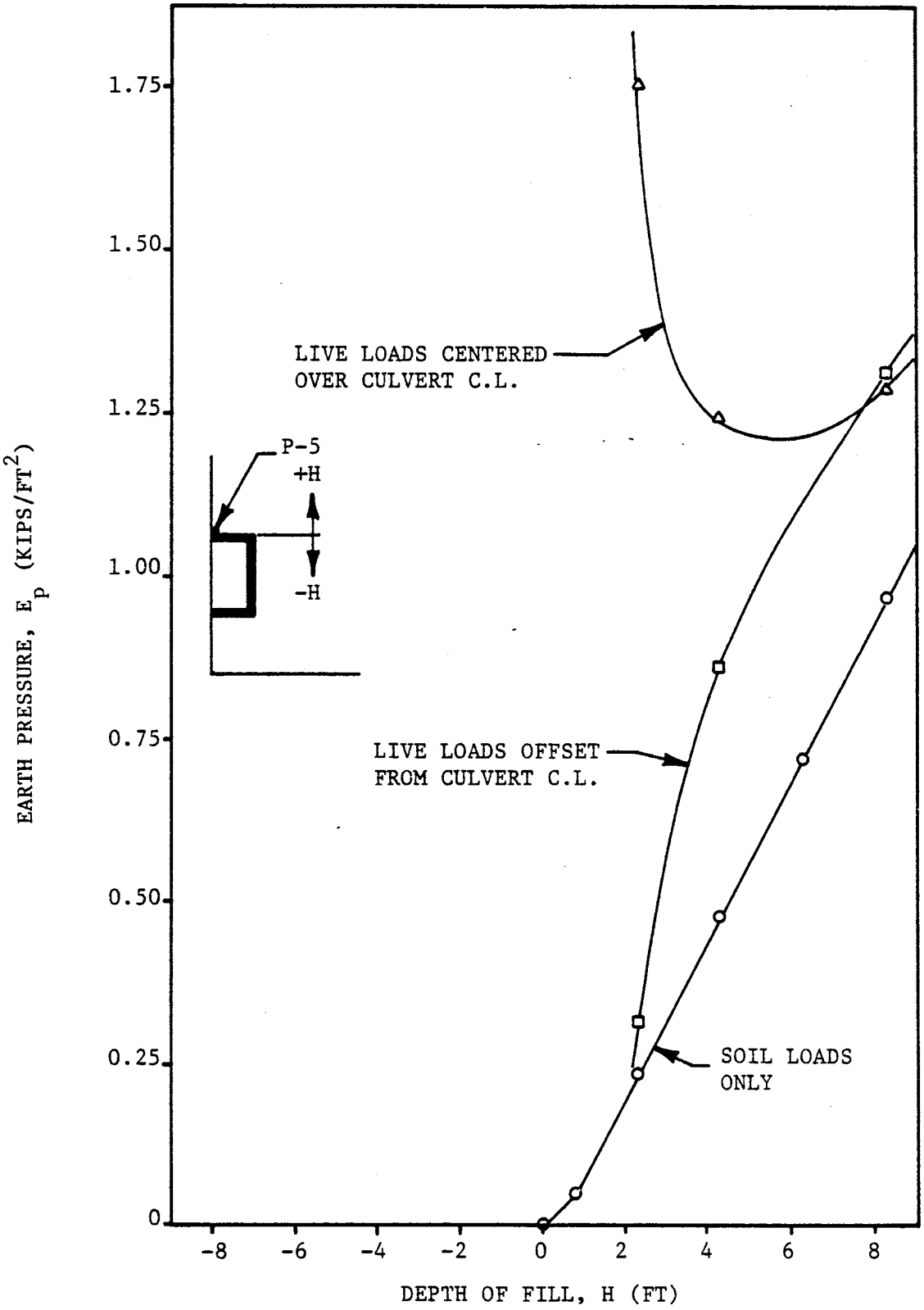

Variation of Earth Pressure with Depth
of Fill for Pressure Cell P-5

FIGURE 4-10

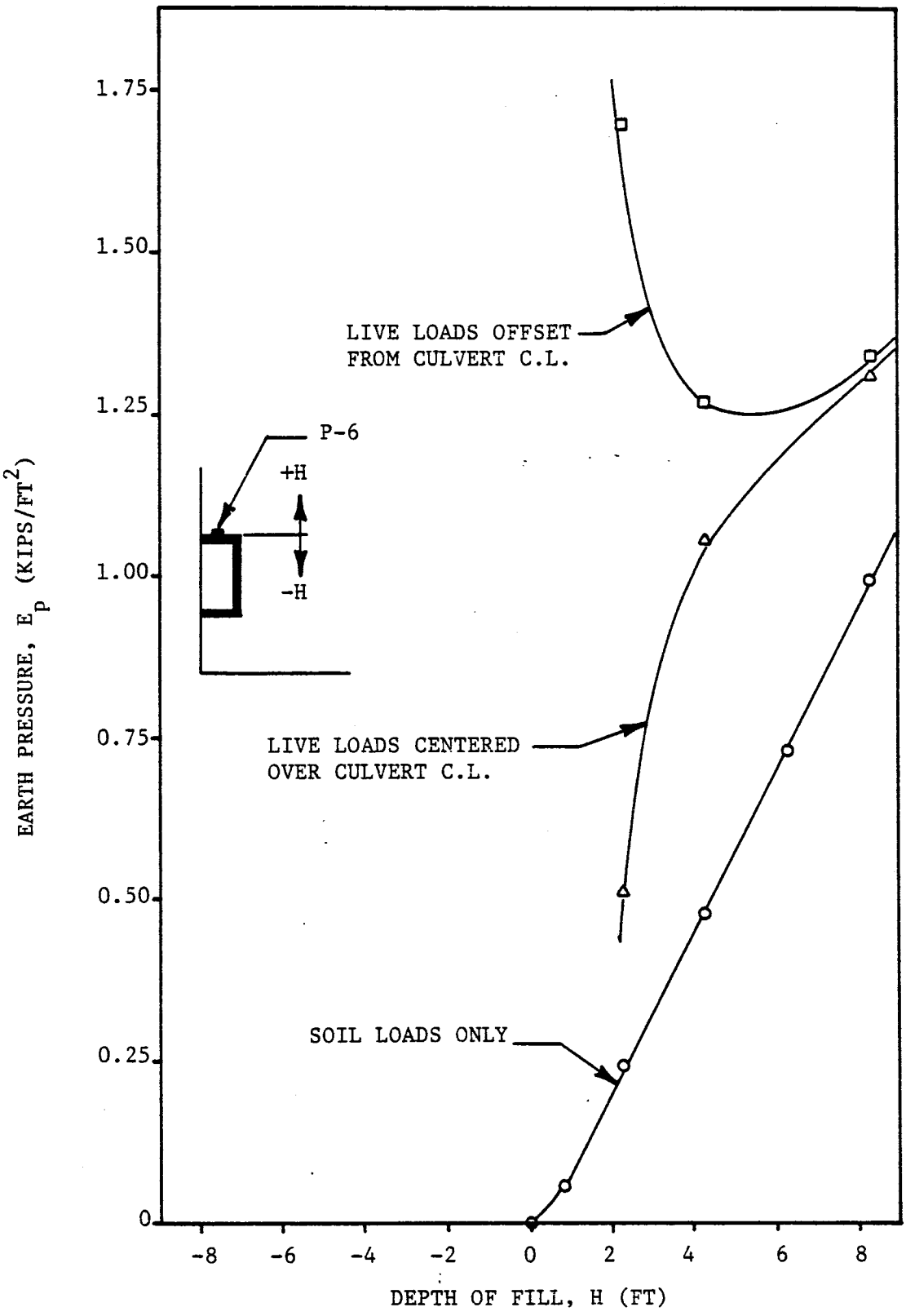

Variation of Earth Pressure with Depth of Fill for Pressure Cell P-6

FIGURE 4-11

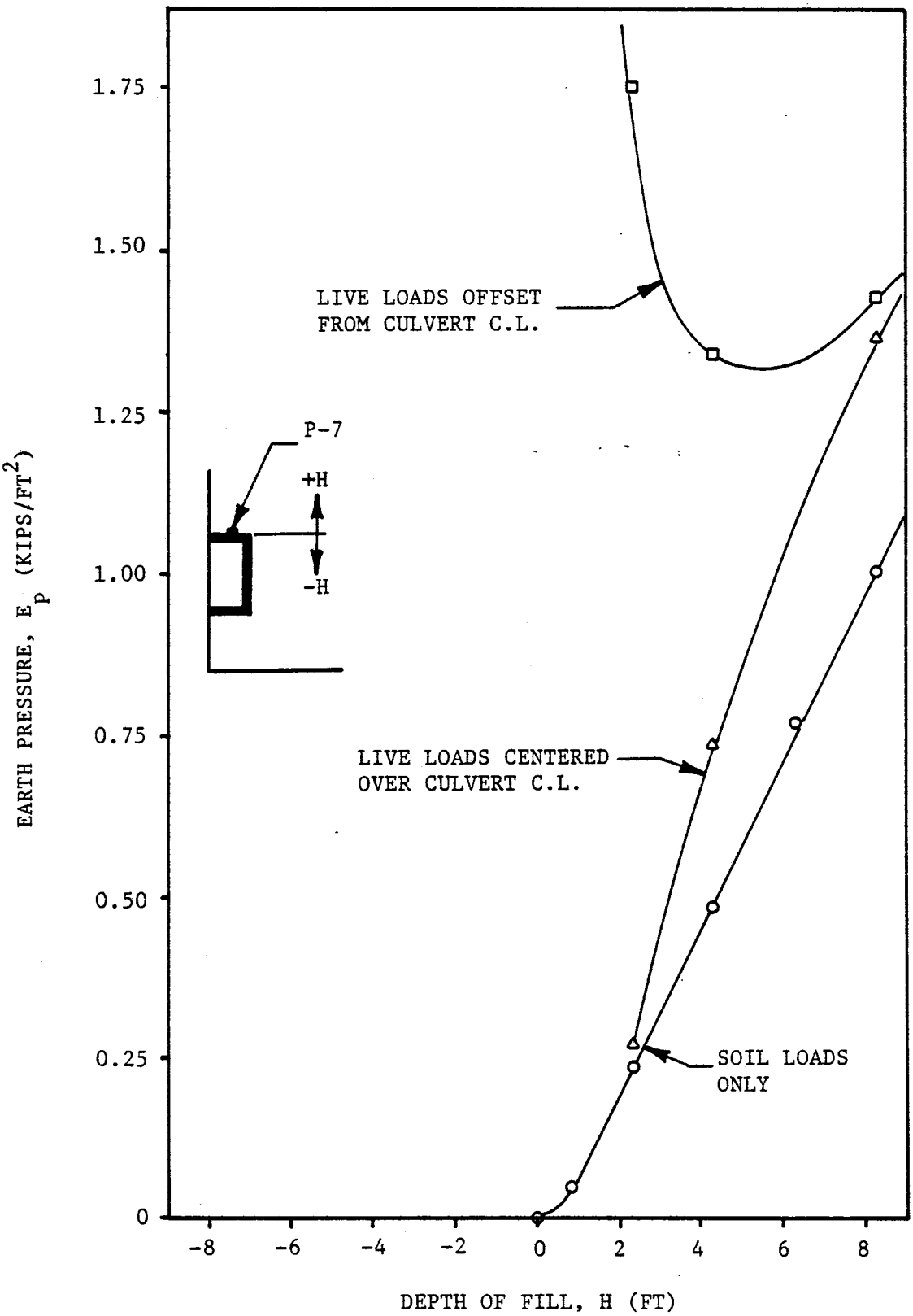

Variation of Earth Pressure with Depth
of Fill for Pressure Cell P-7

FIGURE 4-12

of application of the offset load, Figure 4-11 shows the same general trend. Here, the earth pressure for the offset load starts high with a small height of fill, and decreases with increasing depth. As before, the pressures tend to approach those values due to backfill only.

For pressure cell P-7, Figure 4-12 shows almost identical results as those in Figure 4-11. The pressures predicted for the offset load are slightly higher in magnitude, due to the fact that the point of application is directly above the pressure cell.

The predicted earth pressure distribution around the culvert for heights of fill of 2, 4, and 8 feet are given in Figures 4-13 through 4-15. In all three cases, the live loads produce very little effect on the bottom and sides of the culvert. The primary difference is produced along the top of the culvert. Here, as expected, as the depth of fill increases, the influence of the live load decreases.

4.3.2 Bending Moments

The distribution of bending moment around the culvert for depths of fill of 2, 4, and 8 feet are shown in Figure 4-16 to 4-18. As with the earth pressure distributions, there is very little difference due to the live load along the bottom and side of the culvert. The top slab exhibits the primary effects, with the 2 foot depth being the most critical. Also, it may be seen that the entire side of the culvert exhibits a negative moment, which indicates that this side is bowing outward due to the live load. This is very different from the bending moments induced by backfill loads alone, which exhibit points

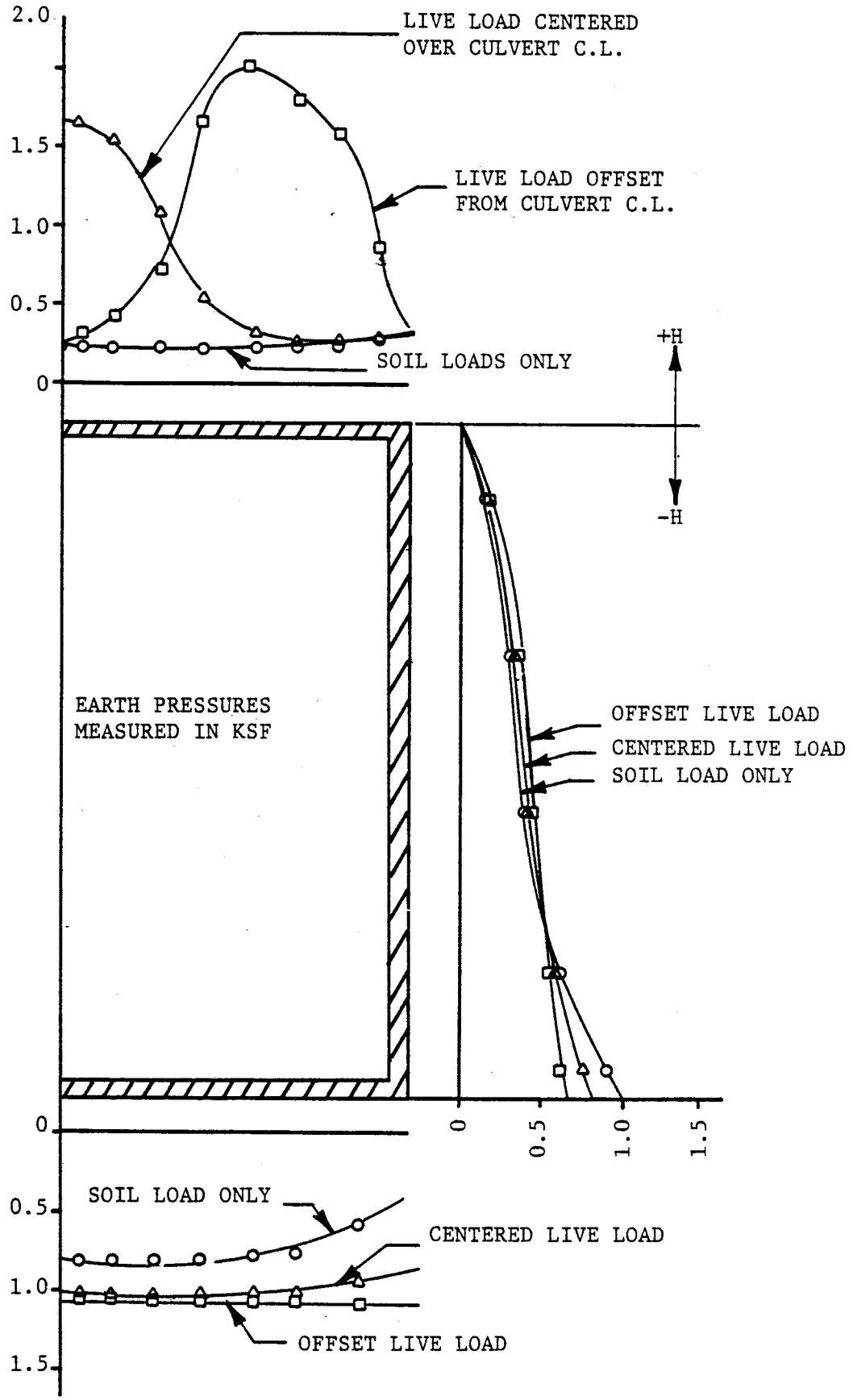

Distribution of Earth Pressure Around the Structure; H = 2'

FIGURE 4-13

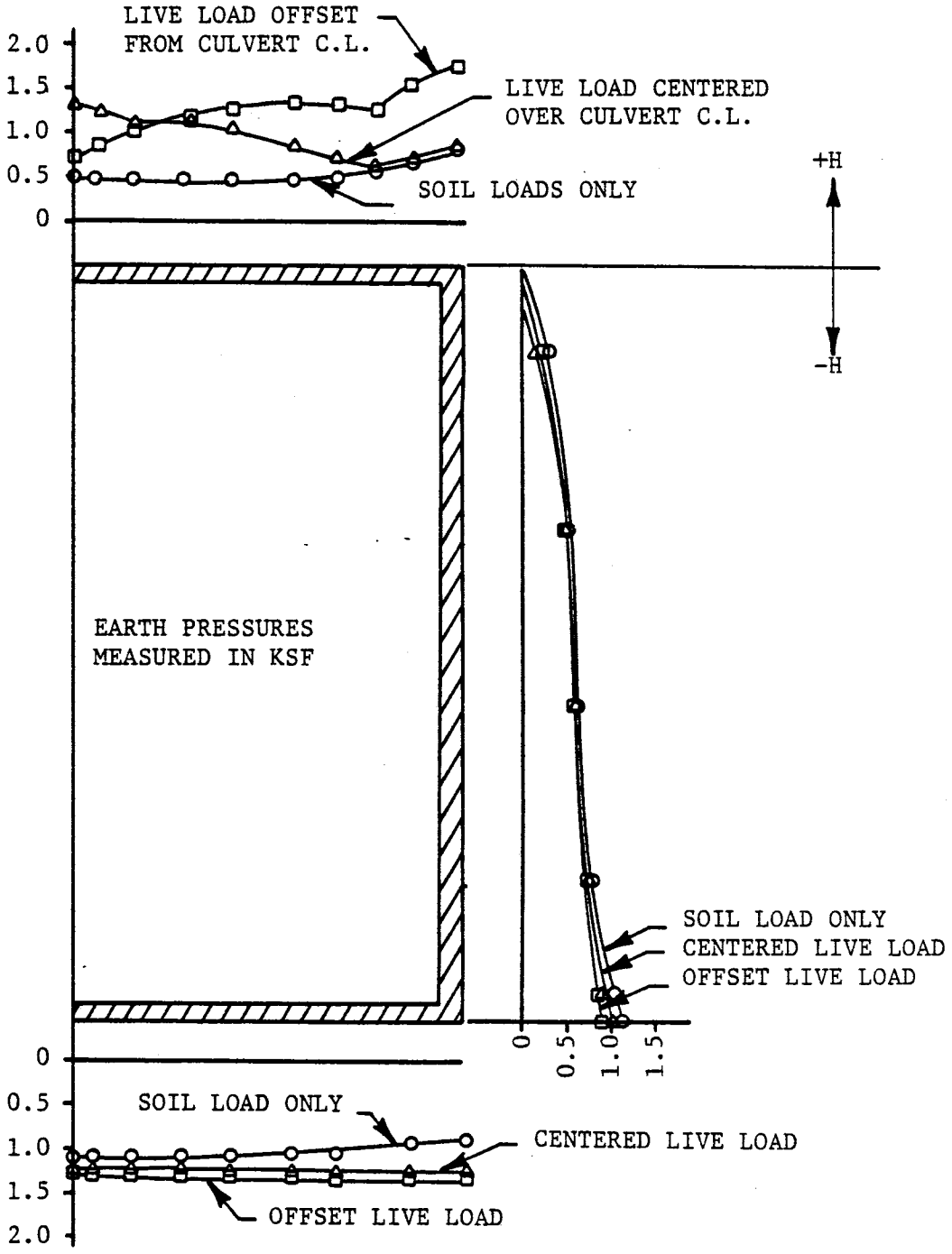

Distribution of Earth Pressure Around
the Structure; H = 4'

FIGURE 4-14

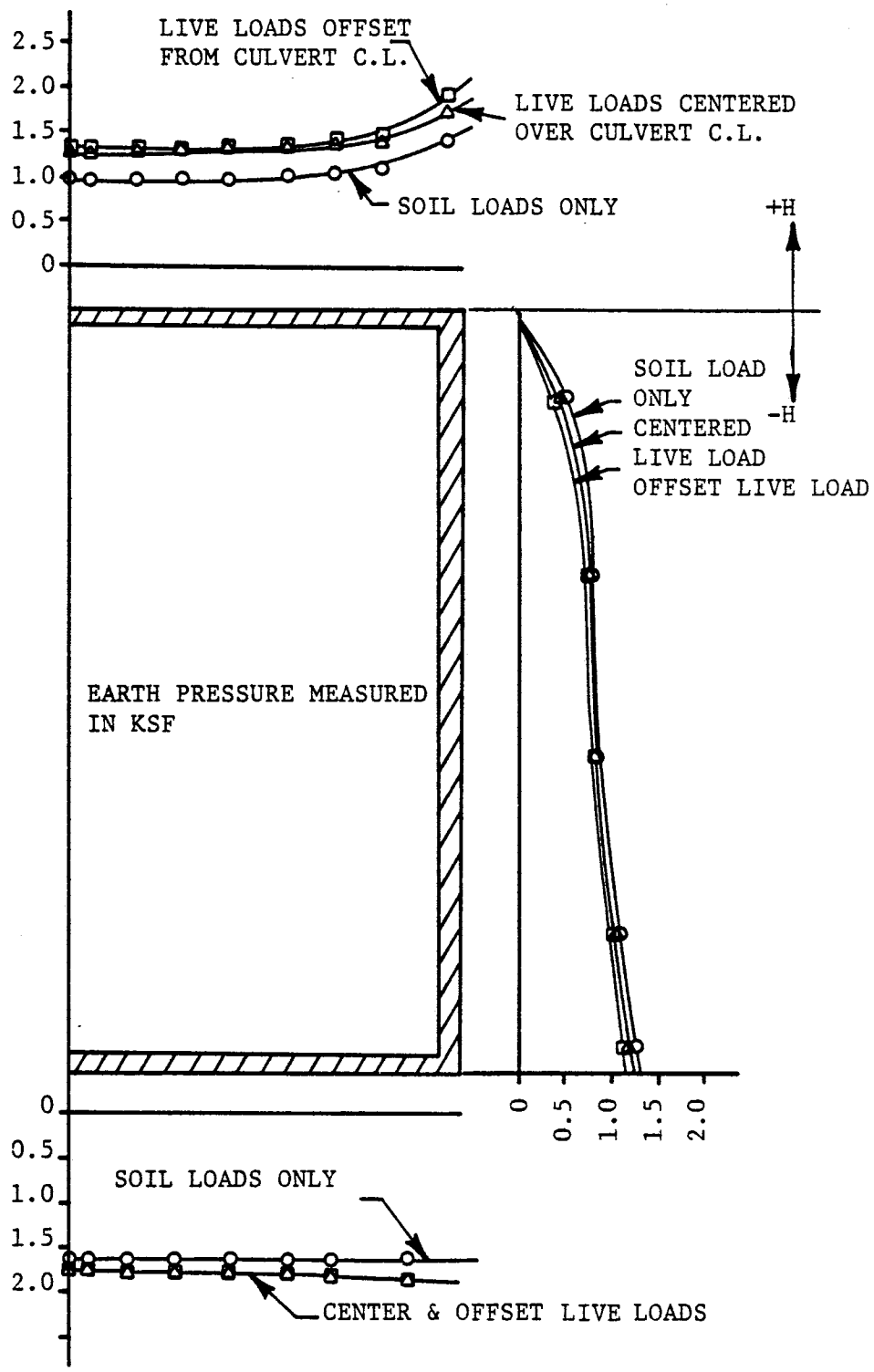

Distribution of Earth Pressure Around the Structure; H = 8'

FIGURE 4-15

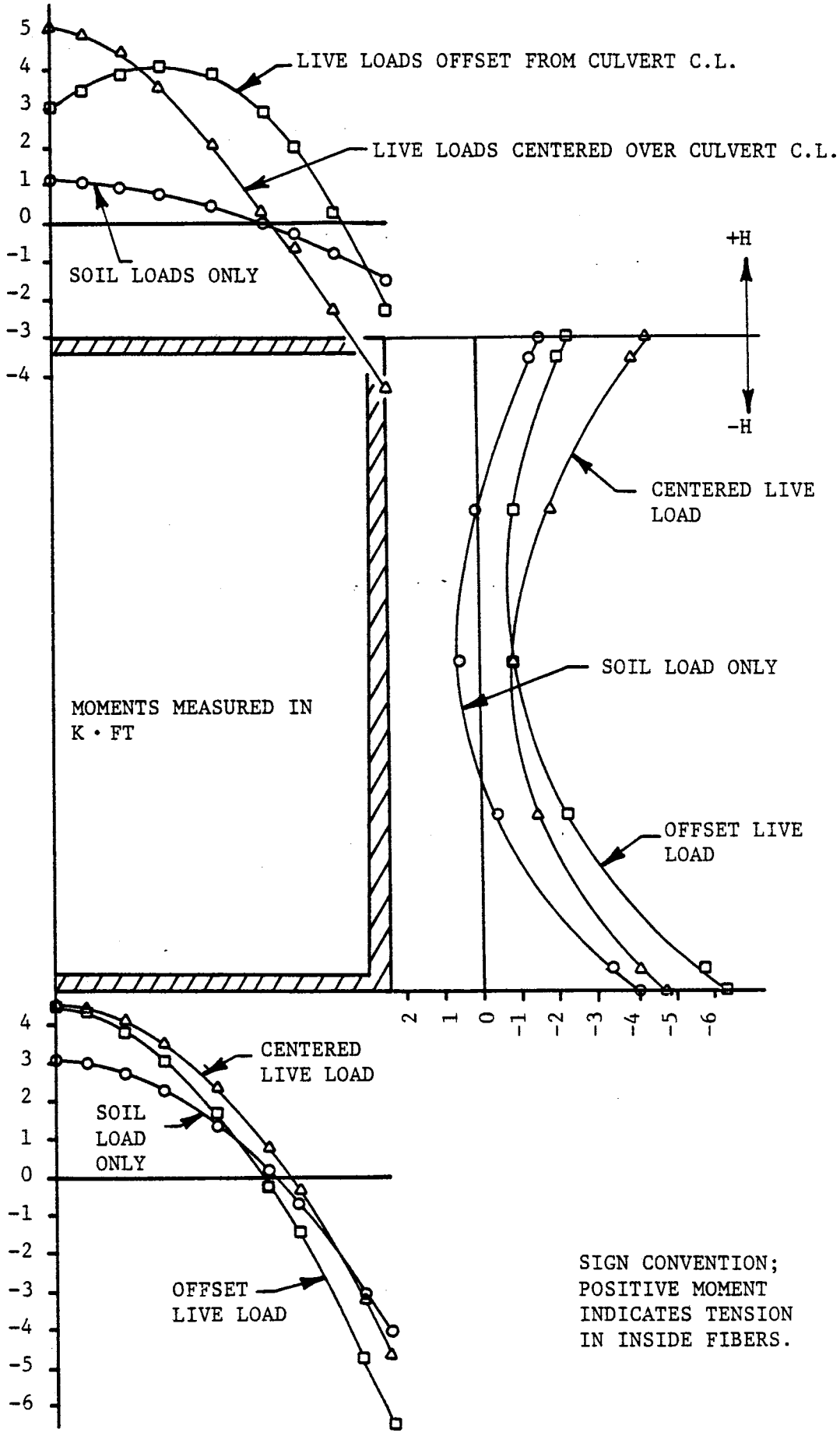

Moment Distribution Around Structure with H = 2'

FIGURE 4-16

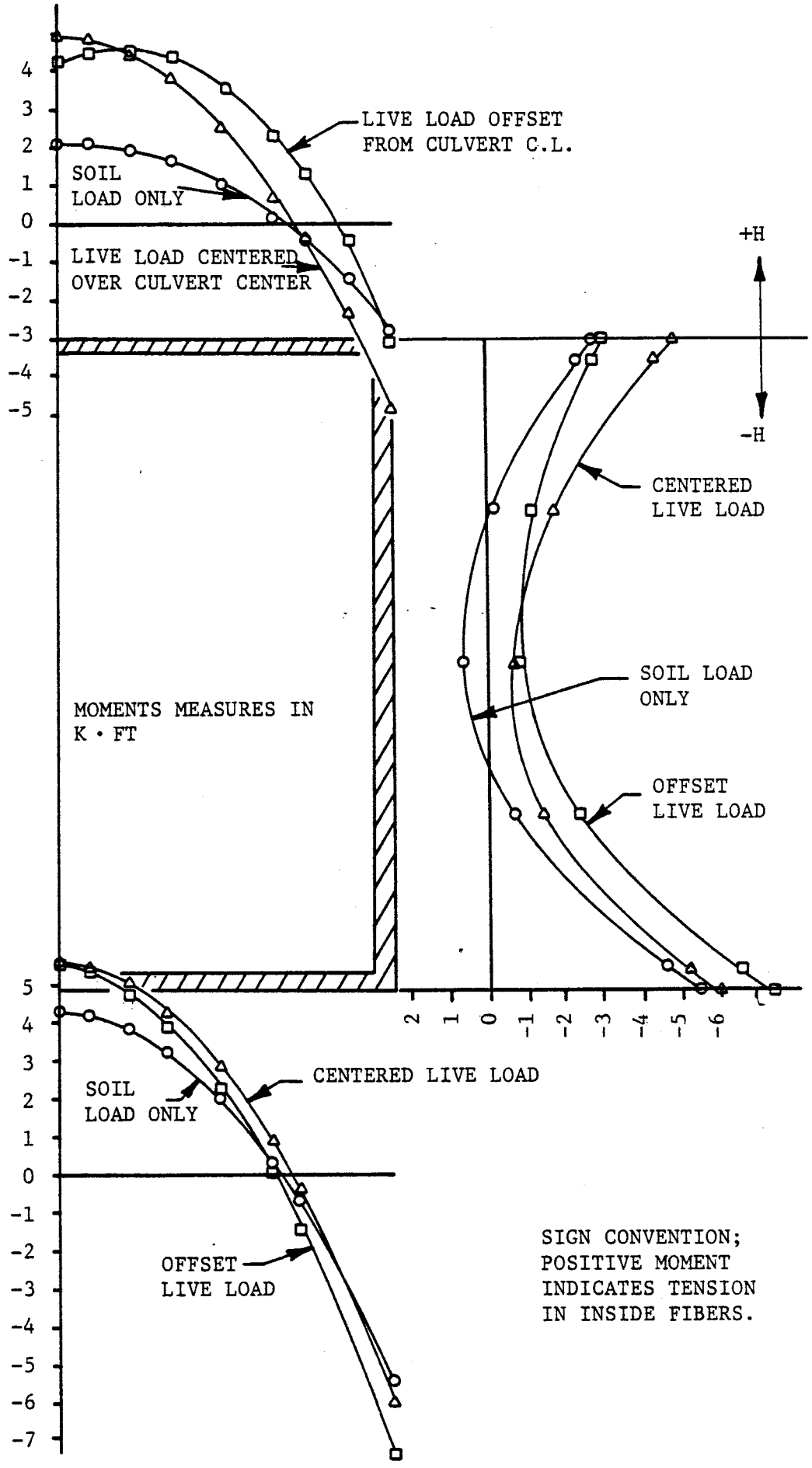

Moment Distribution Around Structure with H = 4'

FIGURE 4-17

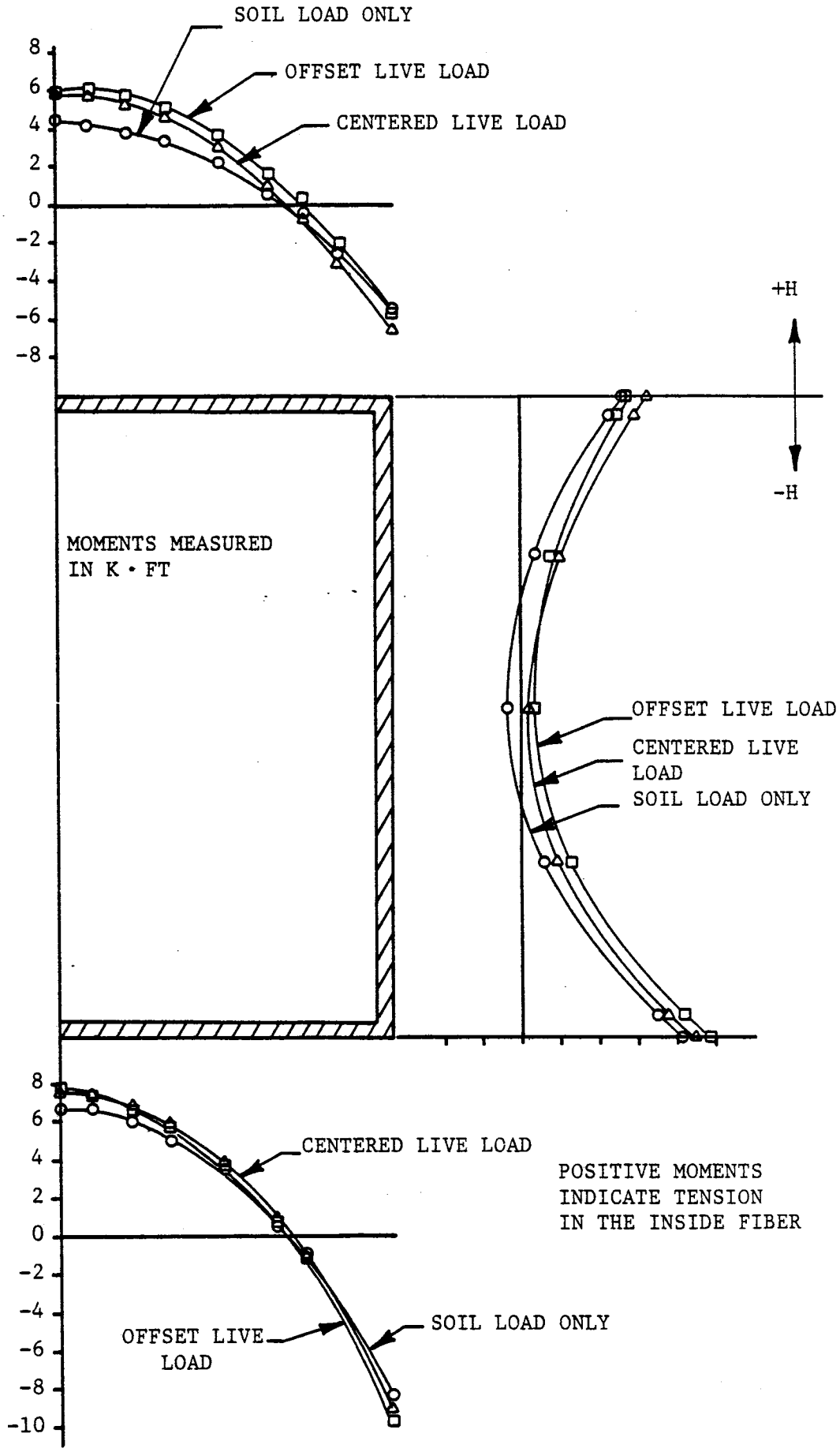

Moment Distribution Around the
Structure with H = 8'

FIGURE 4-18

of inflection and a region of positive moment in the center of the wall.

4.3.3 Shear Forces

The shear force distribution around the culvert for depths of fill of 2, 4, and 8 feet are shown in Figures 4-19 to 4-21. As with the earth pressures and bending moments, the live loads produce negligible effects in the bottom slab and the walls. Along the top slab, the center load produces the greatest shear values for a depth of fill of 2 feet. As the depth of fill increases, the effects of the live load decrease and approach the values due to backfill only.

4.3.4 Stresses and Strains

The variations of stress with depth of fill for the extreme fibers of critical sections are shown in Figure 4-22 to 4-25. The critical sections considered include the center of the top slab, and the top corner of the culvert. These points correspond to the placement of electrical strain gages in the companion field study.

The inside fiber stresses for the top center of the culvert are shown in Figure 4-22. The application of live loads causes an increase in the stresses of this section. Also, the center loading condition exhibits the most critical results. Both loading conditions seem to begin to approach the results of the soil loads only as the depth of fill increases.

Similar trends are shown for the outside fiber stresses in Figure 4-23. The centered live load produces the greatest difference, and

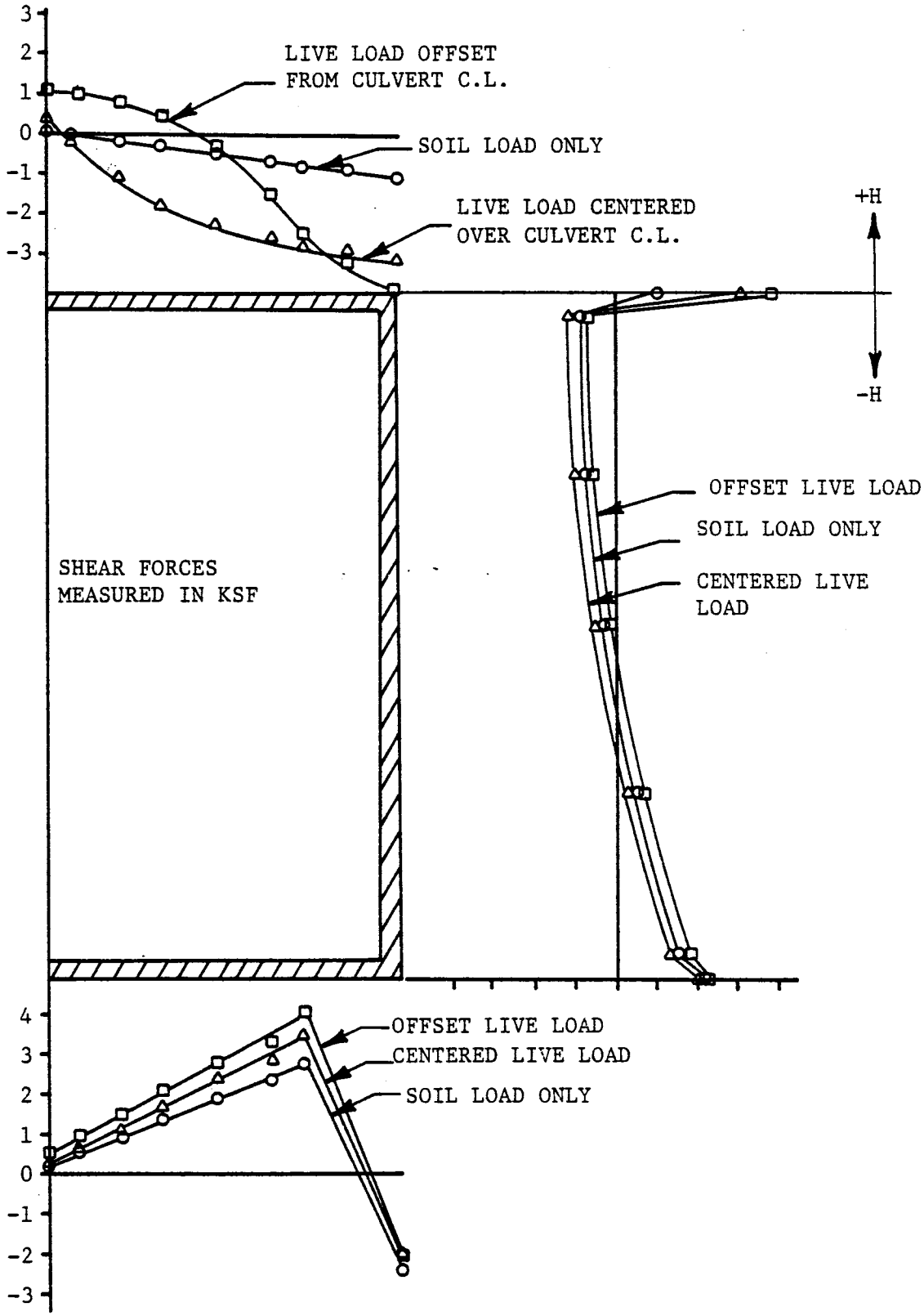

Distribution of Shear Force
with H = 2'

FIGURE 4-19

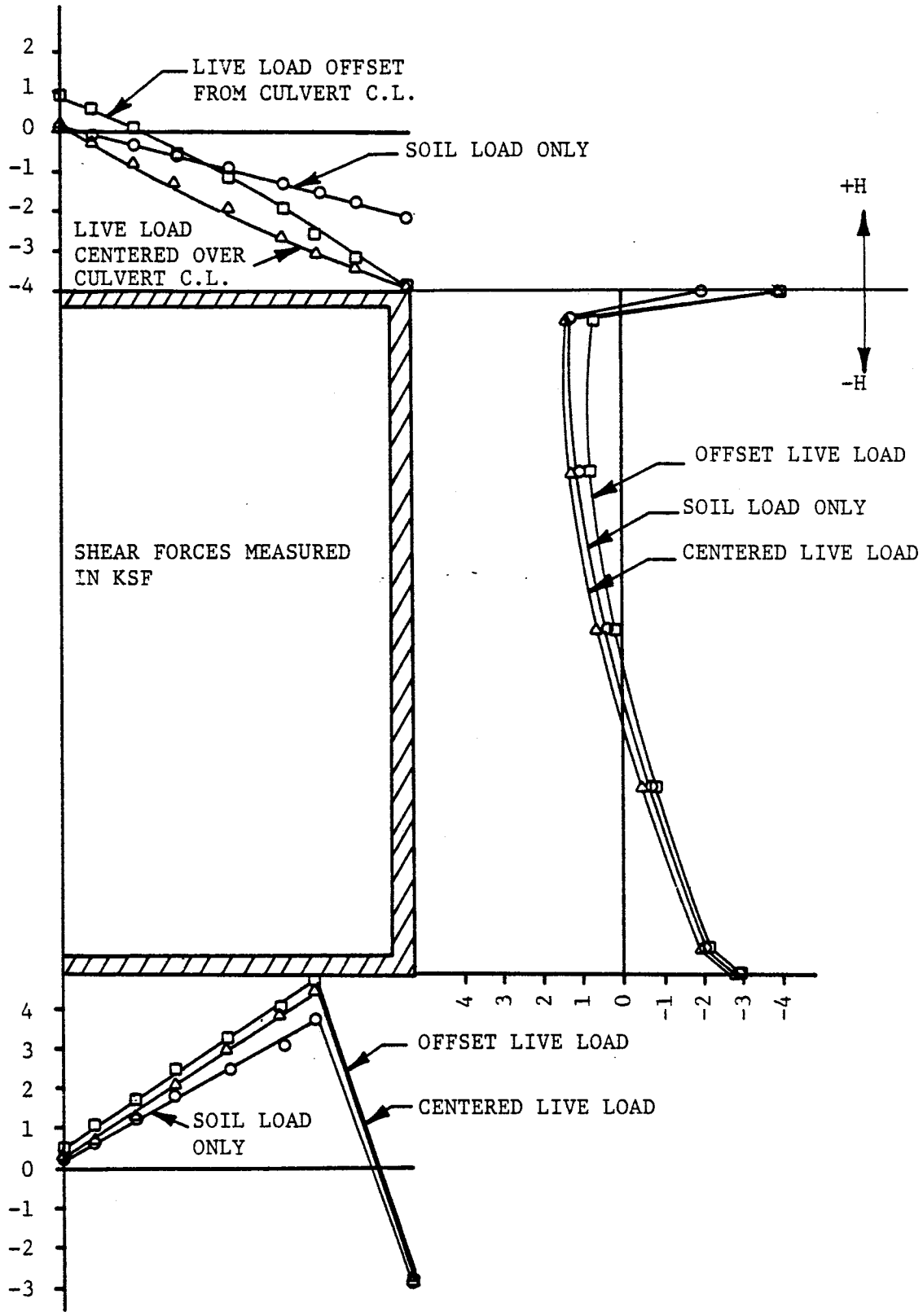

Distribution of Shear Force
with H = 4'

FIGURE 4-20

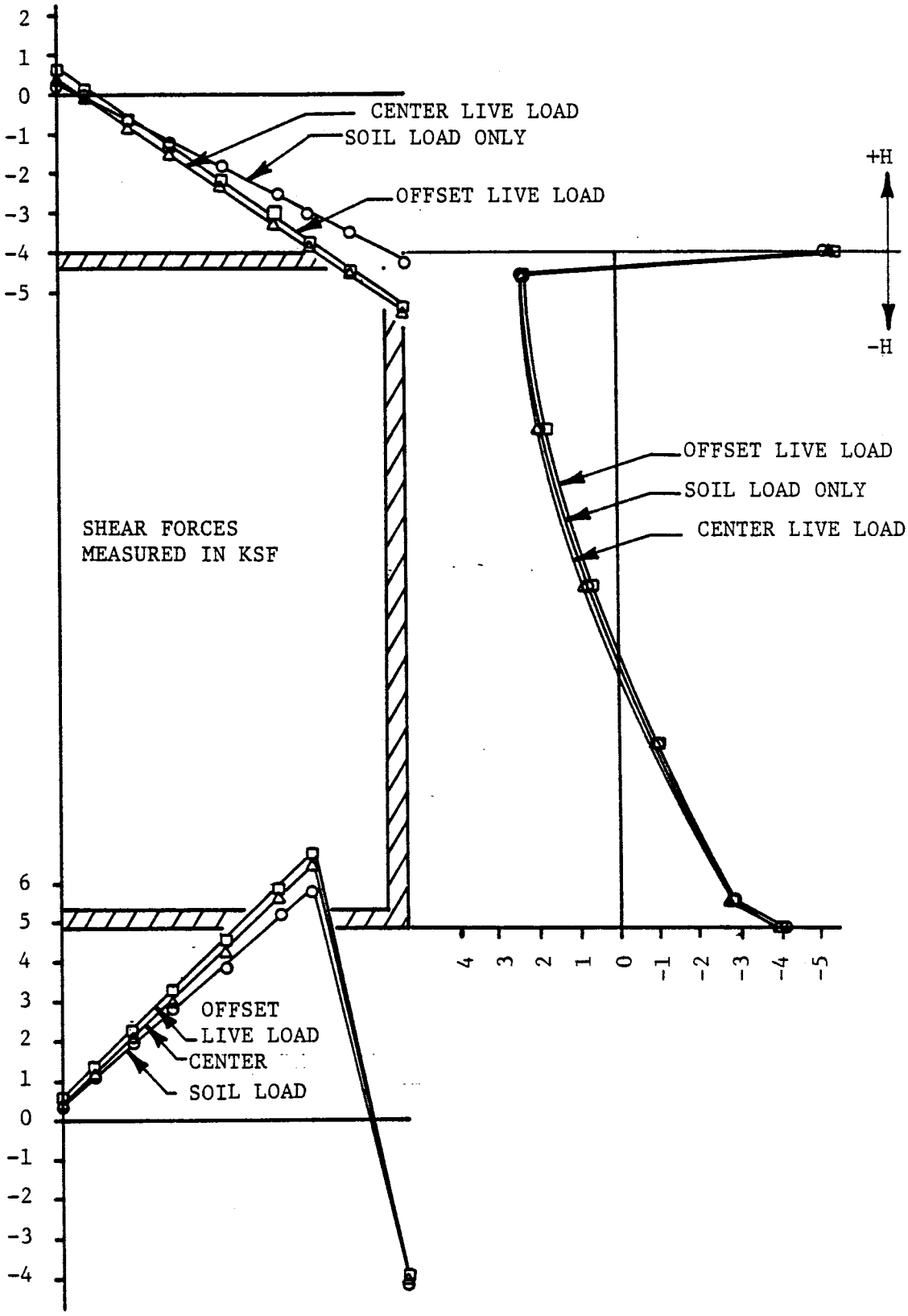

Distribution of Shear Force
with H = 8'

FIGURE 4-21

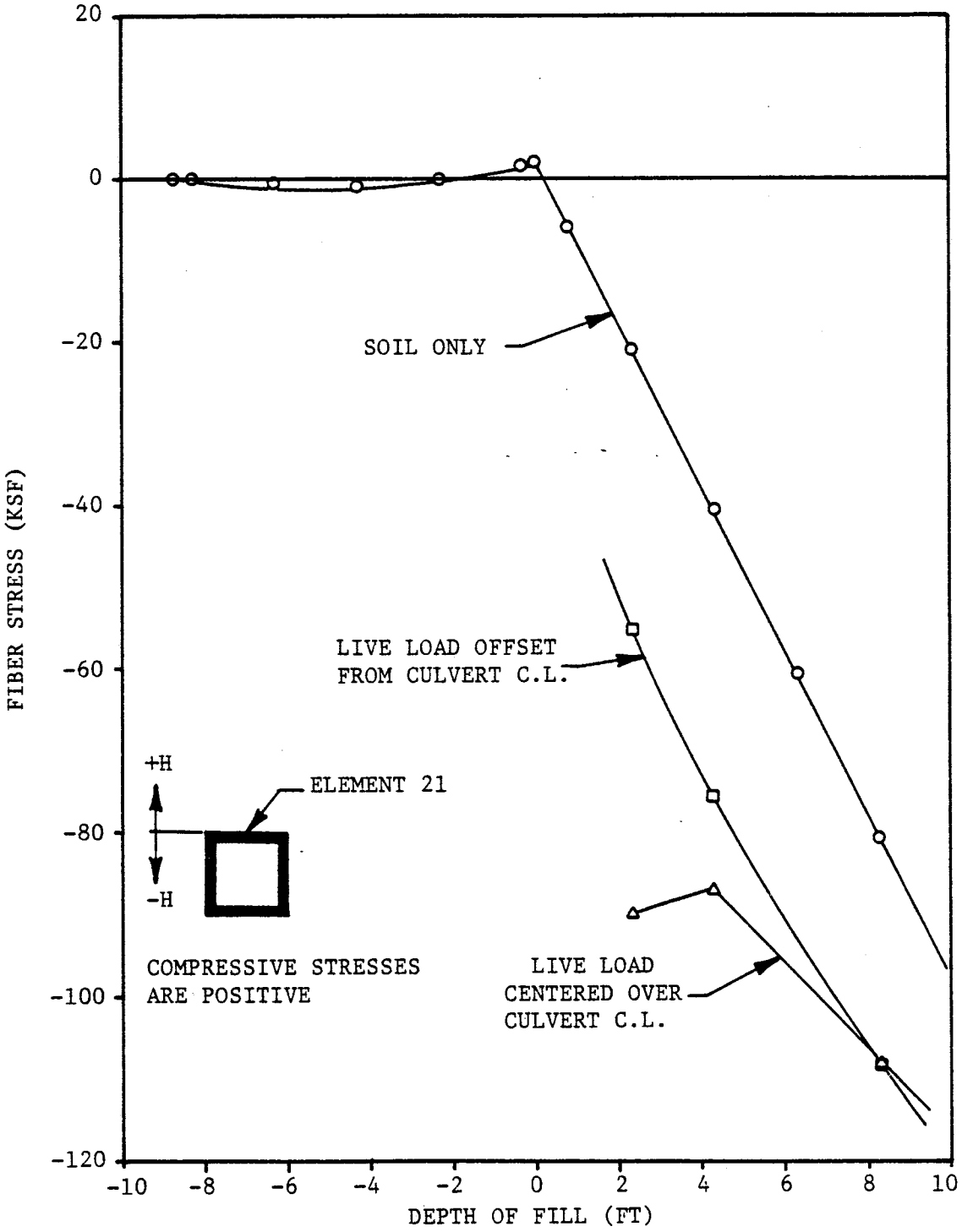

Variation of Fiber Stress with Depth
Inside Stress, Element 21

FIGURE 4-22

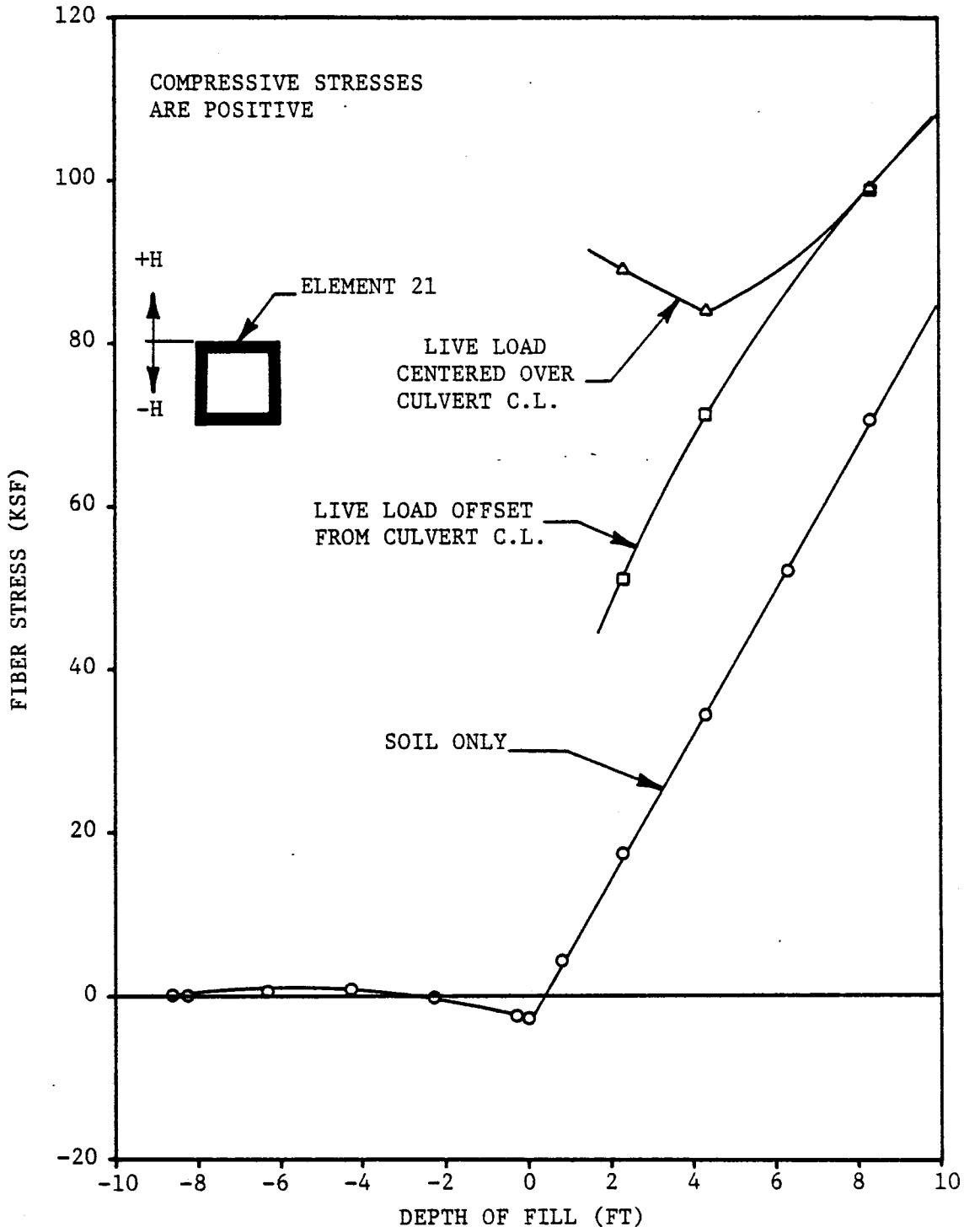

Variation of Fiber Stress with Depth
Outside Stress, Element 21

FIGURE 4-23

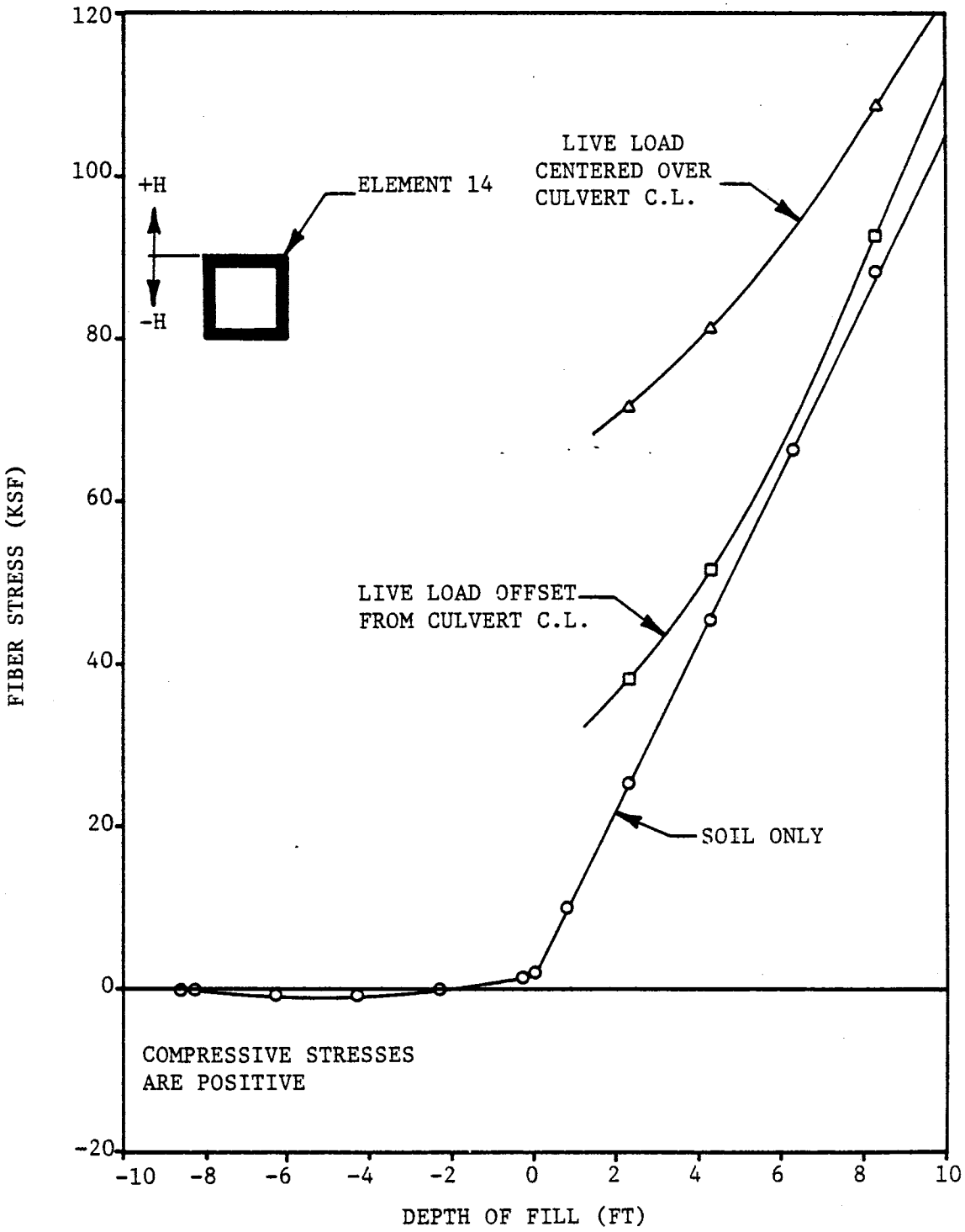

Variation of Fiber Stress with Depth
Inside Stress, Element 14

FIGURE 4-24

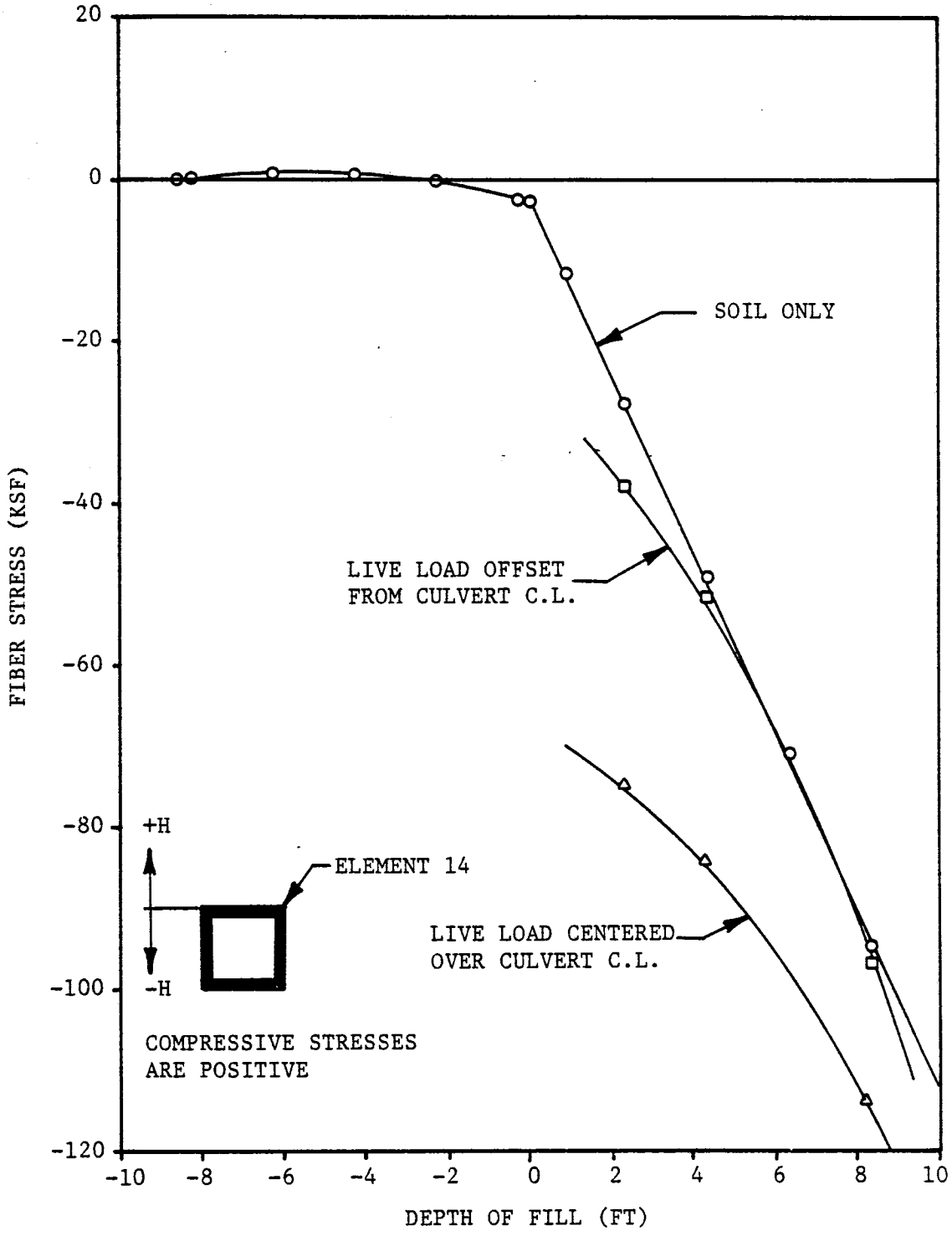

Variation of Fiber Stress with Depth
Outside Stress, Element 14

FIGURE 4-25

the stresses tend to approach those for the soil loads only as the depth of fill increases. There is a decrease in stress as the depth of fill changes from 2 to 4 feet. This may be explained by noting that as the depth of fill increases, greater load distribution is obtained. With only 2 feet of fill, however, significant influence from the live load is noticed as a result of the location of the applied load.

For the top corner of the culvert, the variation of the inside fiber stress with depth of fill is shown in Figure 4-24. Here, there is very little influence from the offset live load. This may be explained by an arching effect around the corner of the culvert, causing a load reduction in this area. This effect was previously shown in the earth pressure diagrams for this same region of the culvert.

The outside fiber stresses for the top corner of the culvert are shown in Figure 4-25. As with the inside fiber stresses, the offset load produces very little effect on the predicted results. Also, as the depth of fill increases, the live load influence decreases.

The variation in strain with depth of fill for the center of the top slab is shown in Figure 4-26. These results were reduced using the fiber stress results and assuming a linear strain distribution across the section. This assumption is considered valid because of the relatively small values of strain encountered in reinforced concrete analysis and design. For this section, the centered live load produces the most critical results due to the application of the load directly above the section being considered.

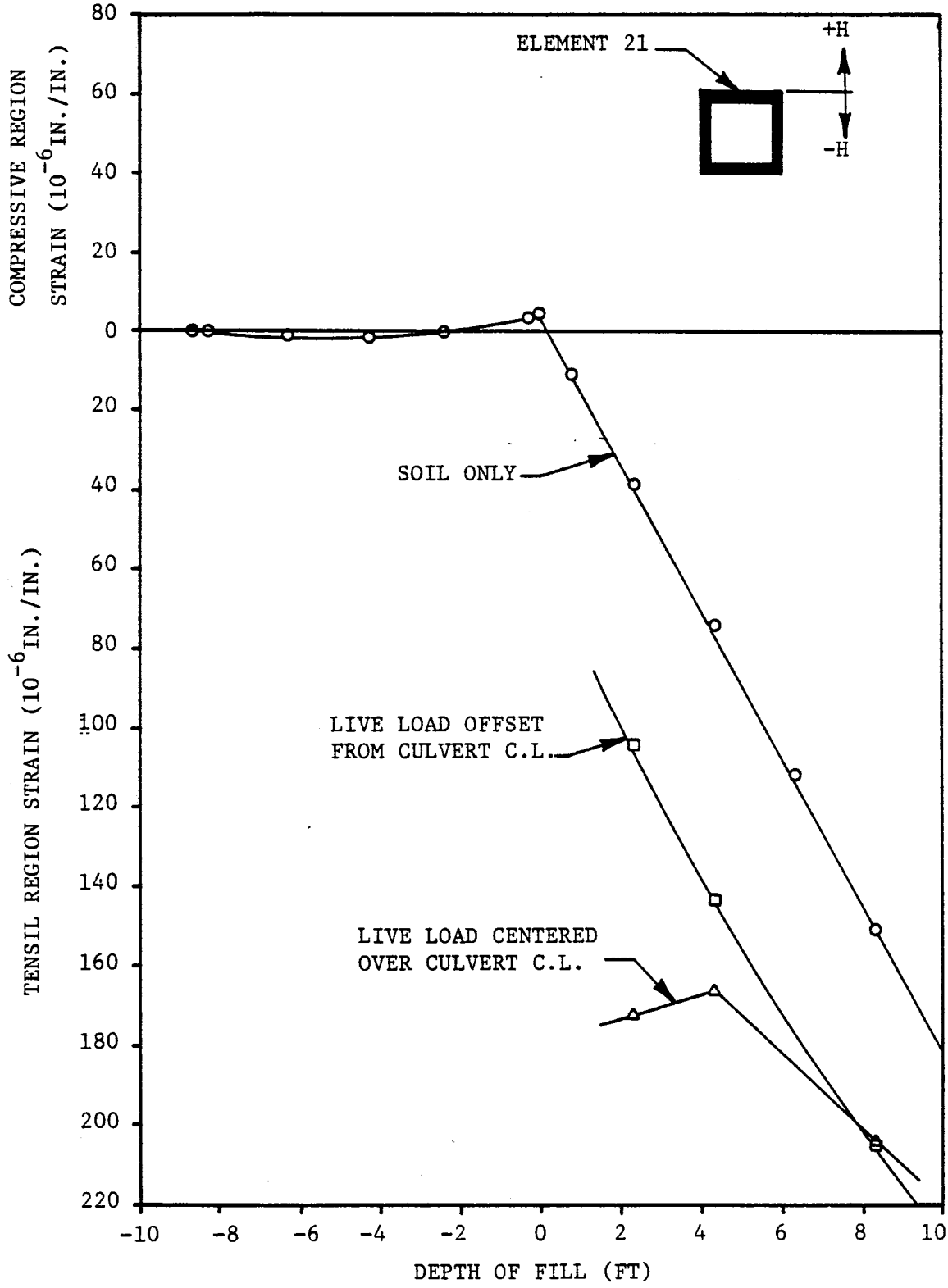

Variation of Strain with Depth
Strain Gage SG-1, Element 21

FIGURE 4-26

For the top corner of the culvert, the variation in strain with depth of fill is shown in Figure 4-27. The center live load produces the largest effect, with very little influence produced as a result of the offset live load. The values tend to approach those of the soil loads only as the depth of fill increases.

4.3.5 Deflections

The predicted variation in crown deflection with depth of fill is shown in Figure 4-28. The applied live loads produce slightly greater deflections, with the deflection increasing linearly with depth of fill. The effects of both centered and offset live loads seem to be identical, with the influence of the applied live load decreasing as the depth of fill increases.

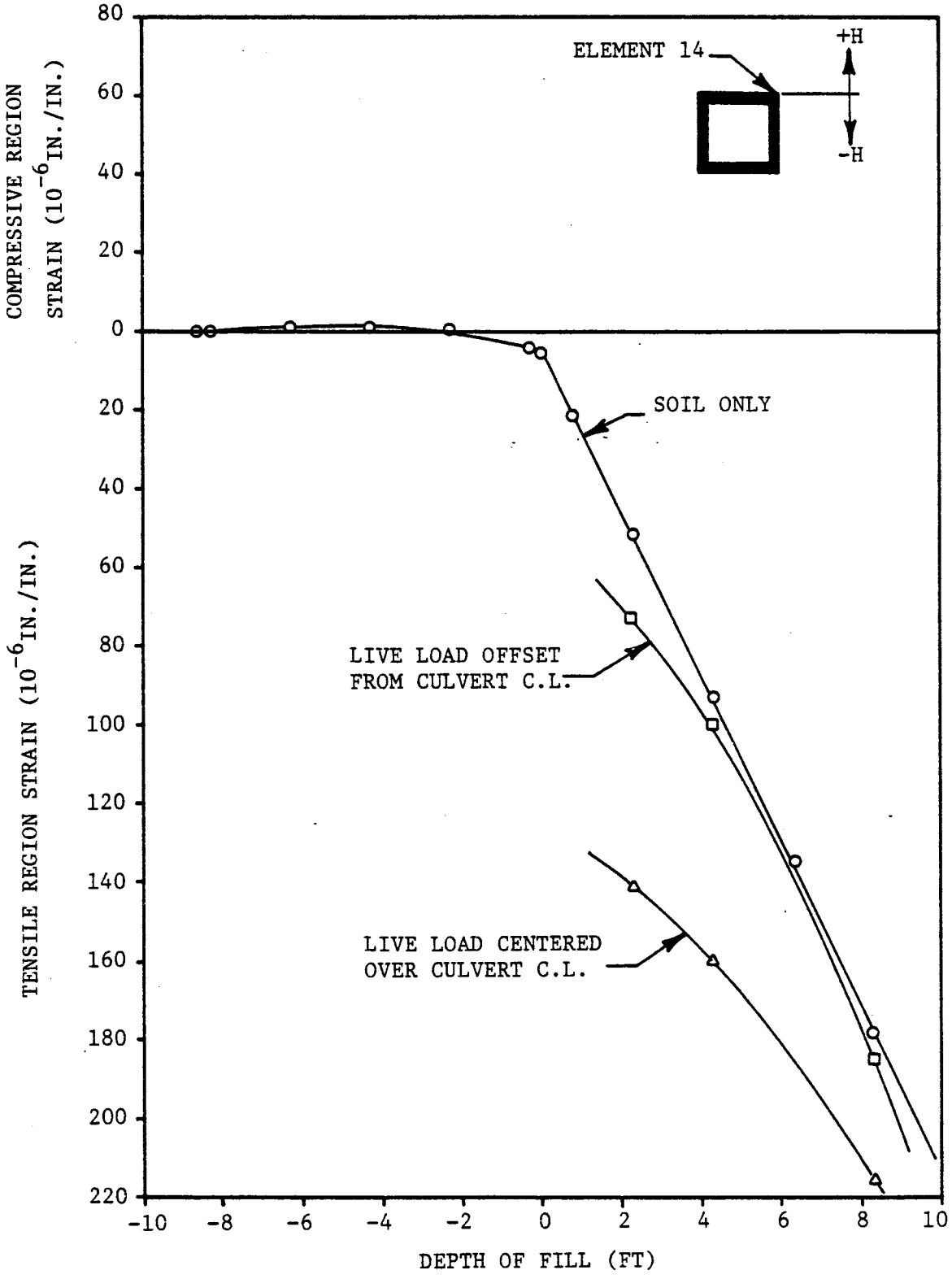

Variation of Strain with Depth
Strain Gage SG-2, Element 14

FIGURE 4-27

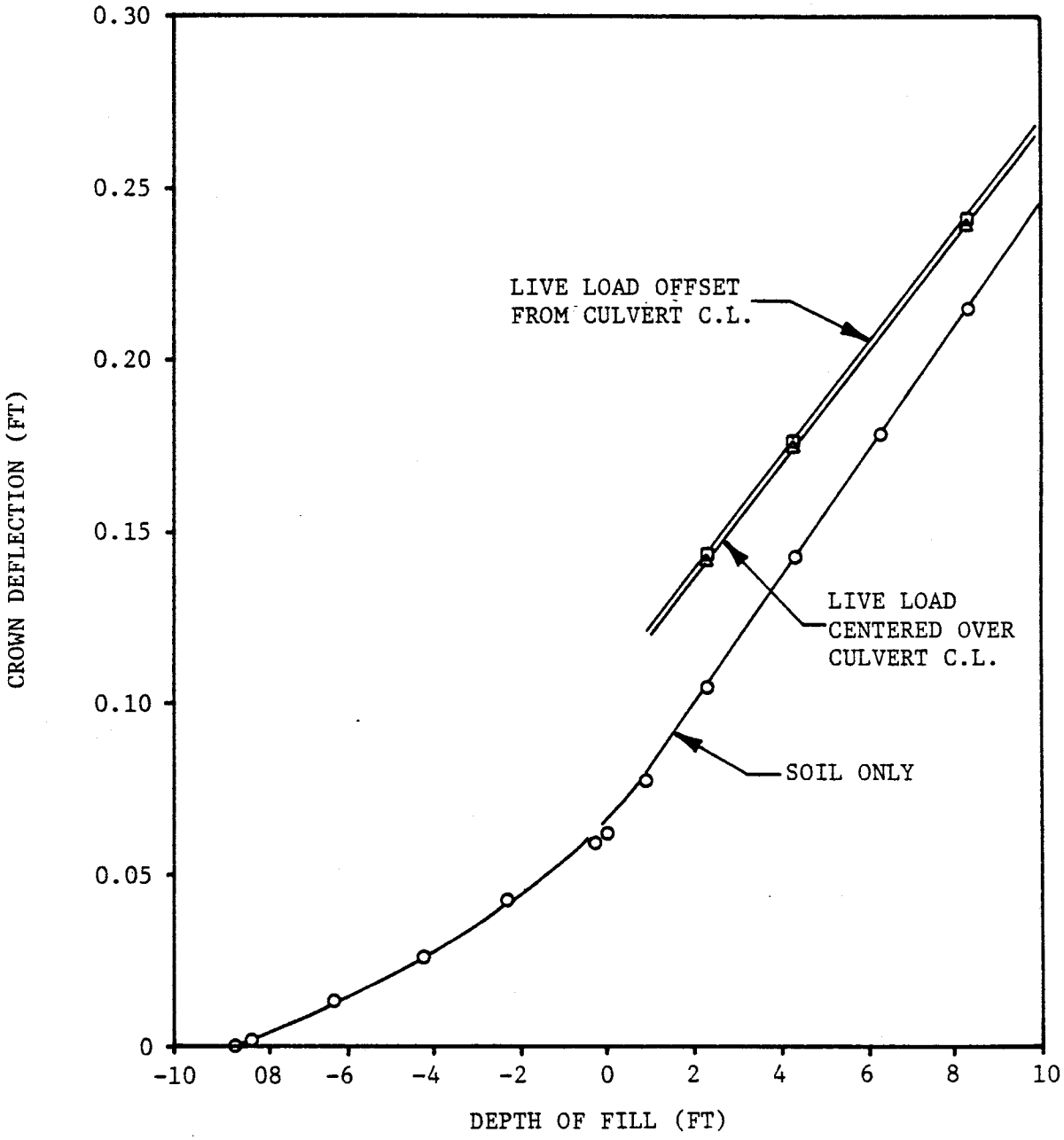

Variation of Crown Deflection with
Depth of Fill

FIGURE 4-28

CHAPTER 5

COMPARISON OF FINITE ELEMENT RESULTS WITH FIELD OBSERVATIONS

5.1 Introduction

In order to verify the validity of the finite element predictions of the behavior of the R. C. box culvert, a comparison of the results of the analyses and the field data from the instrumented box culvert has been made. The field measurements were limited to measured earth pressures under fill heights of up to 8 feet above the crown of the culvert. The field data presented herein are somewhat of limited scope, therefore the results of this section should not be considered for design without further reference to the final results of the field instrumentation study presently being conducted by the Texas Transportation Institute, Texas A&M University, Study No. 2-5-81-294, entitled "Determination of Earth Pressures on Reinforced Concrete Box Culvert".

5.2 Field Measurements

Field instrumentation of the 8' x 8' R.C. box culvert consists of 15 Terra-Tec T9010 pressure cells, and 5 Slope Indicator 51482 pressure cells. These cells are located on both vertical walls, and on the top slab of the box culvert as shown in Figure 5.1 The Slope Indicator cells are shown as cell numbers 1 through 4, and 20, with the remaining cells being Terra-Tec pressure cells.

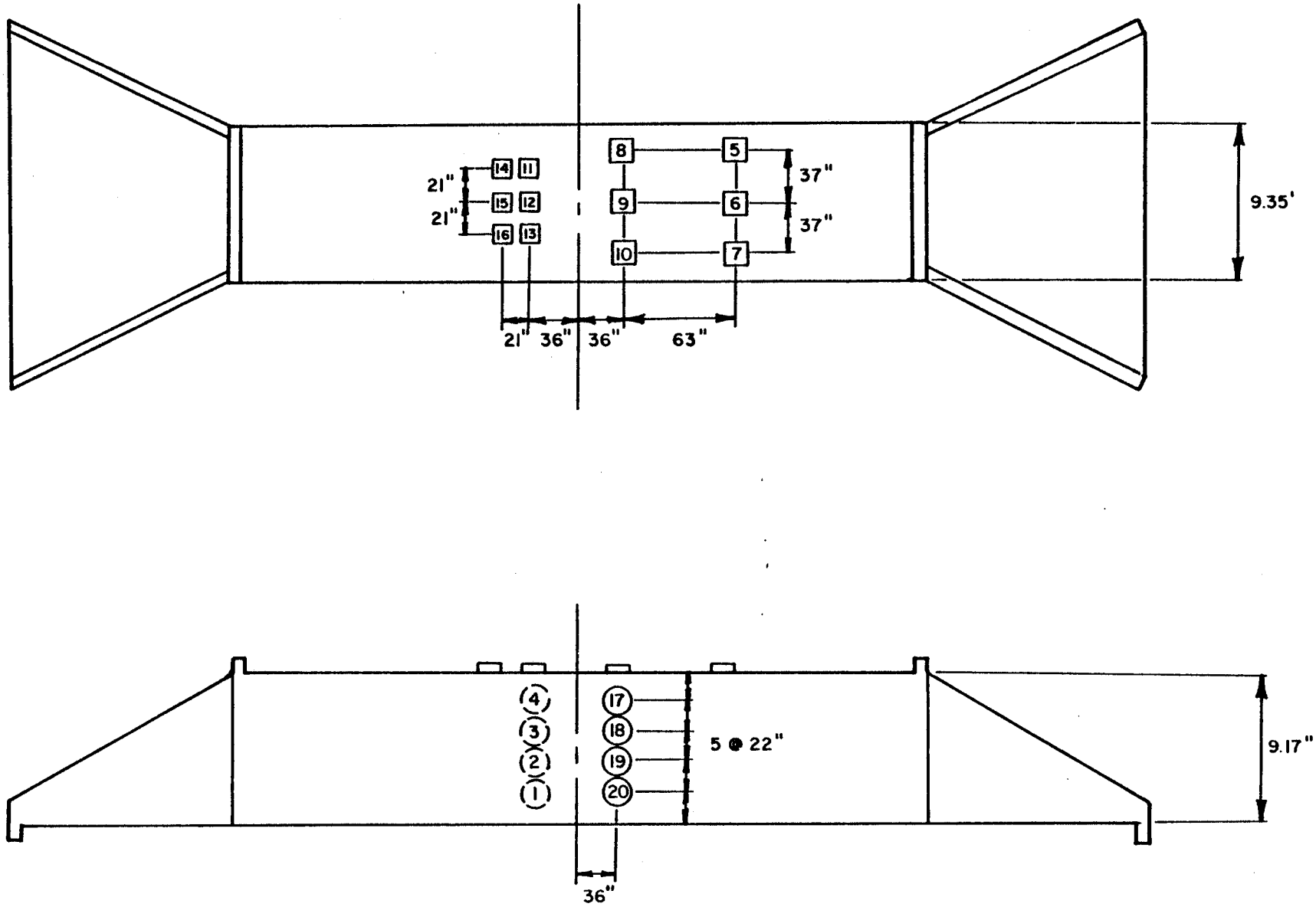

Instrumentation of the R. C. Box Culvert

FIGURE 5-1

Calibration procedures for the pressure cells include temperature and offset pressure corrections and a hydraulic calibration of the cells to test the accuracy of their measurements. In order to calibrate the cells for temperature effects and offset pressures, pressure measurements were taken after the cells had been mounted on the culvert, but prior to any placement of backfill. These readings were taken at temperatures ranging from 49°F to 80°F in order to determine the variation of measured pressure with temperature. Using these data, a relationship between the pressure and the temperature was developed. Subsequent pressure cell measurements were accompanied by temperature readings so that the appropriate correction could be applied to the pressures measured. This correction also includes the effects of the offset pressure built into the pressure cell itself. This offset pressure is a small preload built into the cell to insure that no negative pressures are measured. By calibrating the cells at zero pressure and at various temperatures, this offset pressure correction can be included.

In order to test the accuracy of the pressure cells, a hydraulic pressure calibration procedure was performed in the laboratory. This involved the use of a hydraulic pressure tank in which a pressure cell was mounted so that a known constant pressure could be applied to the cell. Pressures ranging from 0 to 40 psi were used to test the pressure cell. It was determined that above 20 psi the pressure cells gave reasonably accurate measurements. However, below 2 psi the pressures measured were erratic, and should be considered as such in the field measurements. It should be noted that much of the data available

were less than 2 psi, therefore scatter in the data is unavoidable.

In addition, the accuracy and the reliability of pressure cells of this type are known to depend on various other parameters, including the flow rate of nitrogen used during pressure measurements and the procedures used for the installation of these pressure cells on the culvert. A careful control of these parameters is required to insure the reliability of the results.

The variation in measured earth pressure with depth of fill for pressure cells 1 and 20 is shown in Figure 5-2. When the depth of fill is 2 feet from the bottom of the culvert (-6 feet from the crown), unreasonably high earth pressures were recorded. At this point, only 2 inches of fill was covering the pressure cells, therefore the measured earth pressure should be very close to zero. It is thought that this measurement could have been influenced by the movement of construction equipment around the culvert at the time these measurements were taken.

The earth pressures measured for pressure cell 20 are greater than those for cell 1, with the difference being as great as 0.30 ksf at higher fill levels. This may be an indication of uneven compaction of fill material, or simply a natural variance in pressure cell readings at very low pressures.

With the height of fill at 8 inches above the crown of the culvert, earth pressure measurements were taken on a number of days. The pressures changed with time, but there appears to be no correlation between the length of time and the changes in measured earth pressures.

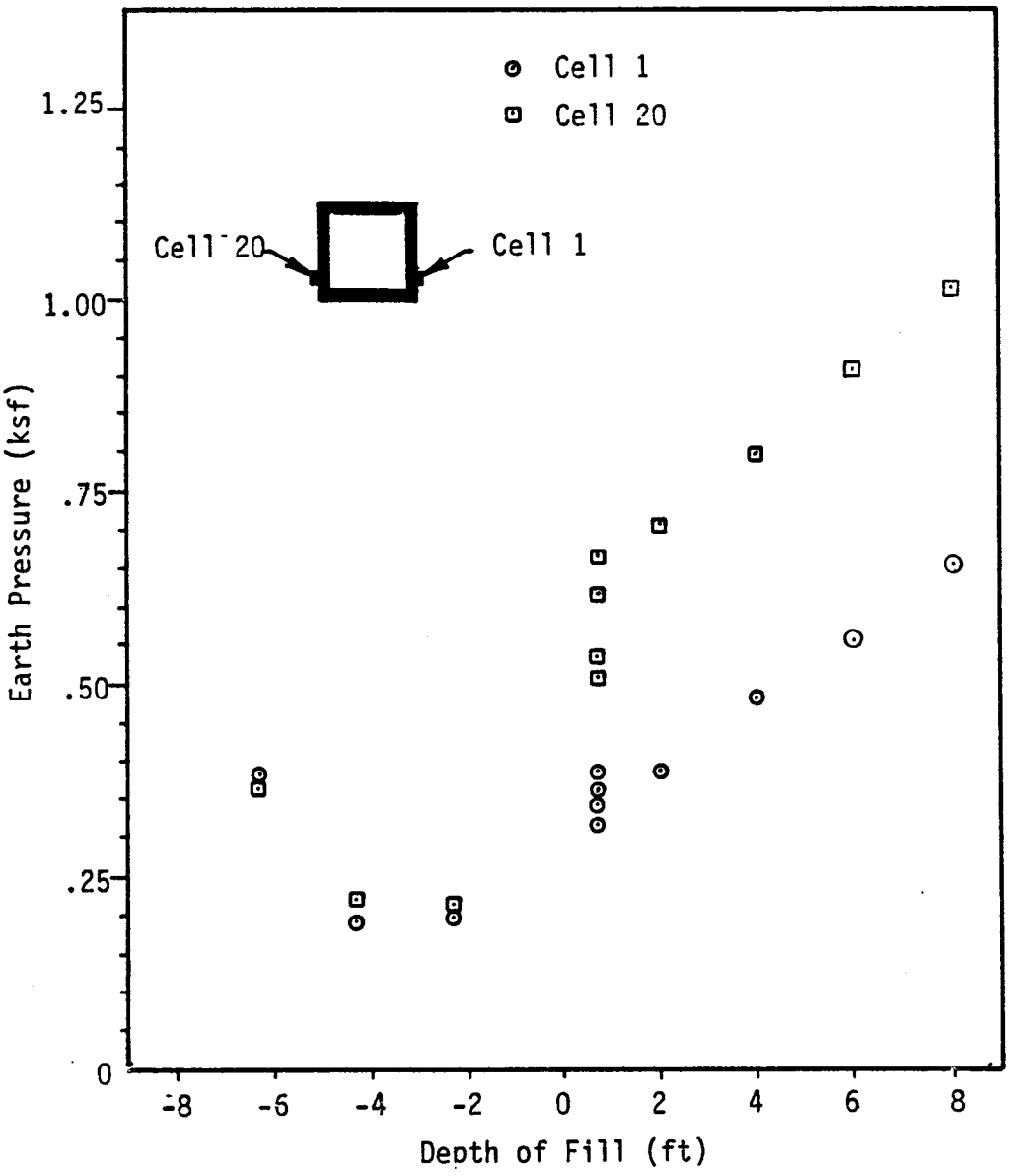

Field Data for Pressure Cells 1 and 20; Soil Loads Only
Variation of Earth Pressure with Depth of Fill

FIGURE 5-2

The variation in measured earth pressure with depth of fill for pressure cells 2 and 19 is shown in Figure 5-3. The values seem to be reading 0.20 ksf too high, as shown by the measured earth pressures at a height of fill of -6 feet, when no backfill material has been placed above the level of the pressure cells. This may be an indication that the total effect of the offset pressure has not been completely subtracted out of the measured values. Also, for lower levels of fill, the measured earth pressures for pressure cell 2 are larger than those for pressure cell 19. However, when the depth of fill exceeds the crown of the culvert, the pressures measured by cell 19 become greater than those for cell 2. This may be due to the difference in the type of pressure cells. As stated previously, cell 2 is a Slope Indicator cell, while pressure cell 19 is a Terra-Tec cell.

The variation in earth pressure with depth of fill for pressure cells 3 and 18 is shown in Figure 5-4. Before the level of fill exceeds the height of the pressure cells, both cells indicate almost zero pressure. However, after only a few inches of fill has been placed above the height of the pressure cells, measurements of approximately 0.40 ksf are shown. These values seem unreasonably high for the small amount of backfill material covering the pressure cells. As the level of fill exceeds the height of the pressure cells, there seems to be a linear increase in pressure with depth of fill. Also, as with pressure cells 2 and 19, the measured earth pressures for pressure cell 3 are greater than those for pressure cell 18 for lower fill heights. However, as the height of fill increases, the measured earth pressures for cell 18 become greater than those of cell 3. This may in part be due to the difference in the type of pressure cells, or may be due to

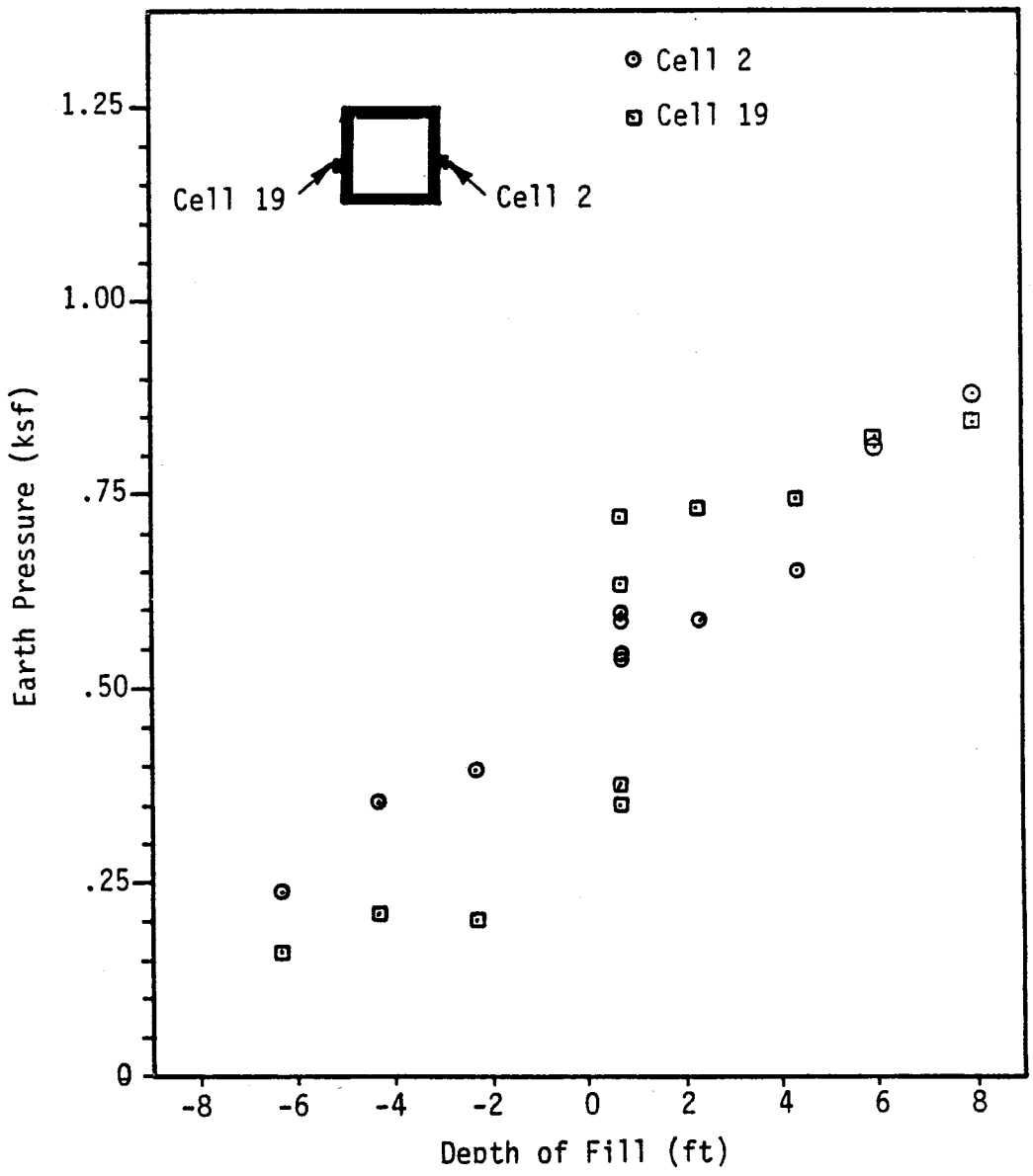

Field Data for Pressure Cells 2 and 19; Soil Loads Only
Variation of Earth Pressure with Depth of Fill

FIGURE 5-3

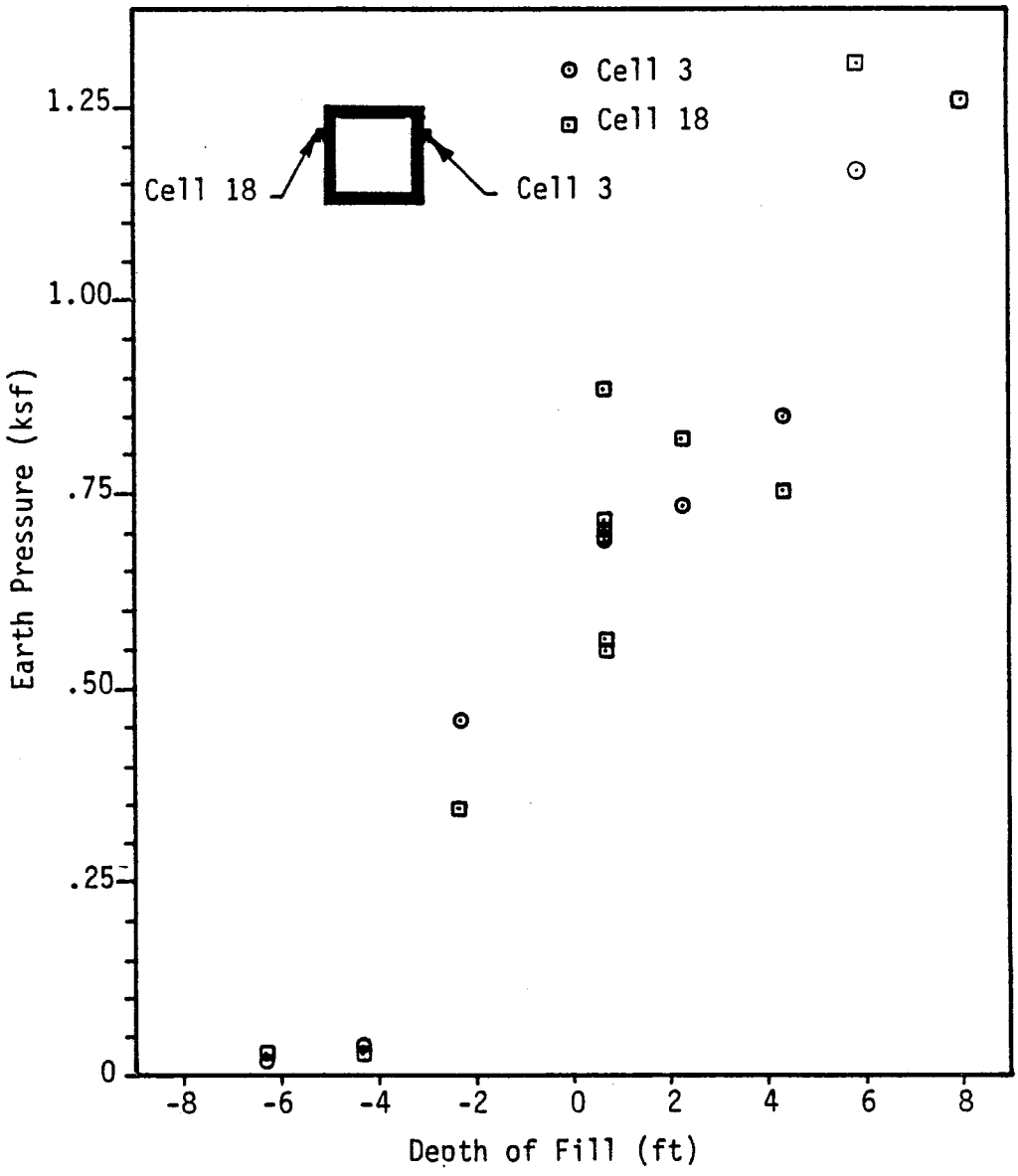

Field Data for Pressure Cells 3 and 18; Soil Loads Only
Variation of Earth Pressure with Depth of Fill

FIGURE 5-4

uneven degrees of compaction during the construction sequence. Cells 2 and 3 are on the same wall of the culvert.

The variation of measured earth pressure with depth of fill for pressure cells 4 and 17 is shown in Figure 5-5. Initially, there is a small pressure indicated before any fill is placed above the level of the pressure cells. As noted before, when the depth of fill is 8 inches above the crown of the culvert, earth pressure measurements were taken on a number of different days. Both pressure cells show an increase in measured pressure with time. This may be due to primary consolidation and compaction after placement of the fill material. Also, the measured earth pressures appear to increase linearly with depth of fill.

For pressure cells located on the top of the culvert, the variation in earth pressure with depth of fill for pressure cells 6, 9, 12 and 15 along the centerline of the culvert is shown in Figure 5-6. All of the pressure cells indicate some measured pressure before the level of fill exceeds the crown of the culvert, with pressure cell 15 consistently showing high values. There is a wide range of pressures for depth of fill 8 inches above the crown of the culvert, with measured pressures varying from almost zero to 0.45 ksf. The variation of pressure with depth is not linear, and the reasons for the deviations in the data are fully understood. Thermally induced soil pressures are possibly the cause of some of this deviation.

The variation in earth pressure with depth of fill for pressure cells 11, 13, 14 and 16 is shown in Figure 5-7. These pressure cells are located on the top of the culvert, 21 inches from the centerline on either side. Before the level of fill exceeds the crown of the culvert, all cells measure essentially zero earth pressure. For a depth of fill

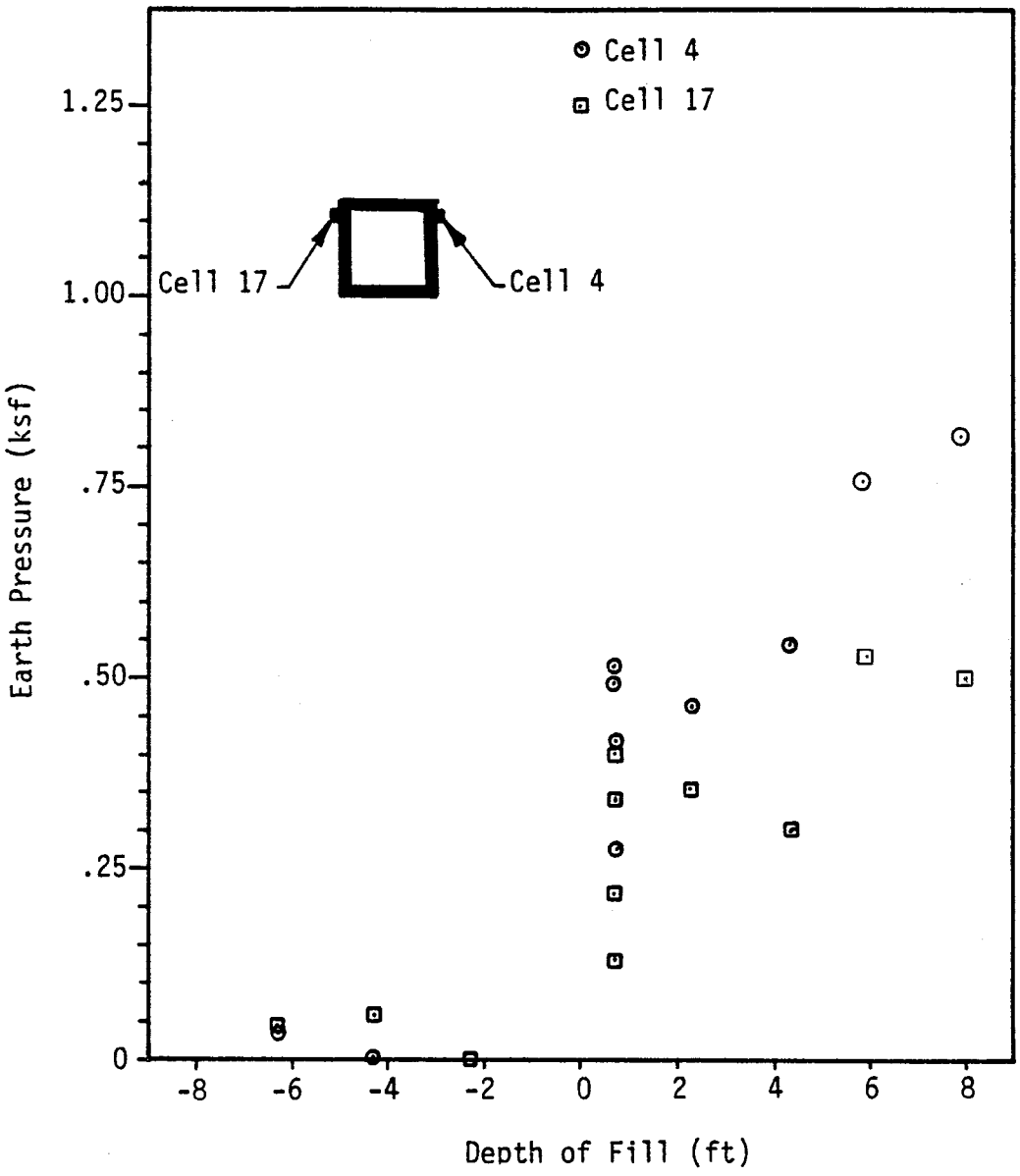

Field Data for Pressure Cells 4 and 17; Soil Loads Only
Variation of Earth Pressure with Depth of Fill

FIGURE 5-5

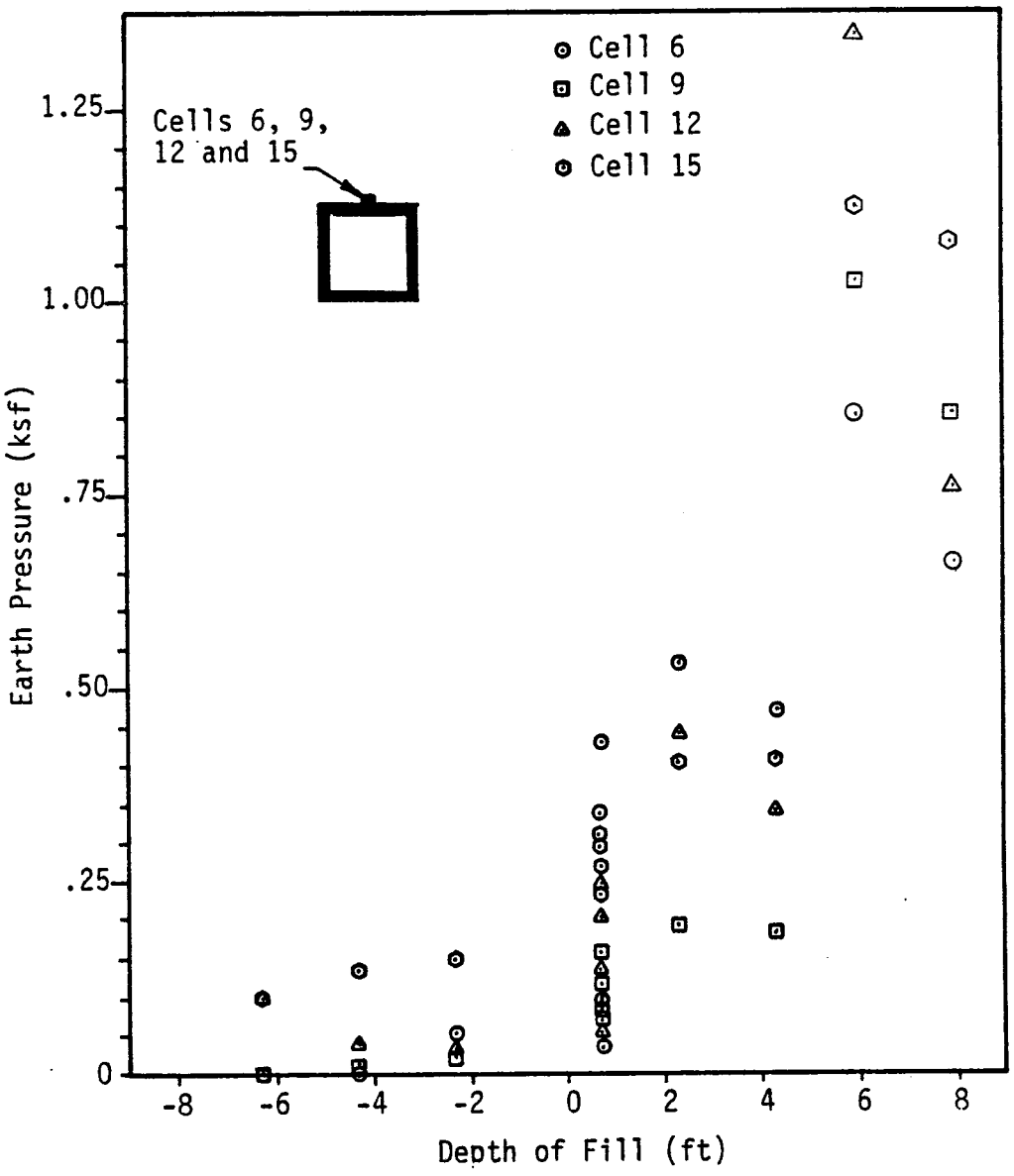

Field Data for Pressure Cells 6, 9, 12, 15; Soil Loads Only
Variation of Earth Pressure with Depth of Fill

FIGURE 5-6

of 2 feet above the crown of the culvert, pressure cells 11 and 13 indicate unreasonably high values of earth pressure, while pressure cells 14 and 16 show more realistic measurements.

Finally, the variation in earth pressure with depth of fill for pressure cells 5, 7, 8 and 10 is shown in Figure 5-8. These pressure cells are located on the top of the culvert, 37 inches on either side of the centerline. Again, a large variation of measured earth pressures is shown for a depth of fill of 8 inches above the crown of the culvert. Also, the earth pressure tends to increase linearly with height of fill.

It should be noted that the large variation of measured earth pressures for a fill height of 8 inches above the crown of the culvert is probably due to the construction and testing sequence involved. At this height of fill, a number of preliminary live load earth pressure measurements were taken. Therefore, the effects of the large truck, as well as other construction equipment, moving around on top of the culvert with this small amount of fill covering the pressure cells seems to have increased the values of earth pressure obtained. In other words, there seems to be some residual stresses existing in the fill material due to compaction.

Also, for small values of earth pressure, the accuracy of the pressure cells is somewhat questionable, and thermally induced earth pressures may be important. This could affect the measured values enough to explain part of the wide variations in the field measurements shown.

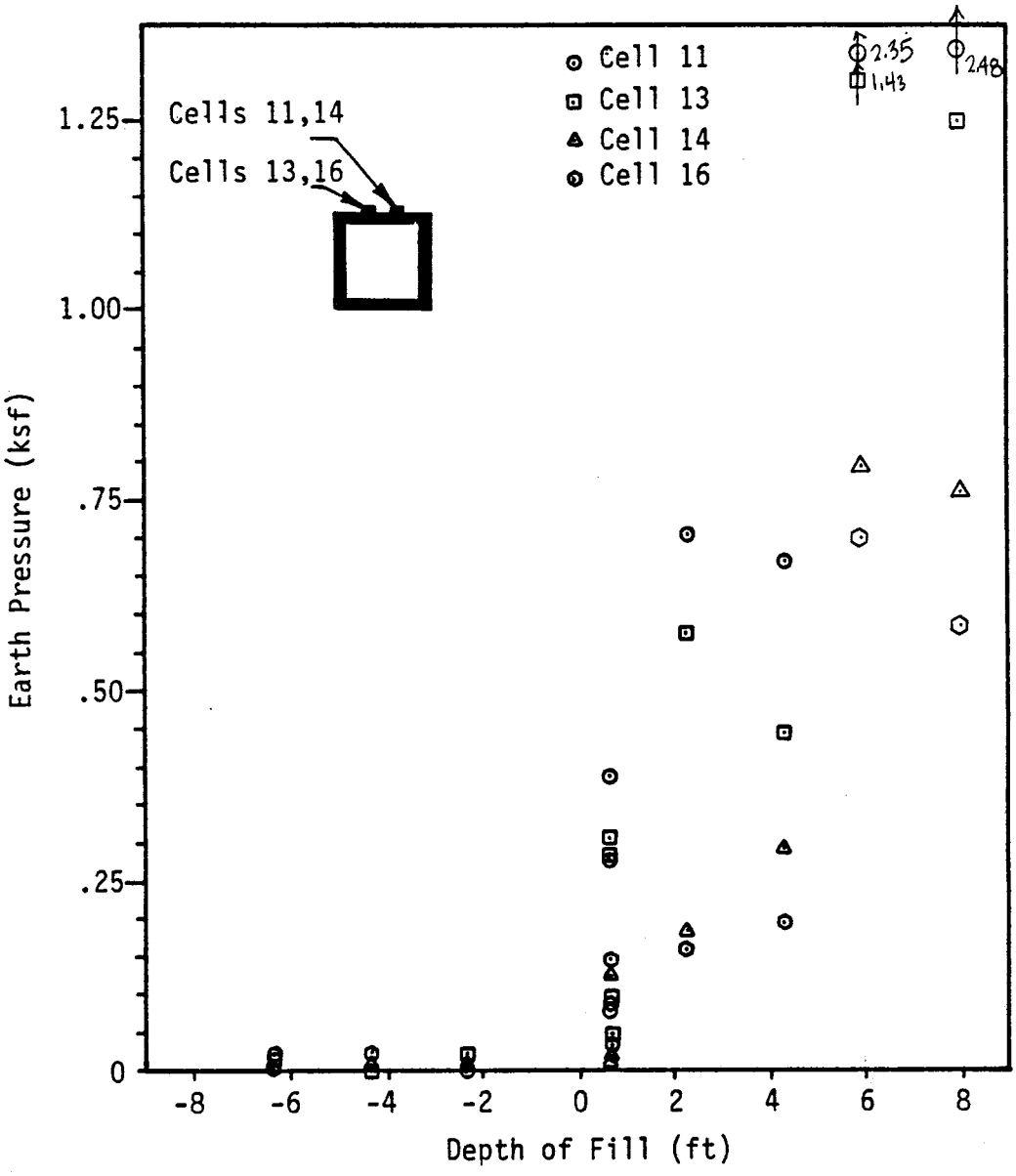

Field Data for Pressure Cells 11, 13, 14, 16; Soil Loads Only
Variation of Earth Pressure with Depth of Fill

FIGURE 5-7

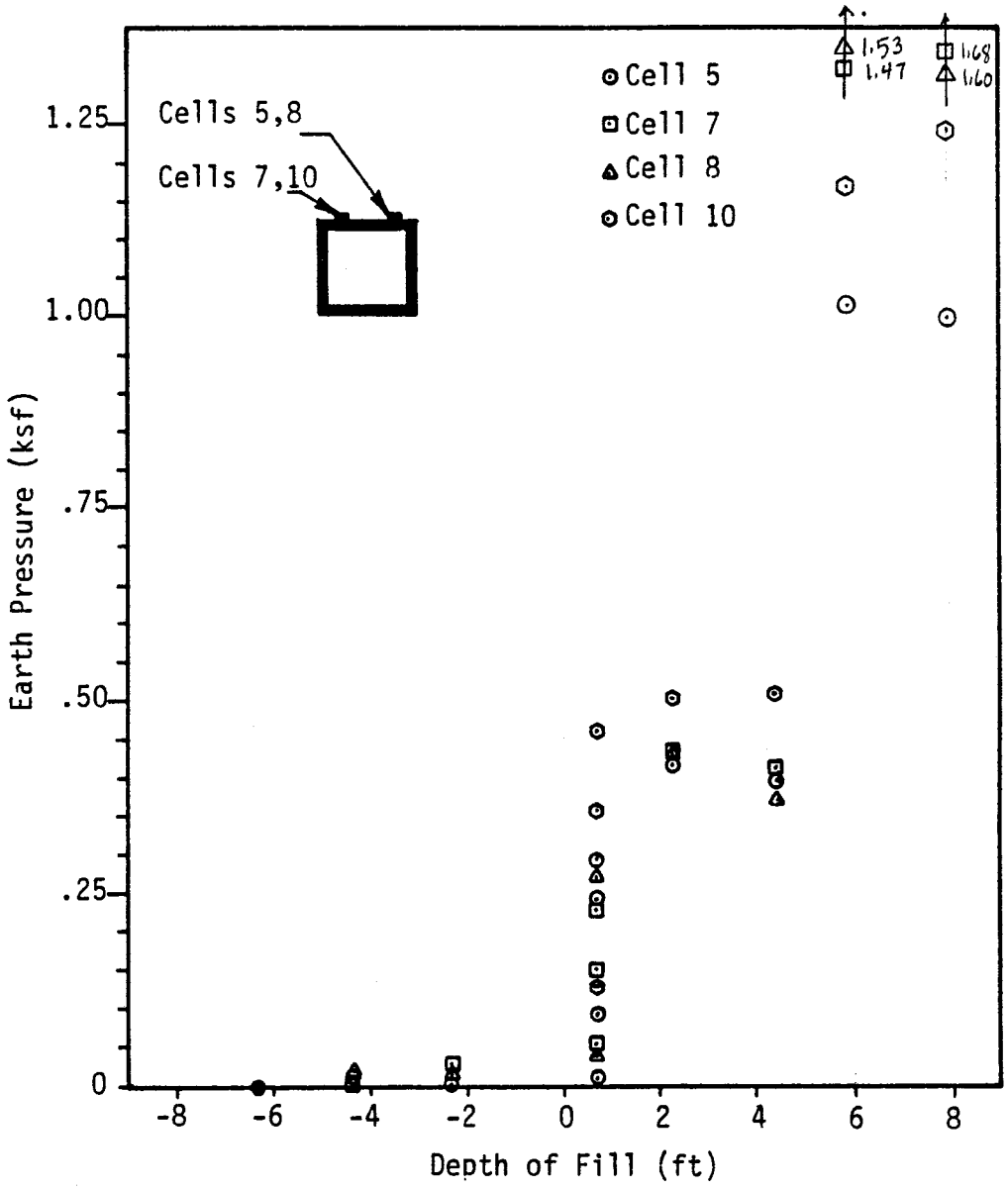

Field Data for Pressure Cells 5, 7, 8, 10; Soil Loads Only
Variation of Earth Pressure with Depth of Fill

FIGURE 5-8

5.3 Comparison of Finite Element Predictions and Field Measurements

5.3.1 Dead Loads

In order to compare the field measurements of earth pressure with the predictions from the finite element method analyses, the predicted values for earth pressure were superimposed on the plots of field measurements shown previously. In this manner, a comparison of the results is easily made.

For pressure cells 1 and 20, the comparison of predicted and measured earth pressures is shown in Figure 5-9. Except for the measured earth pressures at -6 feet, a very good correlation is seen between the prediction and data from cell 20. Cell 1 indicates a significantly lower pressure. At a depth of fill of -6 feet, the measured values seem unreasonably high. At this point, only a few inches of backfill material are covering the pressure cells.

For pressure cells 2 and 19, the comparison of predicted and measured earth pressures is shown in Figure 5-10. The predicted values seem to be much less than the measured earth pressures. However, at -6 feet, although no fill has been placed above the level of the pressure cells, measurements of approximately 0.20 ksf for the earth pressures are obtained. This indicates that there may be a correction of 0.20 ksf necessary so that zero pressures are measured when zero pressure is applied to the cells. After reducing the measured earth pressures by this amount, the comparison appears to be much better, as shown in Figure 5-11. Here, the predicted earth pressures fall well within the range of measured values, giving a better correlation. Whether the increasing deviation of the predicted pressures from measured pressures at increasing depth of fill is significant or is due to scatter in the

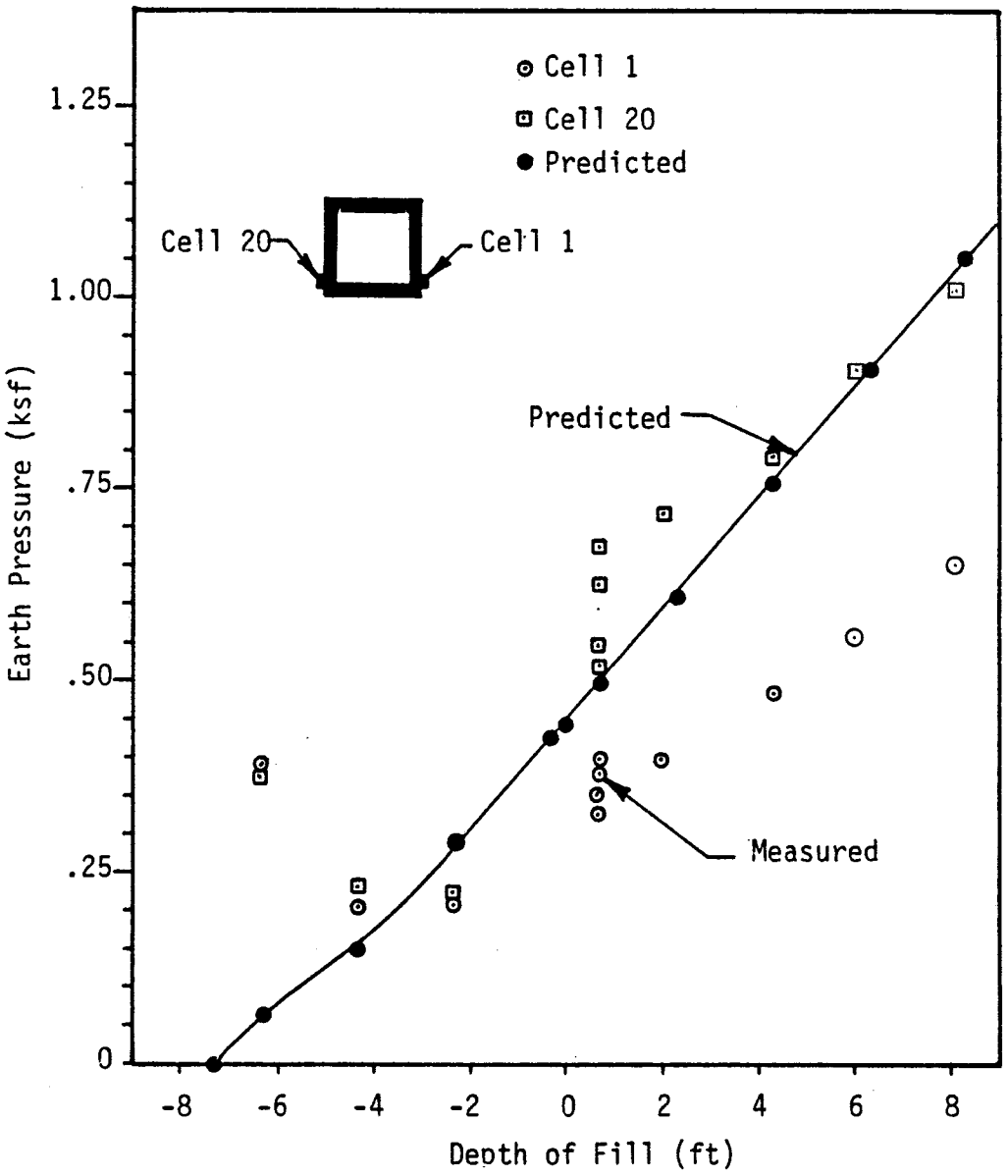

Comparison of Predicted and Measured Earth Pressures
For Pressure Cells 1 and 20;
Variation in Earth Pressure With Depth of Fill

FIGURE 5-9

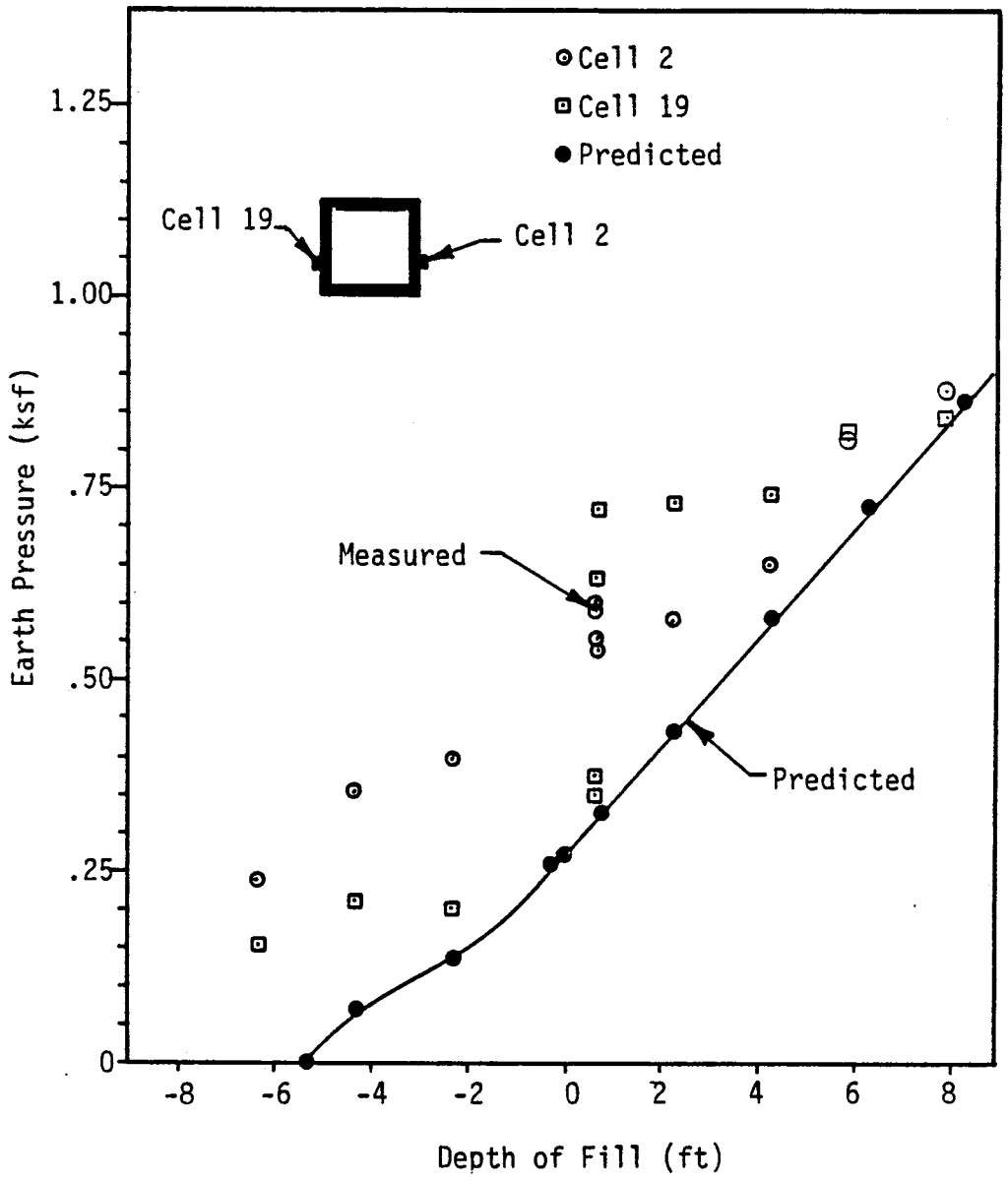

Comparison of Predicted and Measured Earth Pressures
For Pressure Cells 2 and 19;
Variation of Earth Pressure With Depth of Fill

FIGURE 5-10

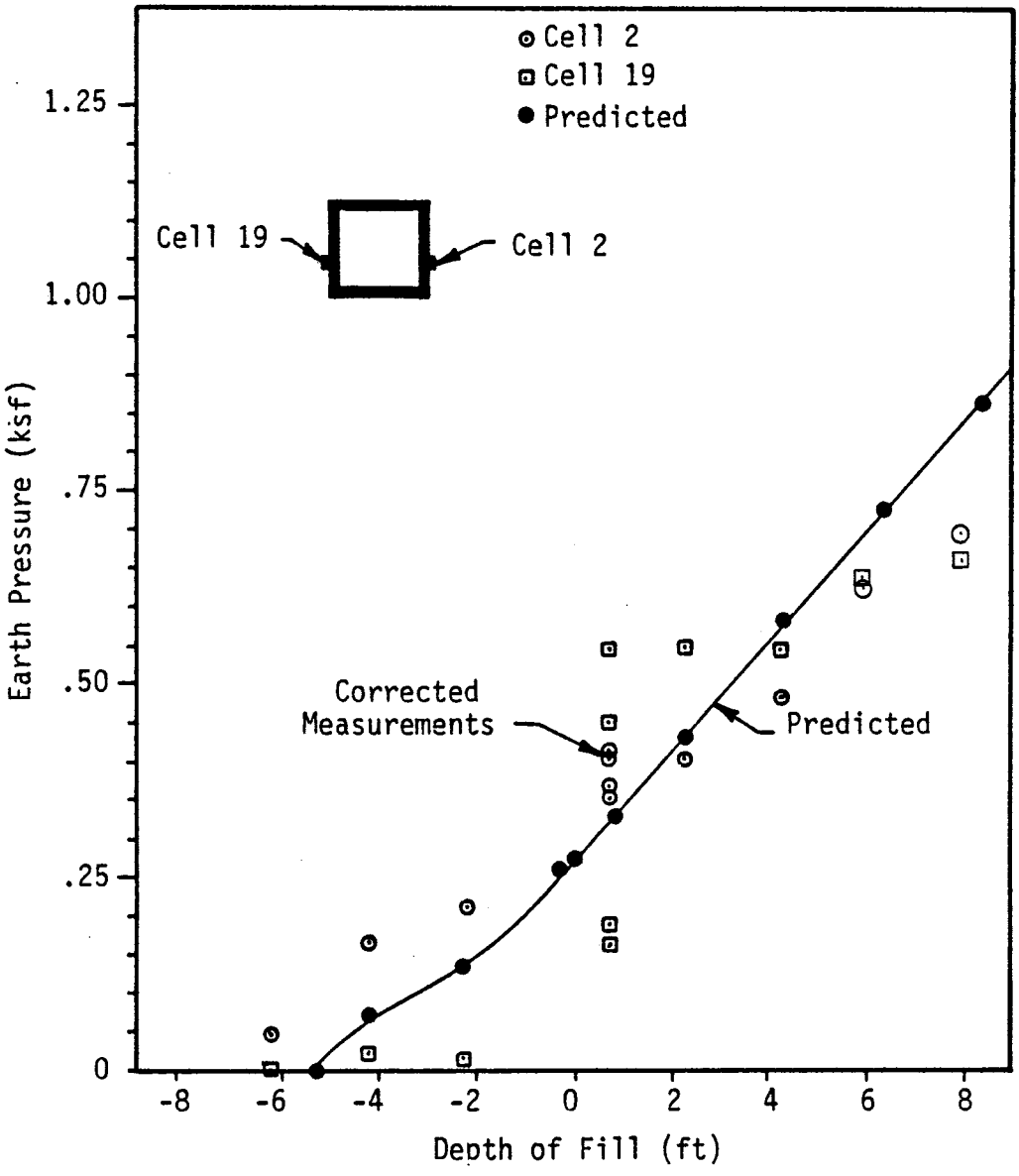

Comparison of Corrected Measurements
From Cells 2 and 19
With Predicted Earth Pressures

FIGURE 5-11

data cannot be conclusively determined.

For pressure cells 3 and 18, the comparison of predicted and measured earth pressures is shown in Figure 5-12. The predicted earth pressures are approximately 40% of the measured values. It is possible that there are measurement errors of unknown origin in these two cells. One likely source is residual compaction stresses. This reasoning is supported by the fact that a depth of fill of -2 feet, when only a few inches of fill are covering the cells, unreasonably high values of earth pressure are measured.

The comparison of predicted and measured earth pressures for pressure cells 4 and 17 is shown in Figure 5-13. The predicted values are slightly less than those measured, however there does seem to be some variation in measured pressures before any backfill is placed above the cells. This indicates the possibility of some scatter in the data, as was noted previously. Here, the predicted values may be slightly unconservative, but it is felt that they represent actual field condition reasonably well.

The comparison of predicted and measured earth pressures for pressure cells 6, 9, 12 and 15 is shown in Figure 5-14. These cells are located on the top of the culvert along the centerline. Although there is a fairly good correlation before any further correction of field measurements, it is noted that some correction may be required to offset readings before any fill is placed above the level of the cells. Here, the data has been reduced by 0.05 ksf, as shown in Figure 5-15. The correlation of predicted and measured values is better, with the predicted values falling slightly less than the average measured pressure at each depth of fill.

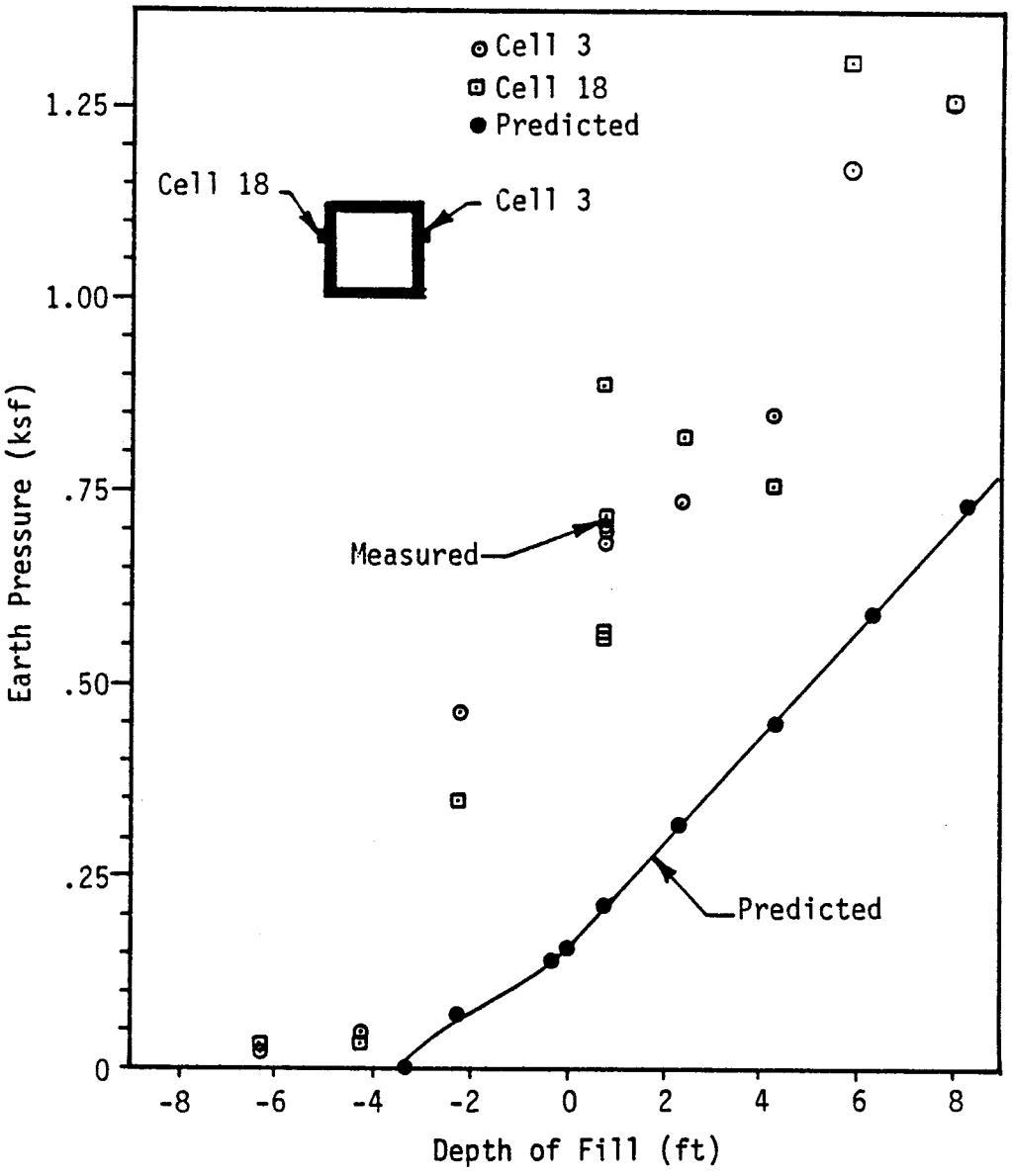

Comparison of Predicted and Measured Earth Pressures
For Pressure Cells 3 and 18;
Variation of Earth Pressure With Depth of Fill

FIGURE 5-12

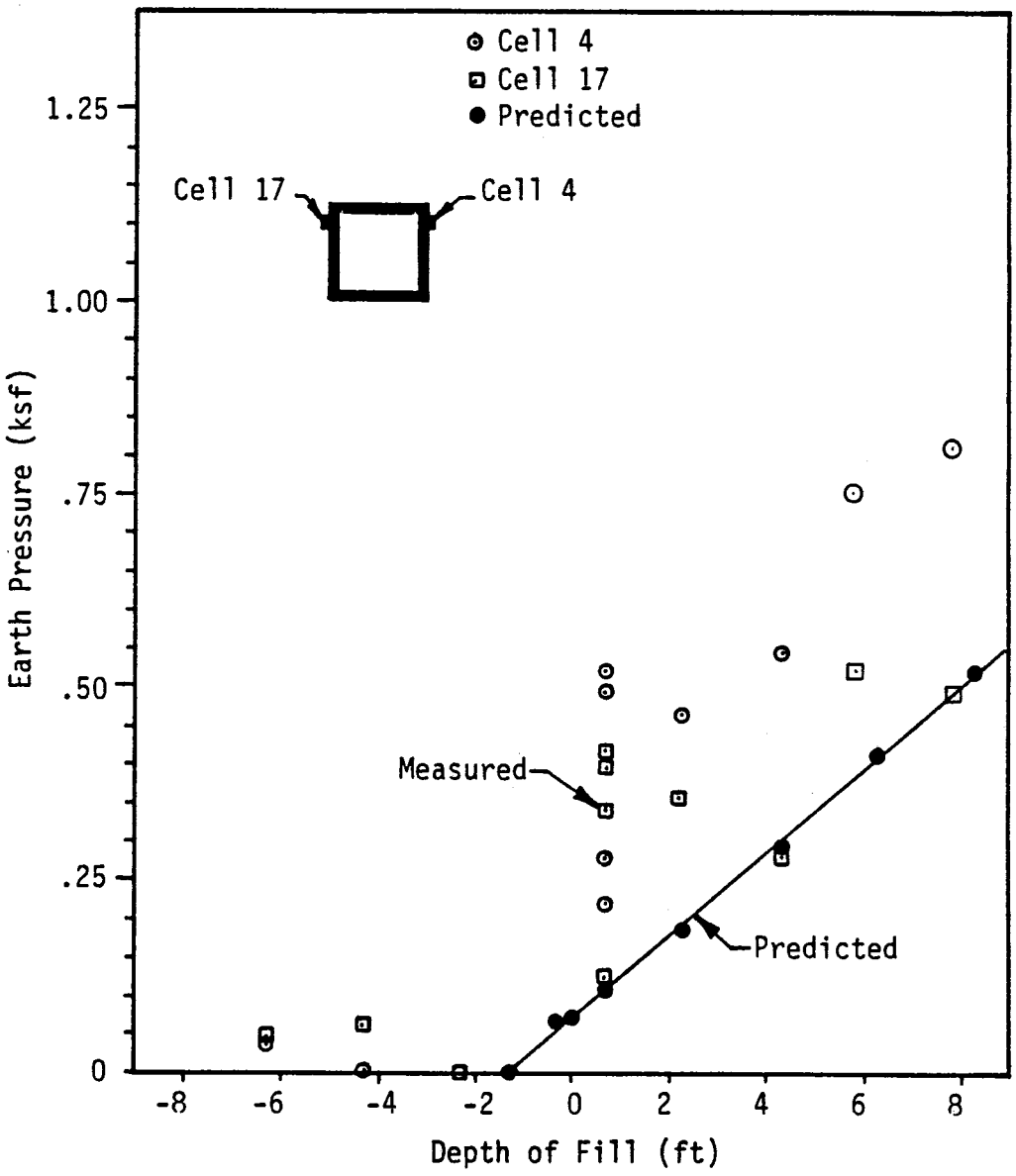

Comparison of Predicted and Measured Earth Pressures
For Pressure Cells 4 and 17;
Variation in Earth Pressure With Depth of Fill

FIGURE 5-13

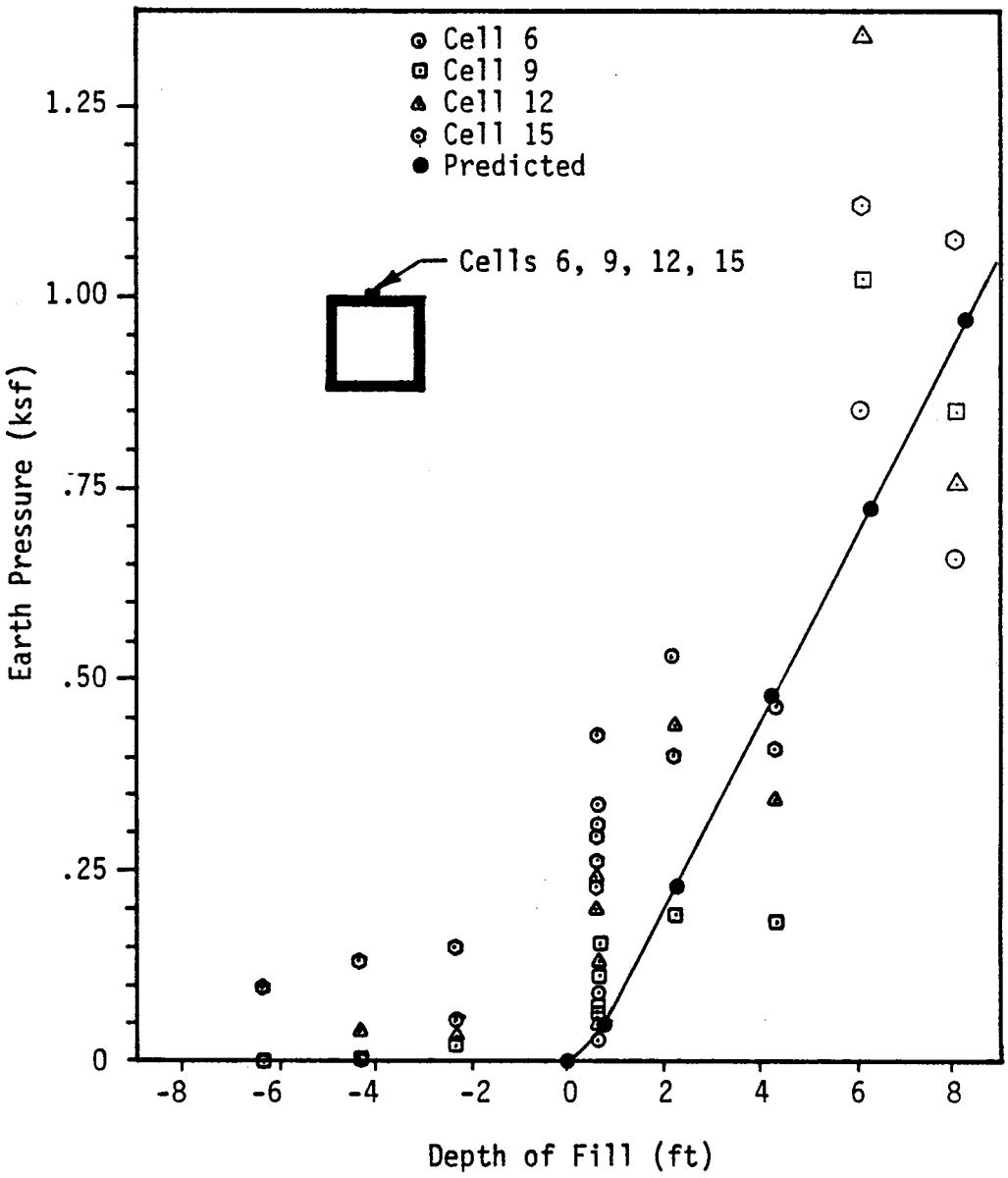

Comparison of Predicted and Measured Earth Pressures
For Pressure Cells 6, 9, 12, and 15
Variation in Earth Pressure With Depth of Fill

FIGURE 5-14

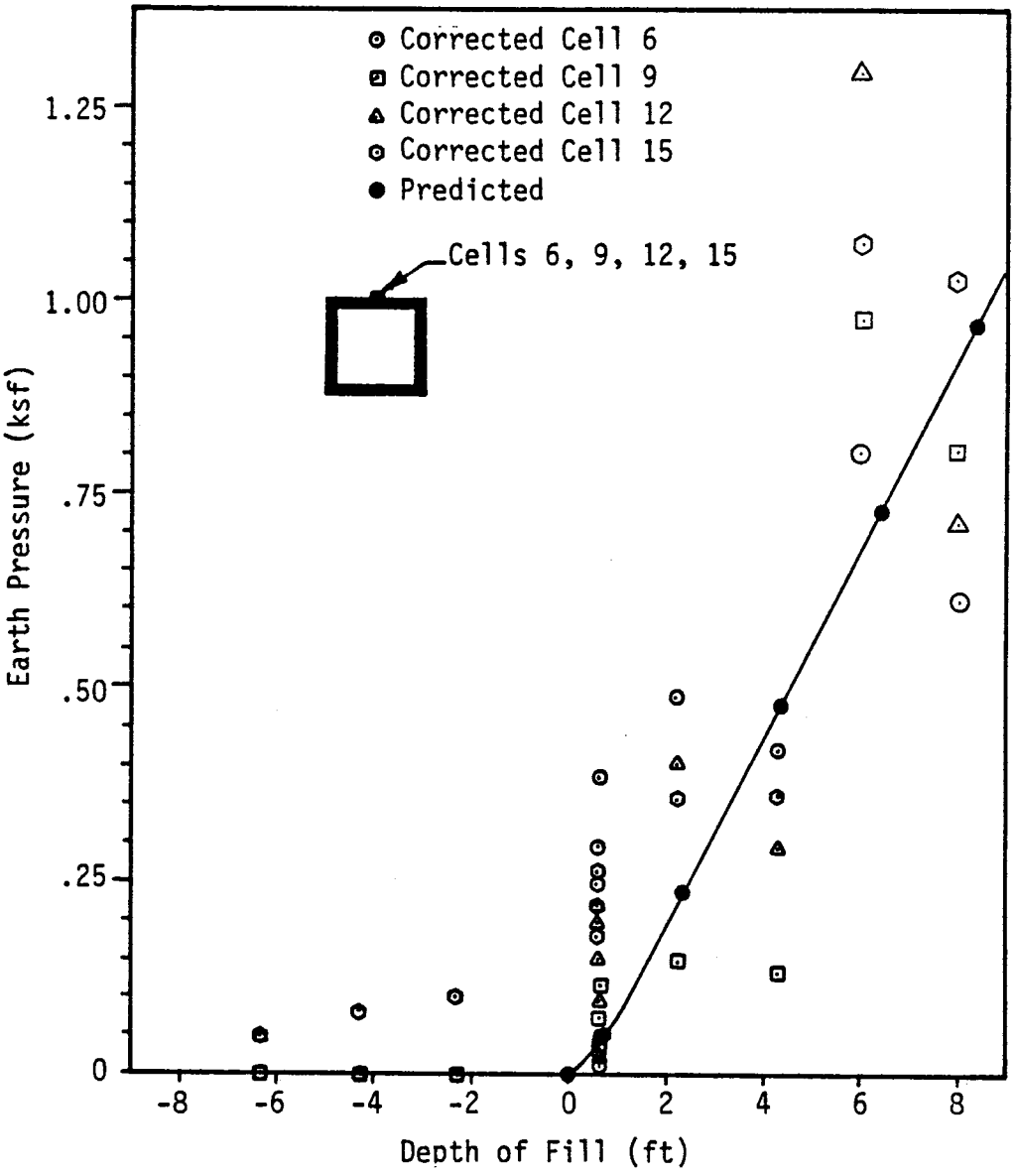

Comparison of Corrected Measurements From Cells 6, 9, 12, and 15 With Predicted Earth Pressures

FIGURE 5-15

The comparison of predicted and measured earth pressures for pressure cells 11, 13, 14 and 16 is shown in Figure 5-16. Here a reasonably good agreement is found between the predicted and measured values. Although some nonzero readings are seen prior to the level of fill exceeding the level of the cells, these values are rather small and therefore no correction has been made. Considerable scatter of unknown origin is evident in the measured pressures at 6-8 feet covers.

Finally, the comparison of predicted and measured pressures for cells 5, 7, 8 and 10 is shown in Figure 5-17. These cells are located on the top of the culvert, 37 inches offset from the centerline on either side. There is a fair agreement of data, with the predicted values being less than the measured values. As with the other cells, there seems to exist a linear relationship between the depth of fill and the earth pressure.

5.3.2 Live Loads

A comparison of measured and predicted pressures for 2 feet of cover is shown in Figure 5-18. Here the measured pressures beneath the line of wheel loads are plotted, superimposed on the predicted pressures for a centered stripload presented earlier in Figure 4-13. Measured pressures due to soil loads only are generally greater than predicted pressures. This observation was discussed in the section on dead load earth pressures. The possibility of experimental errors exists, however the errors would have to be systematic to account for the difference. The live load induced incremental measured and predicted pressures appear to be in good qualitative agreement, except for the location of

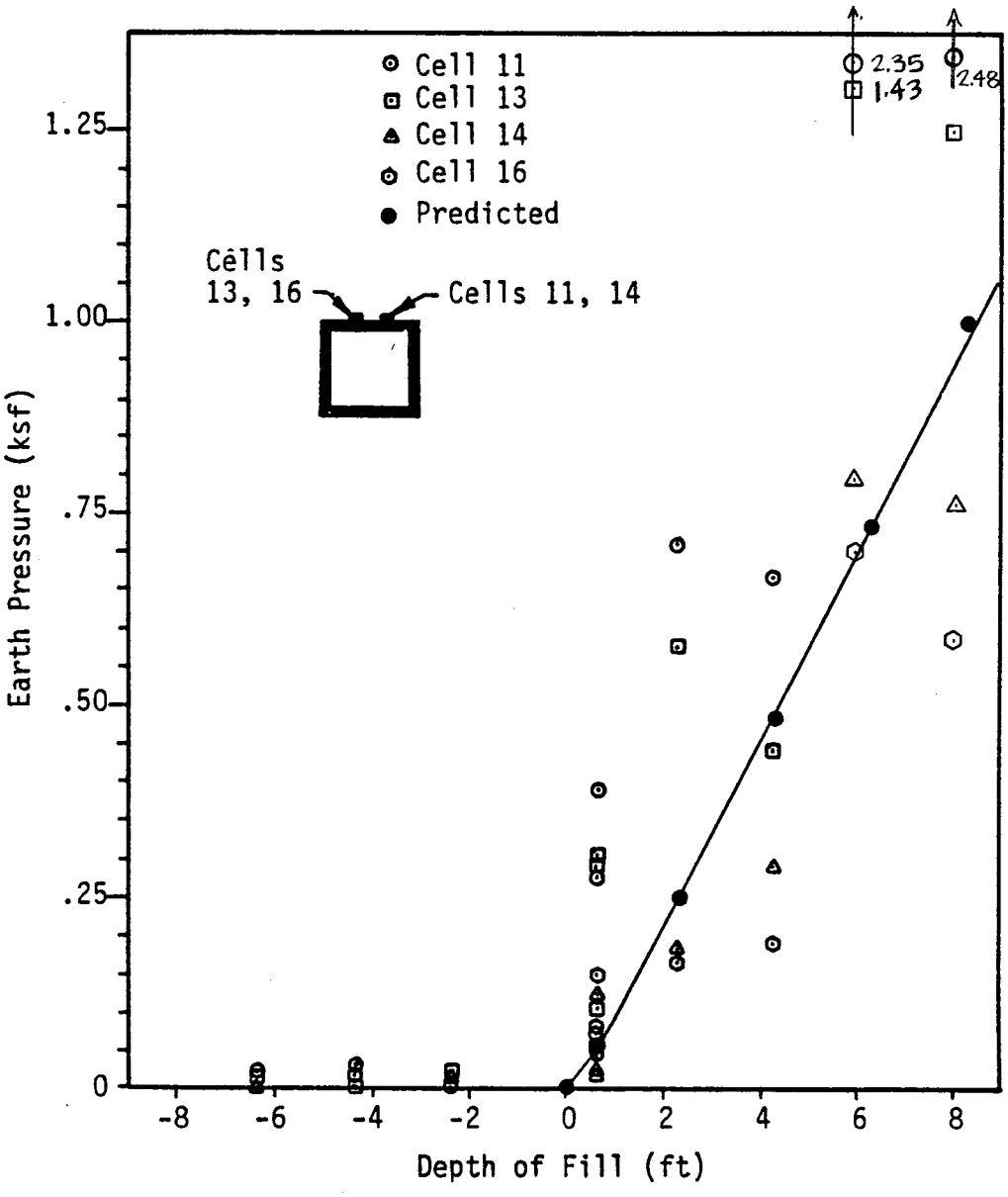

Comparison of Predicted and Measured Earth Pressures
For Pressure Cells 11, 13, 14 and 16
Variation of Earth Pressure With Depth of Fill

FIGURE 5-16

the maximum pressures. The peak measured pressure is indicated by pressure cells 11 and 13, which are nearly beneath the applied wheel loads. The predicted maximum pressure at the top slab midspan is significantly less than the measured maximum pressure, in spite of the fact that the unit strip load is expected to cause greater predicted live load maximum pressures than each of the experimental 24 kip axles.

The predicted live load earth pressures for 4 ft cover, presented earlier in Figure 4-14, are compared to measured earth pressures in Figure 5-19. Here the scatter in the experimental data is of the same magnitude as the live load induced pressure. Still, the predicted dead load only and dead load plus live load pressures are in reasonable agreement, with much less deviation than was observed in the data for 2 ft cover.

The predicted live load earth pressures for 8 ft cover, presented earlier in Figure 4-15, are compared to the measured earth pressures in Figure 5-20. Again, the scatter in the measured data is large, however the data do not appear to significantly deviate, on the average, from the predictions.

In general, there is reasonably good agreement between the predicted and measured live load earth pressures. The data at 2 ft cover is the exception. The reasons for the differences at 2 ft are not known. While it is possible that the differences can be attributed to experimental errors, it is not considered likely since large systematic errors are not expected.

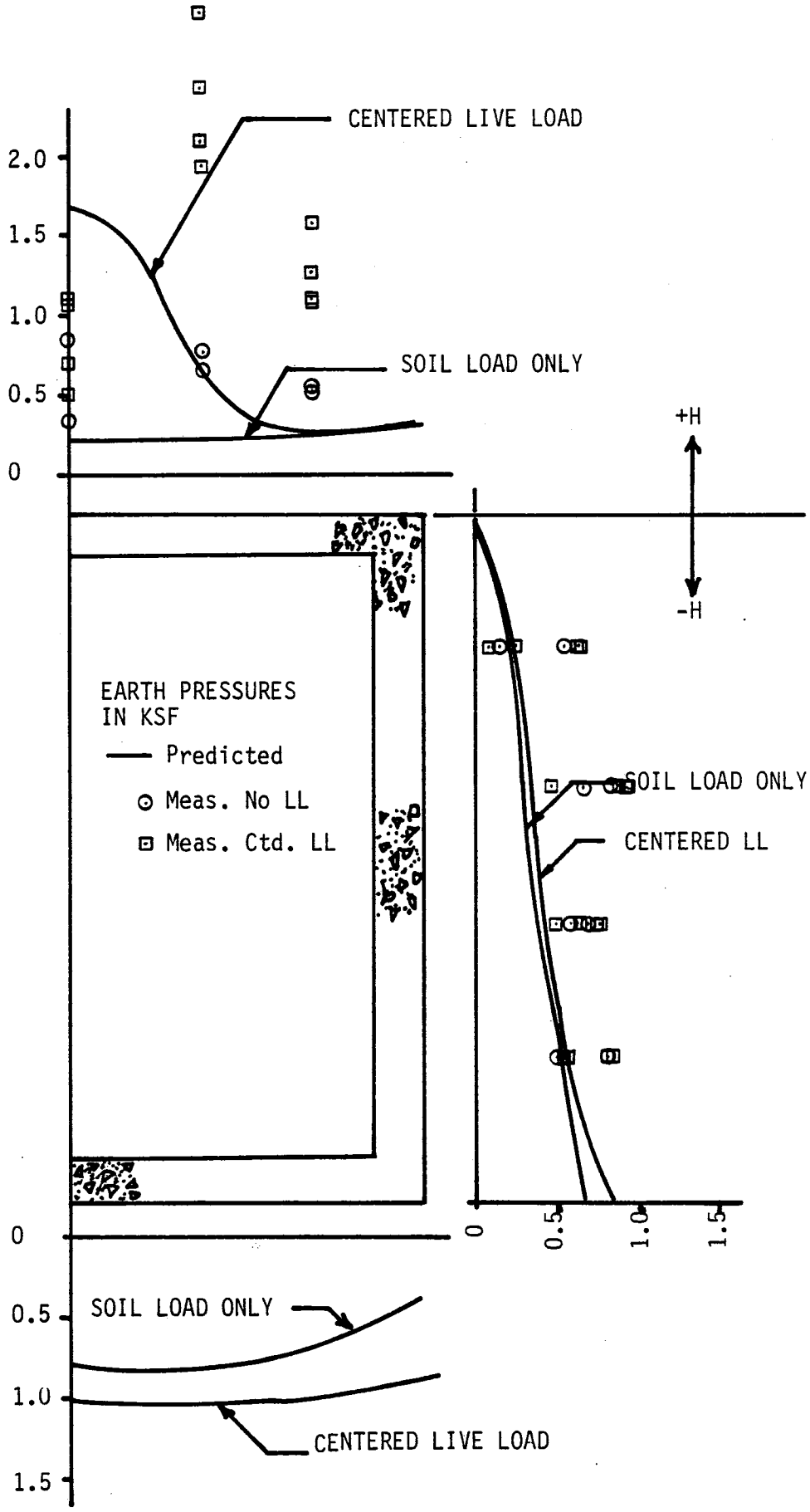

Comparison of Predicted (equiv. unit strip) and Measured (48 kip tandem) Earth Pressures; H=2 ft

FIGURE 5-18

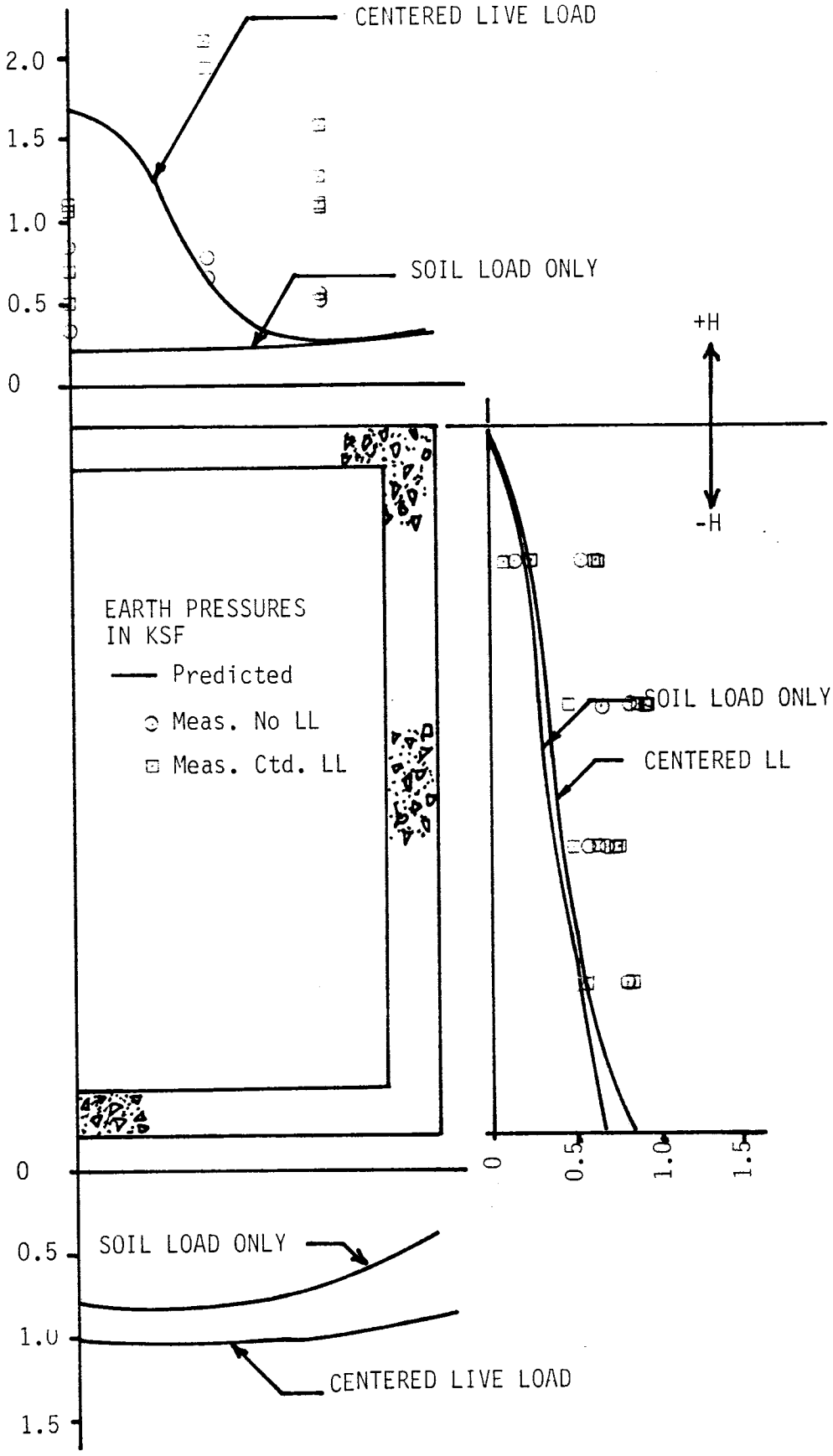

Comparison of Predicted (equiv. unit strip) and Measured (48 kip tandem) Earth Pressures; H=2 ft

FIGURE 5-18

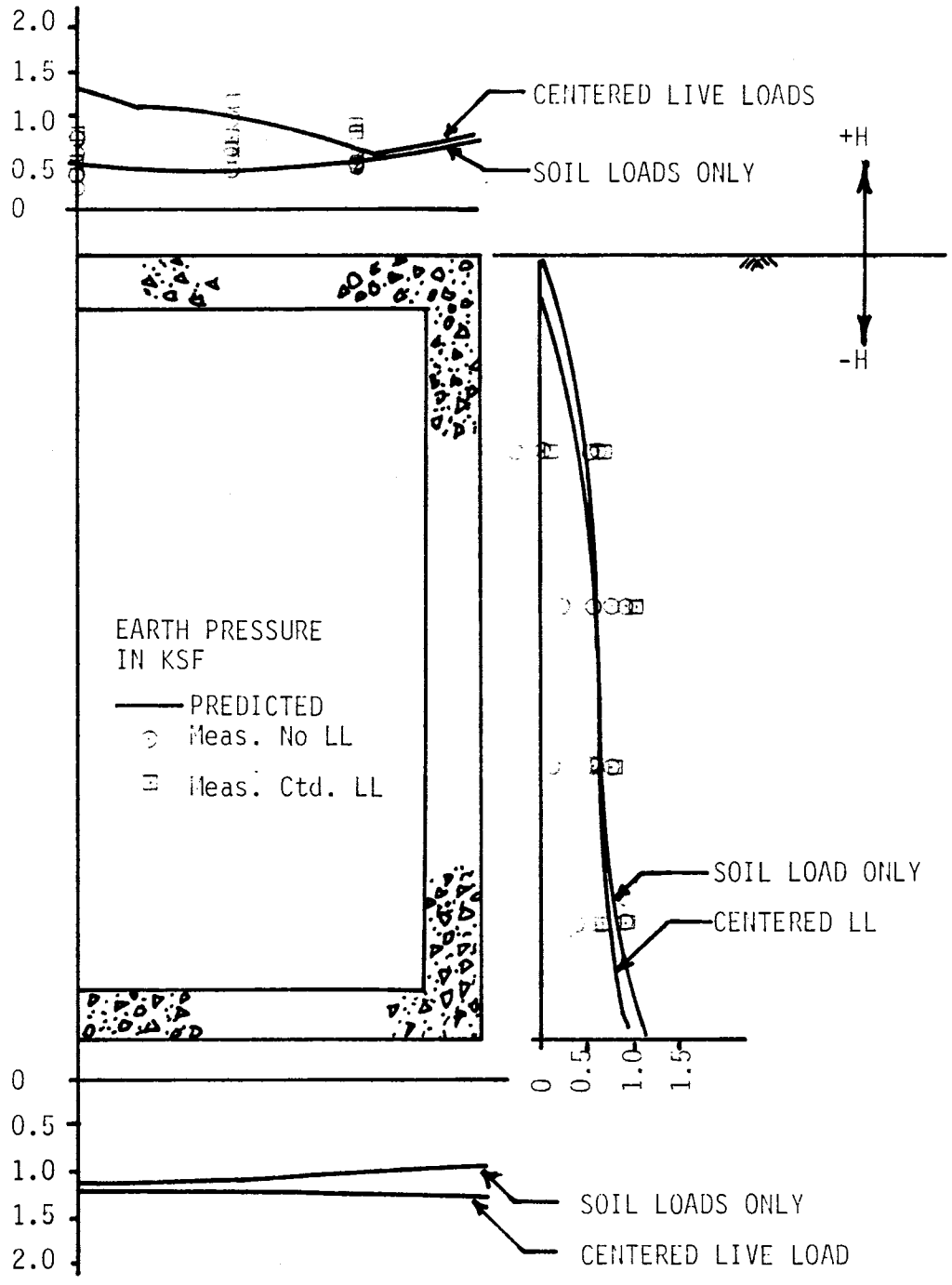

Comparison of Predicted (equiv. unit strip) and Measured (48 kip tandem) Earth Pressures; H=4 ft

FIGURE 5-19

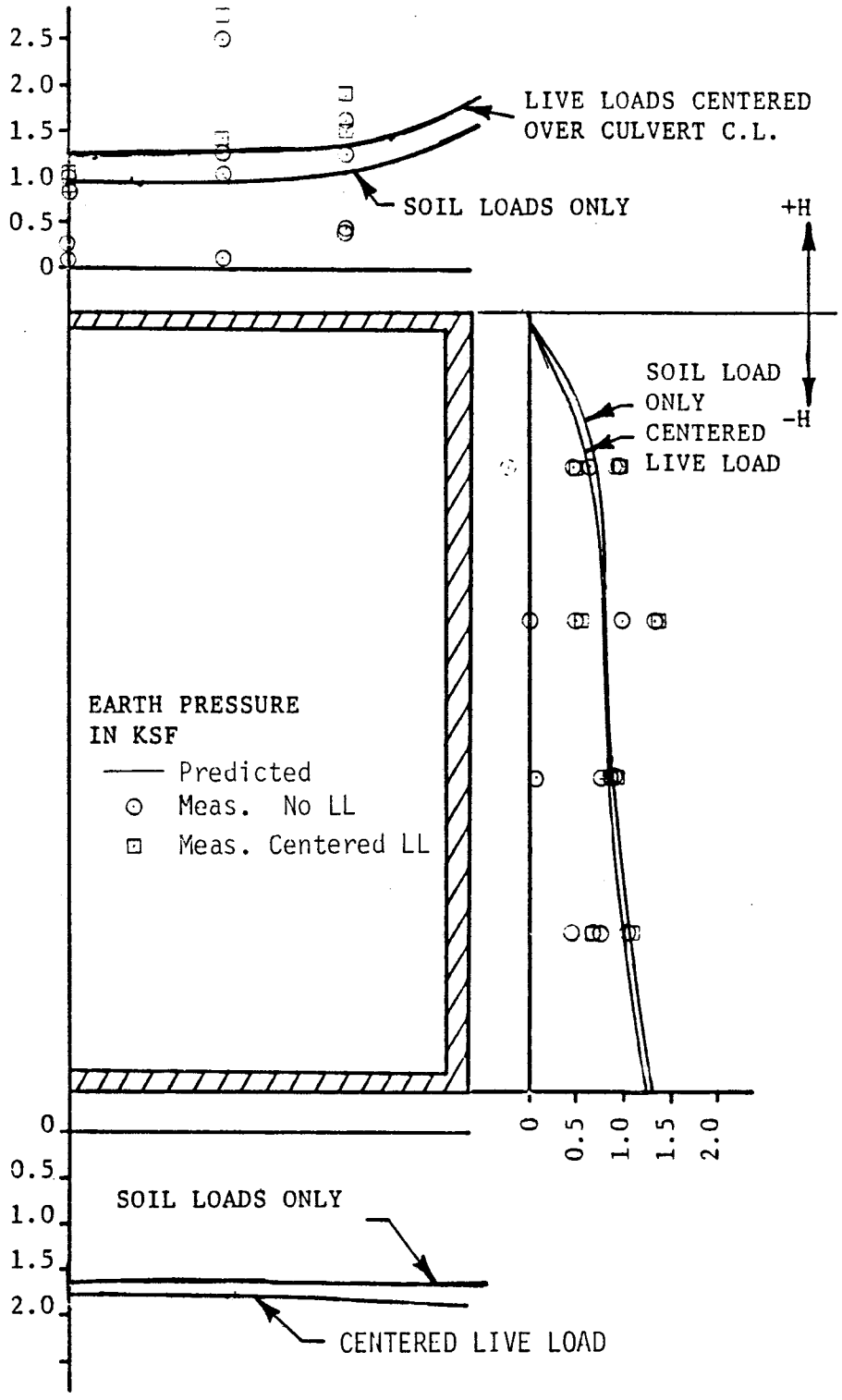

Comparison of Predicted (equiv. unit strip) and Measured (48 kip tandem) Earth Pressures; H=8 ft

FIGURE 5-20

CHAPTER 6

SUMMARY, CONCLUSIONS, AND RECOMMENDATIONS

6.1 Summary

The computer program SSTIPN has been used to predict earth pressure distributions as well as stresses, strains and internal stress resultants in a reinforced concrete box culvert. The predicted earth pressures have been compared to measured earth pressures resulting from a parallel experimental study. The loading is simplified as an equivalent strip load of width equal approximately to one wheel footprint length. The tandem axle loading has been approximated by equivalent single strip load for computational convenience.

6.2 Conclusions

The computer program SSTIPN can be applied to the analysis of reinforced concrete box culverts. Predicted pressures are in reasonable agreement with measured pressures except for shallow depths of fill, where predicted pressures appear to be unconservatively low. The differences in predicted and measured pressures may be partly due to the method chosen to model the loading; by a two-dimensional single equivalent strip loading applied the length of the culvert. The actual loading is over four contact areas, which results in measured earth pressure distributions showing local maximums beneath each wheel contact area. A more sophisticated loading case could improve the model. Because of the difference in the magnitudes of the maximum predicted and

measured pressures, it is concluded that either a more sophisticated soil model or a more sophisticated load model is required, especially when high wheel load earth pressures are expected to dominate the solution.

The application of a live load to the box culvert system appears to exert very little influence on the lateral earth pressures acting on the culvert walls for depths of fill greater than 2 feet above the crown of the culvert. A significant reduction in lateral earth pressures at the top corner of the culvert appears to exist. This implies an "arching" effect as a result of the application of the live loads and the soil-culvert interaction.

Along the top surface of the culvert, both the symmetrical and unsymmetrical live loads influence the earth pressures significantly. This influence decreases with increasing depth of fill, although not as quickly as previously expected. At a depth of fill 8 feet above the crown of the culvert, there is approximately a 30% increase in earth pressure as a result of the application of symmetrical and unsymmetrical live loads.

Moments, shear forces, stresses, and strains exhibit the same trend as found with earth pressures in that the primary influence of the live loads occurs along the surface of the culvert, with very little effect on the sides or bottom of the culvert.

6.3 Recommendations

While SSTIPN has been shown to be applicable to the soil-structure interaction problem of a box culvert with dead and live load induced earth pressures, enough differences between the predicted pressures and

measured pressures exist to require further study before its adoption for routine analysis and design. Further study of better load and soil modelling techniques is recommended, specifically:

1. Better representation of the wheel loads is required for more accurate prediction of live load induced pressures at shallow cover depths, and
2. An evaluation is recommended of the applicability of the soil model chosen, especially when subject to the combination of shallow cover depths and multiple wheel loads.

REFERENCES

1. Allgood, J. R. and Takahashi, S. K., "Balanced Design and Finite Element Analysis of Culverts", U.S. Naval Civil Engineering Lab., 1968.

2. American Association of State Highway and Transportation Officials, "Interim Specification for Precast Reinforced Concrete Box Sections for Culverts, Storm Drains, and Sewers", [AASHTO Designation: M259-75I], 1976.

3. American Society for Testing Materials, "Standard Specifications for Precast Reinforced Concrete Box Sections for Culverts, Storm Drains, and Sewers", [ASTM Designation: C789-79], 1979.

4. Armco Drainage and Metal Products, Inc., "Handbook of Culvert and Drainage Practice", 1948, Middletown, Ohio.

5. Davis, R. E. and Bacher, A. E., "Californias' Culvert Research Program - Description, Current Status, and Observed Peripheral Pressures", Highway Research Record 249, 1968, pp. 14-23.

6. Department of the Army, Office of the Chief of Engineers, "Conduits, Culverts, and Pipes", Engineering Manual No. 110-2-29-2, 1969.

7. Duncan, J. M. and Chang, C. Y., "Nonlinear Analysis of Stress and Strain in Soils", Journal of the Soil Mechanics and Foundation Division, ASCE, Vol. 96, No. SM5, Proceedings Paper 7513, 1970.

8. Duncan, J. M., Byrne, P. M., Wong, K. S., and Mabry, P. N., "Hyperbolic Volume Change Parameters for Nonlinear Finite Element Analyses of Stresses and Movements in Soil Masses", Geotechnical Engineering Report, University of California, Berkeley, 1978.

9. Duncan, J. M. and Jeyapalan, J. K., "Summary of Finite Element Analyses of the Below Ground Section of the Arco-Kuparak Oil Pipeline", Report to Arco Corp. & William Brothers Co., November, 1979.

10. Duncan, J. M. and Jeyapalan, J. K., "Deflection of Flexible Culverts Due to Backfill Compaction", Report to Kaiser Aluminum Chemical Sales Corp., California, October, 1979.

11. Heger, F. J., "Structural Design Method for Precast Reinforced Concrete Pipe", Simpson, Gumphertz, and Heger, Inc., Cambridge, MA.

12. Huang, A., Gill, S. A., and Gnaedinger, J. P., "The Study of Earth Pressures on Concrete Box Culverts", Soil Testing Services Inc., Northbrook, Illinois.

13. Katona, M. G., "Soil-Structure Analysis and Evaluation of Buried Box Culvert Designs", May 1981, Presented at ASCE 1981 International Convention.

14. Karadi, G. M. and Krizek, R. J., "Culvert Design in Some European Countries", 1969, Highway Research Record, No. 262.

15. Marston, A., "The Theory of External Loads on Closed Conduits in the Light of the Latest Experiments", Iowa Engineering Experiment Station, Bulletin No. 96, 1930.

16. Nielson, F. D., "Soil Structure Arching Analysis of Buried Flexible Structures", Highway Research Record 185, pp. 36-50, 1967.

17. Olander, H. C., "Stress Analysis of Concrete Pipe", U.S. Bureau of Reclamation, Engineering Monograph No. 6, October 1950.

18. Polack, S. P. and DeGroot, A., Culverts and Tunnels, International Textbook Company, Scranton, PA, 1941.

19. Portland Cement Association, Concrete Culverts and Conduits, Skoakie, IL, 1975.

20. Poulos, H. G. and Davis, E. H., Elastic Solutions for Soil and Rock Mechanics, John Wiley and Sons, Inc., New York, 1974.

21. Quigley, D. W., Earth Pressures on Conduits and Retaining Walls, Ph.D. dissertation, University of California, Berkeley, 1978.

22. Selig, Ernest T., "Subsurface Soil-Structure Interaction: A Synopsis", Proc. Symp. on Soil Structure Interaction, Univ. of Arizona, 1964.

23. Watkins, R. K., "Characteristics of the Modulus of Passive Resistance of Soil", Unpublished Ph.D. disseration, Iowa State University, 1957.

24. Watkins, R. K. and Nielson, F. D., "Development and Use of the Modpares Device in Predicting the Deflection of Flexible Conduits Embedded in Soil", ASCE Pipeline Journal, Jan. 1964.